PROTEOMIC ANALYSIS OF BENZYLISOQUINOLINE ALKALOID (BIA) BIOSYNTHESIS IN DIFFERENT OPIUM POPPY CULTIVARS AND EXAMINATION OF DIFFERENTIALLY EXPRESSED PROTEINS IN RELATION TO BIA CONTENT

A Thesis Submitted to
the Graduate School of
Izmir Institute of Technology
in Partial Fulfillment of the Requirements for the Degree of

MASTER OF SCIENCE

in Molecular Biology and Genetics

by
İrem TAŞDEMİR

December 2024
İZMİR

We approve the thesis of **İrem TAŞDEMİR**

Examining Committee Members:

Prof. Dr. Anne FRARY
Molecular Biology and Genetics,
Izmir Institute of Technology

Asst. Prof. Şerife AYAZ GÜNER
Molecular Biology and Genetics,
Izmir Institute of Technology

Asst. Prof. Athanasia PAVLOPOULOU
Genomics and Molecular Biotechnology,
Izmir International Biomedicine and Genome Institute

11 December 2024

Prof. Dr. Anne FRARY
Supervisor, Molecular Biology and Genetics
Izmir Institute of Technology

Prof. Dr. Özden YALÇIN ÖZUYSAL
Head of the Department of
Molecular Biology and Genetics

Prof. Dr. Mehtap EANES
Dean of the Graduate School

ACKNOWLEDGEMENTS

First and foremost, I would like to express my deepest gratitude to my thesis advisor Prof. Dr. Anne Frary and Prof. Dr. Sami Doğanlar, for their invaluable guidance, support, and encouragement throughout this thesis. Their expertise and mentorship have been pivotal in shaping this work and my academic journey.

My heartfelt thanks go to my committee members, Assist. Prof. Dr. Şerife Ayaz Güner and Assist. Prof. Dr. Athanasia Pavlopoulou, for their insightful feedback and constructive suggestions, which greatly enhanced the quality of this research.

I extend my deepest thanks to Dr. Hüseyin Güner for his assistance and support during the course of my work. His expertise and guidance have been crucial in overcoming several challenges during this research. I also owe a debt of gratitude to Prof. Dr. Bernhard Küster and Sarah Brajkovic for their support and mentorship during my internship at the Technical University of Munich. Their help and encouragement have enriched this thesis and provided me with invaluable learning experiences.

This thesis was also supported by the Scientific and Technological Research Council of Türkiye (TÜBİTAK) under the 1001 program, with grant number 123O370. I would like to express my gratitude to TÜBİTAK for their support.

I am profoundly grateful to my precious family members, my mother Gül Taşdemir, my father Halil Taşdemir, and my sister Gonca Şahin, and to my best friend, Setenay Çevik, whose endless love, patience, and encouragement have been a cornerstone of my strength and motivation. Their steadfast belief in me and constant support have inspired me to keep going in the most challenging moments.

Lastly, a special thanks to my boyfriend, Kubilay Can, whose unwavering presence has been my anchor throughout this journey. From the very first day in the opium poppy fields, he stood by my side with endless patience, love, and support in the hardest days. For being my constant source of comfort and encouragement, I am forever grateful.

To all women who dared to dream and all those who continue to fight for their place in the world…

ABSTRACT

PROTEOMIC ANALYSIS OF BENZYLISOQUINOLINE ALKALOID (BIA) BIOSYNTHESIS IN DIFFERENT OPIUM POPPY CULTIVARS AND EXAMINATION OF DIFFERENTIALLY EXPRESSED PROTEINS IN RELATION TO BIA CONTENT

The opium poppy (*Papaver somniferum*) is a strategic crop due to its production of benzylisoquinoline alkaloids (BIAs), valuable pharmaceuticals used for pain relief, cough suppression, and as narcotics. Opium poppy is the sole feasible source for commercial BIA production. Türkiye's opium poppy cultivars, bred for high BIA content, require yield improvement to maintain global competitiveness. This study employed a proteomic approach to compare protein profiles from various organs of different cultivars with varying BIA content. Three Turkish cultivars were analyzed: TMO T (thebaine), Ofis 2 (morphine), and Ofis NM (noscapine). Protein extracts from specific tissues were examined using LC-MS/MS, and BIA content in dry capsules was quantified via TLC/HPLC analysis. This enabled investigation of connections between protein expression patterns in different organs and cultivars with alkaloid accumulation. Mature capsules exhibited the highest number of significant differentially expressed proteins (DEPs), with Ofis 2 diverging significantly from TMO T and Ofis NM across all tissues in terms of protein expression. Key enzymes in the BIA pathway showed significant up- and down-regulation in mature capsules and latex-containing stems. These findings provide insights into differential proteome profiles involved in BIA biosynthetic and regulatory pathways. Future research should focus on unannotated protein functions, multi-omics integration, tissue-specific enzyme localization, and functional gene studies to enhance understanding of BIA biosynthesis. This could facilitate the development of high-yield opium poppy cultivars, ensuring sustainable pharmaceutical production.

ÖZET

FARKLI HAŞHAŞ ÇEŞITLERINDE BENZİLİZOKİNOLİN ALKALOİD (BİA) BİYOSENTEZİNİN PROTEOMİK ANALİZİ VE DİFERANSİYEL OLARAK İFADE EDİLEN PROTEİNLERİN BİA İÇERİĞİNE BAĞLI OLARAK İNCELENMESİ

Haşhaş (*Papaver somniferum*), eczacılıkta kullanılan benzilizokinolin alkaloidleri (BIA) üretmesi nedeniyle Türkiye için stratejik öneme sahip bir bitkidir. Yalnızca haşhaş bitkisinden elde edilebilen bu alkaloidler, ağrı kesici, öksürük kesici ve narkotik amaçlı ilaç olarak yaygın şekilde kullanılmaktadır. Türkiye'nin haşhaş çeşitleri, yüksek BIA içeriği hedeflenerek geliştirilmiş olup küresel rekabet için verimlerinin artırılması gerekmektedir. Bu çalışmada, farklı haşhaş çeşitlerinin belirli organlarındaki protein seviyelerinin değişen BIA içeriği ile ilişkili olarak karşılaştırılmasını içeren proteomik bir yaklaşım kullanılmıştır. Çalışmada, belirli alkaloidler açısından öne çıkan üç Türk haşhaş çeşidi kullanılmıştır: tebain (TMO T), morfin (Ofis 2) ve noskapin (Ofis NM). Haşhaş bitkisinin belirli dokularından alınan protein ekstraktları, LC-MS/MS kullanılarak incelenmiş ve ardından kuru kapsüllerdeki BIA miktarı TLC/HPLC analizleriyle ölçülmüştür. Bu şekilde, farklı haşhaş çeşitlerinin ve organlarının protein ekspresyon modelleri ile kapsüllerdeki alkaloid birikimi arasındaki bağlantılar araştırılmış ve BIA metabolizmasının biyosentetik ve düzenleyici yollarına dair bilgi edinilmiştir. İncelenen beş doku arasında, olgun kapsüller en yüksek sayıda anlamlı farklı şekilde ifade edilen proteini gösterirken, Ofis 2 protein ifade profilleri açısından tüm dokularda TMO T ve Ofis NM'den belirgin şekilde ayrışmıştır. BIA yolağındaki kilit enzimler, üç haşhaş çeşidinin kapsülleri ve lateks içeren gövdeleri arasında anlamlı yukarı ve aşağı regülasyon göstermiştir. Gelecekteki araştırmalar, BIA biyosentezini aydınlatmak ve manipüle etmek için karakterize edilmemiş proteinlerin işlevlerini, çoklu omik entegrasyonunu, dokuya özgü enzim lokalizasyonunu ve işlevsel gen çalışmalarını araştırabilir. Bu sayede farmasötik amaçlar için yüksek verimli haşhaş çeşitlerinin geliştirilmesine olanak sağlanabilir.

TABLE OF CONTENTS

LIST OF FIGURES

Figure **Page**

Figure **Page**

LIST OF TABLES

Table **Page**

CHAPTER 1

INTRODUCTION

1.1. Opium Poppy (*Papaver somniferum* L.)

Papaver somniferum (common name: opium poppy) is an annual, diploid (2n = 22), flowering plant in the Papaveraceae. It originates from southeastern Europe and western Asia and bears white, pink, red or purple flowers. The opium poppy has been grown for thousands of years for its pharmaceutical purposes, as food, and for industrial uses. It represents a crossroads of history, medicine, and legal regulation that shaped societies and economies worldwide (Norn et al., 2005).

1.1.1. Industrial and Medicinal Importance of Opium Poppy

Due to its immense economic and medicinal benefits, the opium poppy has become one of the most highly valued plants to be studied scientifically, and that makes it an attractive topic of research. For humans, the two most important parts of *P. somniferum* are the seeds and the seed capsule. Seeds are a source of food for animals, as well as humans, but they also form the source of poppy oil, an aromatic oil rich in both oleic and linoleic fatty acids (Singh et al., 1990). In general, seeds of poppy find application in baking and can be found ready ground or even roasted. Poppy oil is valuable in beauty products and art supplies; the oilcake that remains is also a good fertilizer and feed for animals (Özgen et al., 2017). In 2022, Türkiye exported 23,480 t of poppy seeds, with a total export value of 91 million USD. (FAOSTAT, 2024; http://www.fao.org/faostat/).

The capsules of poppy seeds have medicinal and pharmaceutical value owing to their high alkaloid concentration. Opium is the term used for the milky latex that is produced by the opium poppy, which is the exclusive source of benzylisoquinoline alkaloids (BIAs). BIAs are a diverse group of plant-derived secondary metabolites

characterized by a benzylisoquinoline molecular backbone (Ozber and Facchini, 2022). They help defend against herbivores and pathogens in plant. The latex is produced by laticifers, which are elongated cells found within the plant's vascular tissue (Bird et al., 2003). The latex alkaloids with the most economic significance include morphine, noscapine, thebaine, codeine, and papaverine. Medicinally important drugs often incorporate these BIAs as their main ingredients (Hagel and Facchini, 2013). Morphine is the primary pain-relieving alkaloid in opium which has been used as a painkiller for centuries. Codeine is a narcotic pain reliever that acts on the central nervous system to reduce or relieve pain (Chahl, 1996; Singh et al., 2019). Thebaine has a stimulating impact on the central nervous system and is used by the pharmaceutical industry to produce different opioids (Lee et al., 2013). Noscapine and papaverine do not have any pain-relieving or addictive properties, yet they are still considered to be medically beneficial. According to Heinrich et al. (2021), noscapine is mainly utilized as a cough suppressant, while papaverine is used to improve blood flow and relax smooth muscles.

1.1.2. Legal Cultivation of Opium Poppy in Türkiye

Growing and processing opium poppies must be done under strict control and with government permission because of the narcotic, habit-forming qualities and worldwide illegal trade of its products. In addition, the growing and processing of opium poppy are kept separate to be able to extract alkaloids from the capsule and harvest seeds. Türkiye, a major traditional producer of opium poppy, allows legal cultivation of the plant in thirteen cities under the control of the Turkish Grain Board (TMO) (Windle, 2014).

The United Nations has accepted India, Hungary, Australia, France and Spain as the other major legal producers of opium poppy. BIAs in Türkiye are obtained by grinding dried, un-milked capsules via a capsule straw method as opposed to extraction from raw opium latex (TMO, 2019). Opium poppy varieties are not exchanged between nations as they are a key worldwide crop for the pharmaceutical sector. Therefore, Türkiye has a variety of unique cultivars, several of which have specific BIA profiles.

The BIA yield of Turkish varieties is acceptable, but it falls short compared to the higher yields of cultivars in some competitor countries (Ceylan, 2022; Mansfield, 2001; Williams, 2010; Williams, 2013). Therefore, Türkiye should aim to develop cultivars that

have high levels of BIA accumulation with a particular focus on cultivars with specific compound accumulation profiles (Bulut and Türktaş, 2020).

1.1.3. BIA Biosynthesis, Localization and Opium Poppy Varieties with Differing Alkaloid Content

The BIA biosynthesis pathway in opium poppy begins with the conversion of L-tyrosine to tyramine through the action of tyrosine decarboxylase (TYDC) (Figure 1.1). Tyramine is then hydroxylated by tyramine 4-hydroxylase (T4H), producing dopamine (Facchini et al., 2007). Dopamine reacts with 4-hydroxyphenylacetaldehyde (4-HPAA) under the catalysis of norcoclaurine synthase (NCS), resulting in (S)-norcoclaurine. This molecule is methylated by norcoclaurine 6-O-methyltransferase (6OMT) to form (S)-coclaurine, which is further methylated by coclaurine N-methyltransferase (CNMT) to generate (S)-N-methylcoclaurine (Hagel & Facchini, 2013). (S)-N-methylcoclaurine is then hydroxylated by (S)-N-methylcoclaurine 3'-hydroxylase (NMCH), producing (S)-3'-hydroxy-N-methylcoclaurine. This intermediate is further methylated by 3'-hydroxy-N-methylcoclaurine 4'-O-methyltransferase (4'OMT) to create (S)-reticuline (Huang & Kutchan, 2000). Reticuline undergoes epimerization, converting the (S)-isomer to (R)-reticuline. The enzyme salutaridine synthase (SalSyn) then catalyzes the formation of salutaridine, which is subsequently reduced to salutaridinol by salutaridine reductase (SalR). Salutaridinol is acetylated by salutaridinol 7-O-acetyltransferase (SalAT), leading to the formation of thebaine (Ziegler et al., 2009).

In later steps of the pathway, thebaine is transformed into codeinone by the actions of thebaine 6-O-demethylase (T6ODM) and neopinone isomerase (NIPO) and reduced to codeine by codeinone reductase (COR). The final step involves the demethylation of codeine by codeine O-demethylase (CODM) to produce morphine (Ziegler et al., 2009). In parallel, the enzyme berberine bridge enzyme (BBE) converts (S)-reticuline to (S)-scoulerine. (S)-scoulerine is broken down by cytochrome P450 and O-methyltransferase enzymes to produce tetrahydrocolumbamine, canadine and finally noscapine, respectively (Winzer et al., 2012; Dang and Facchini, 2014).

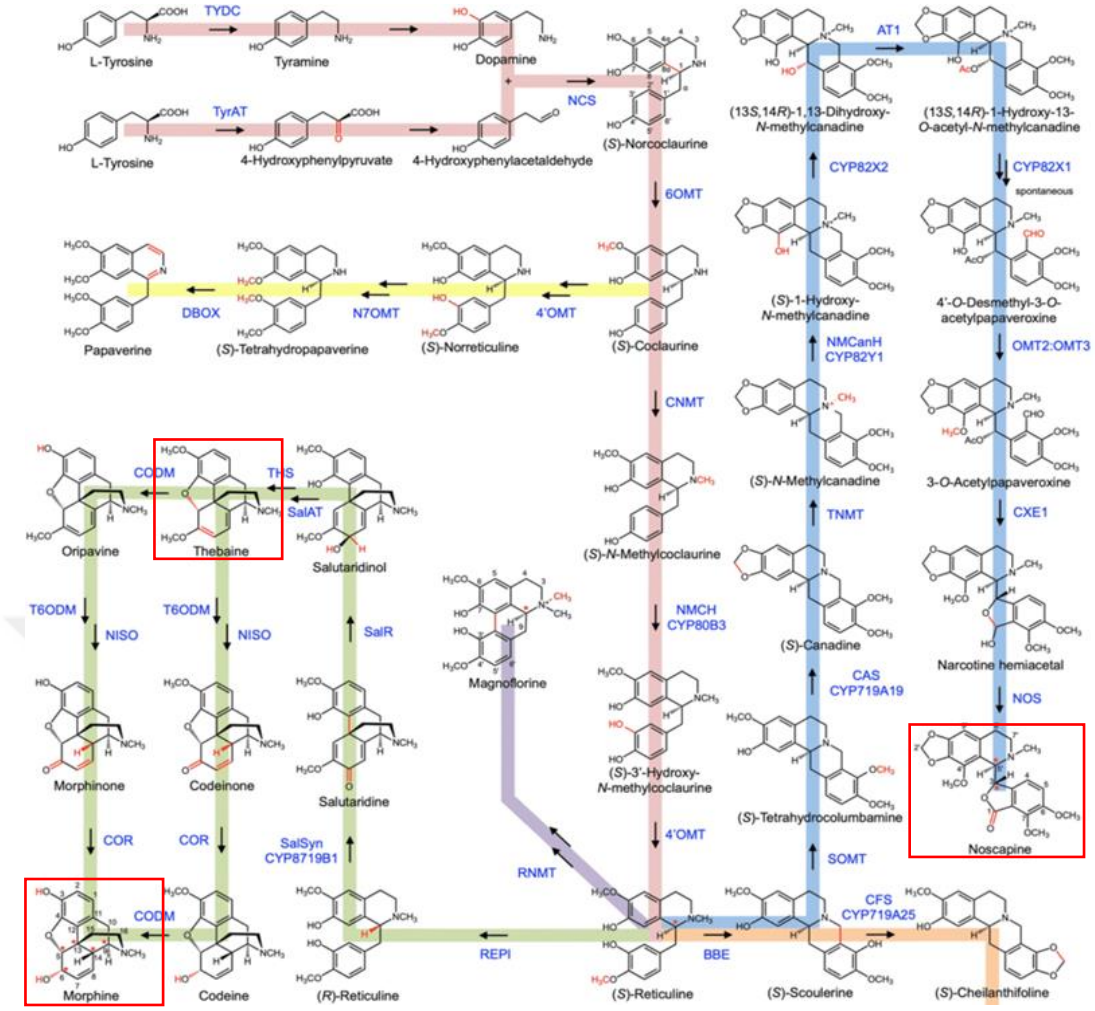

Figure 1.1. Biosynthetic pathways of opium poppy resulting in accumulation of primary BIAs (Singh et al., 2019). BIAs of interest are in red squares. Enzymes are described with the following abbreviations: 3'-hydroxy-N-methylcoclaurine 4'-O-methyltransferase (4'OMT), norcoclaurine 6-O-methyltransferase (6OMT), 1,13-dihydroxy-N-methylcanadine 13-O-acetyltransferase (AT1), berberine bridge enzyme (BBE), canadine synthase (CAS), cheilanthifoline synthase (CFS), coclaurine N-methyltransferase (CNMT), codeine O-demethylase (CODM), codeinone reductase (COR), 3-O-acetylpapaveroxine carboxylesterase (CEX1), 1-hydroxy-13-O-acetyl-N-methylcanadine 8-hydroxylase (CYP82X1), 1-hydroxy-N-methylcanadine 13-O-hydroxylase (CYP82X2), N-methylcanadine 1-hydroxylase (CYP82Y1), dihydrobenzophenanthridine oxidase (DBOX), N-methylstylopine 14-hydroxylase (MSH), norreticuline 7-O-methyltransferase (N7OMT), norcoclaurine synthase (NCS), neopinone isomerase (NISO), N-methylcoclaurine 3'-hydroxylase (NMCH), noscapine synthase (NOS), 4'-O-desmethyl-3-O-acetylpapaveroxine 4'-O-methyltransferase (OMT2:OMT3), protopine 6-hydroxylase (P6H), reticuline epimerase (REPI), reticuline N-methyltransferase (RNMT), salutaridinol 7-O-acetyltransferase (SalAT), salutaridine reductase (SalR), salutaridine synthase (SalSyn), sanguinarine reductase (SanR), scoulerine 9-Omethyltransferase (SOMT), stylopine synthase (SPS), tetrahydroprotoberberine oxidase (STOX), thebaine 6-O-demethylase (T6ODM), thebaine synthase (THS), tetrahydroprotoberberine N-methyltransferase (TNMT), tyrosine decarboxylase (TYDC), tyrosine aminotransferase (TyrAT).

Research on the biosynthetic pathways of morphinan alkaloids in opium poppy unraveled the contributions made by many enzymes in this process. For instance, over-expression of SalAT enzyme induces the accumulation of morphinan alkaloids whereas down-regulation of SalAT leads to accumulation of high salutaridine without affecting the morphinan alkaloid profile in transgenic opium poppy lines (Allen et al., 2008). In a similar manner, over-expression of COR results in a dramatic increase in morphinan alkaloid content while its down-regulation causes an increase in reticuline and some of its methylated derivatives causing a reduction in morphinan (Allen et al., 2004; Larkin et al., 2007). The lack of transcripts of T6ODM in certain varieties of poppy is correlated with high thebaine and oripavine but low codeine and morphine accumulation. Down-regulation of T6ODM also led to increased accumulation of thebaine and oripavine whereas, down-regulation of CODM resulted in increased codeine at the expense of morphine (Hagel and Facchini, 2010). Overall, the above findings emphasize the sensitive balance among the activities of biosynthetic enzymes responsible for BIA profiles in opium poppy.

In parallel with the above work, proteomic analyses carried out using a shotgun methodology elucidated the cell-type-specific localization of morphine biosynthesis in opium poppy (Onoyovwe et al., 2013). In agreement with pre-existing immunolocalization studies, Bird et al. (2003) and Samanani et al. (2006) concluded that enzymes of the morphinan branch upstream of SalR were detected exclusively in sieve elements of phloem. On the contrary, enzymes involved in the pathway from salutaridine to thebaine (namely, SalR and SalAT) were detected in both latex and stem, whereas morphine biosynthetic enzymes (i.e., T6ODM, COR, and CODM) accumulated predominantly in latex, which showed that the conversion of thebaine to morphine occurs in laticifers.

The process by which substances move between sieve elements and latex in morphine biosynthesis is still not fully understood (Onoyovwe et al., 2013). Chen & Facchini (2013) demonstrated that the final step of noscapine biosynthesis also takes place in laticifers in opium poppy. Finally, MS-based proteomics revealed that most of the known enzymes potentially leading to papaverine biosynthesis were not associated with laticifers but sieve elements (Ozber and Facchini, 2022). Another study by Ozber et al. (2022) demonstrated that major latex proteins (MLPs) can alter protein conformation in the presence of specific ligands. Thebaine synthase and neopione isomerase, which are

latex MLP/PR10 proteins, have been found to facilitate key enzymatic reactions in the final stages of morphine biosynthesis, which were previously believed to occur spontaneously. Moreover, introducing these proteins into yeast strains engineered with genes involved in morphine production resulted in a marked improvement in the conversion of salutaridine into morphinan alkaloids.

The amounts of various alkaloids present in opium poppy can vary considerably among different strains due to natural differences (e.g. region, climate, collected organ) as well as breeding efforts (Li et al., 2020b). Poppy varieties used for food usually have low alkaloid levels and also produce very high amounts of seeds, while those grown for medicinal or research purposes have very high alkaloid levels (Skalicky et al., 2014). Yazici and Yilmaz (2021) analyzed the alkaloid levels in capsules of different Turkish opium poppy varieties and found that the morphine content ranged from 0.42 % to 1.66 %, codeine from 0.03 to 0.17 %, thebaine from 0.01 to 0.53 %, noscapine from 0.01 to 0.31 %, and papaverine from 0.00 to 0.10 % in both the parents and hybrids. Molecular studies revealing the association between the phenotypic differences in these Turkish cultivars and their genetic variation are limited (Celik et al., 2016; Guclu et al., 2014; Gurkok et al., 2015; Bulut et al., 2020).

1.2. Multi-omics Analysis of Medicinal Plants

Proteomics is the large-scale functional and structural study of proteins. In general, proteomics studies protein expression, modifications, interactions, and localization in a biological system. It determines the dynamic protein states associated with biological processes and seeks to understand how they change in response to various conditions or stimuli. Methods like MS and bioinformatics are applied to proteomics for protein identification and quantification (Aebersold and Mann, 2003; Aslam et al., 2016).

Proteomics studies have contributed to identifying some target proteins for further investigation of the mechanisms of action of plant-derived medicinal compounds. (Wang et al., 2015). Proteomics can also be valuable in the identification of particular proteins and modifications involved in biosynthesis and regulation of specialized compounds produced by medicinal plants (Martinez-Esteso et al., 2015).

For example, proteomic analysis has been utilized in *Catharanthus roseus* to study the role which MYC transcription factors (TFs) such as CrMYC1 and CrMYC2 play in controlling the synthesis of terpenoid indole alkaloids. These TFs respond to methyl jasmonate signals and regulate the expression of the ORCA genes critical for TIA biosynthesis (Liu et al., 2016). Research has also unraveled the bHLH transcription factors of *Panax ginseng* that regulate the biosynthesis of ginsenosides, bioactive molecules which are presumed to be responsible for the therapeutic effects of these compounds. These proteins impact the expression of genes involved in the ginsenoside biosynthetic pathway, hence influencing the accumulation patterns of these important secondary metabolites (Yang et al., 2022).

The process of analyzing metabolites in cells, tissues, and organisms with an emphasis on their mass and chemical properties is termed metabolomics. This approach helps to map out the biochemical interactions and pathways present in a biological system, offering insights into the underlying metabolic processes (Idle and Gonzalez, 2007).

In plant studies, metabolomics can be used to explore how plants produce various metabolites, how these compounds interact, and how metabolic pathways change in response to environmental conditions, such as light, temperature, or nutrient availability (Hong et al., 2016). By analyzing metabolic profiles, a better understanding of physiological processes and adaptations in plants can be gained, helping to identify key metabolites associated with growth, development, and responses to stress factors. Improved chromatography and mass spectrometry techniques, combined with the development of bioinformatics resources and strategies have made metabolomics very important in research on medicinal plants (Okada et al., 2010; Waris et al., 2022).

This method is now being used in an effective way to screen for the specific bio-active metabolites present in various medicinal plants, and to study the synthesis, regulation, and transport of these metabolites (Quanbeck et al., 2012; Heyman & Dubery, 2016). For instance, the analysis of *Stevia rebaudiana* and *Coptidis rhizome* using the metabolomics platform of GC-MS and HPLC-UV revealed the internal regulation of these plants' metabolic pathways. The resulting evidence confirmed that both glycolysis and the oxidative pentose phosphate pathway OPPEP are crucial factors for plant respiration in both systems. For *C. rhizome*, instead of the main biosynthetic route

involving asparagine depending on tocopheryl and β-carotene, an alternative pathway incorporating proline, phenylalanine, catechollactate, and 2-mono-isobutyrin was found to provide biosynthesis of the major bioactive alkaloids. The other important outcome of this study was the hypothesis that different fatty acids are responsible for enhancing secondary metabolite production in these medicinal herbs (Gu et al., 2018).

Integration of different omics techniques can shed light on various aspects of plant secondary metabolism, which may also provide a cost-effective strategy for developing plant-based pharmaceuticals to benefit humanity. One of these combined omics studies involved the identification of stress-responsive proteins in *Catharanthus roseus* by proteomic analysis, while metabolomic analysis quantified the levels of indole alkaloids under combined stress (Zhu et al., 2015). The major findings showed that binary stress, such as drought and salinity, significantly enhanced the biosynthesis of valuable indole alkaloids, with several proteins and metabolic pathways being up-regulated in response to the stress. Similarly, a study that integrated genetics with transcriptomics (Winzer et al., 2012) described the complex gene cluster in the opium poppy genome which is responsible for noscapine production.

1.2.1. Mass Spectrometry

Liquid chromatography-tandem mass spectrometry, commonly known as LC-MS/MS, is the most frequently used analytical instrument in proteomics studies. The general procedure usually starts with cleavage of proteins using the enzyme trypsin. This results in peptides that can be separated via LC before entering MS (Snyder et al., 2011; Seger and Salzmann, 2020). In the LC process, a complex sample is passed through a column containing a stationary phase. The proteins bind differently to the stationary phase according to their physicochemical properties, and are separated according to their size, charge and hydrophobicity (Snyder et al., 2011). The eluted proteins then can be analyzed by MS/MS. The first step of MS analysis is MS1, in which the peptides are ionized, and their mass-to-charge (m/z) ratio is determined. It is this critical information that allows peptide quantification. MS2, on the other hand, focuses on the scanning of selected precursor ions for their fragmentation into smaller pieces by methods such as collision-induced dissociation (CID) or higher energy C-trap dissociation (HCD) (Cottrell, 2011). In MS2, the fragments from the cleaved peptides create a daughter ion mass spectrum

that assists in the elucidation of the amino acid composition for each peptide. Thus, the amino acid composition identified by MS2 spectra along with their quantitative measurements via MS1 reveal the protein content present in the sample and the relative abundance of individual proteins (Aebersold and Mann, 2003).

LC-MS/MS is able to identify proteins which have varying expression levels across different samples. This approach requires the processing of raw LC-MS/MS data from multiple samples to assess and quantify peptides based on their differential expression patterns between two or more sample conditions (Aebersold and Mann, 2003). This method includes sequence alignment of MS/MS spectra and the assessment of their abundance for relative quantification. This can be done with several comparative quantification methods, such as label-free or metabolic and isotope labeling techniques using methods such as Tandem Mass Tag (TMT) (Zecha et al., 2019). Subsequently, statistical analyses are carried out to reveal which proteins are differentially expressed based on their up- or down-regulation under certain experimental conditions. Deciding on the proper techniques for protein sample preparation and peptide labeling prior to MS is crucial for the success of MS analysis, as they ensure efficient protein digestion, peptide purification, and quantitative accuracy, thereby improving the reliability of the analytical results (Altelaar et al., 2013; Hughes et al., 2019)

1.2.1.1. Single-pot, Solid-phase-enhanced Sample Preparation (SP3)

SP3 (Single-pot, Solid-phase-enhanced Sample Preparation) is a novel, highly efficient method of protein sample preparation in MS. The presence of paramagnetic beads coated with hydrophilic surfaces that allow for the binding of proteins and clearance of MS-incompatible substances in one step drastically improves the preparation process. This method removes the detergents and salts that may interfere in MS, from protein samples while capturing the proteins. SP3 technology also involves simultaneous digestion of the protein by trypsin. Hence, this allows for the complete and uniform cleavage of proteins into peptides, resulting in maximized detection and quantification by MS (Hughes et al., 2019).

Plant proteins naturally occur at low concentrations with high content of secondary metabolites which can sometimes interfere with proteomic analysis. SP3

technology allows successful isolation of proteins from plant tissues with significant repression of the contaminants (Brajkovic et al., 2023). This is an ideal way of increasing the recovery of the proteins with less sample loss for a more efficient and reproducible protein extraction than can be achieved with traditional methods. This approach provides a reliable solution for high-quality proteomic analysis especially when working with relatively low protein abundances (Mikulášek et al., 2021).

1.2.1.2. TMT Labeling

Tandem Mass Tag (TMT) labeling is a quantitative proteomic technique that has found a broad base of application in MS for the purposes of accomplishing simultaneous identification and relative quantification of proteins between many samples. This is enabled through isobaric chemical tags, which label peptides that originate from protein digests, making multiplexed analysis possible in one MS experiment (Zecha et al., 2019).

Each TMT reagent is made up of a reporter group, a balance group (i.e., mass normalizer), and an amino-reactive group, which targets certain peptide residues. The reporter groups have unique reporter masses that differ by a distinct mass-to-charge (m/z) ratio. Thus, various tags in the TMT system include a mass range from 126 to 135 corresponding to heavy carbon atoms in the reporter group (TMT-126, TMT-127 etc.). These different mass-to-charge ratios, upon fragmentation during MS analysis, enable comparative analysis of protein expression levels of different sample conditions with high precision and sensitivity (Altelaar et al., 2013; Li et al., 2020a).

1.2.2. Omics Studies Focused on Opium Poppy

While the power of omics has been successfully demonstrated in many species, in-depth omics studies have recently begun to tackle the complex mechanisms of plant protein expression, including that of metabolic pathways leading to the production of medicinally significant alkaloids like BIAs. Decker et al. (2000) utilized two-dimensional gel electrophoresis and microsequencing to analyze the proteins in the latex of *P. somniferum*. They analyzed a total of 75 protein spots and identified the functions of 69 proteins by comparing them to known proteins. These experiments resulted in the first inventory of soluble latex proteins for opium poppy. A comprehensive database of gene

expression and protein levels in elicitor-treated (i.e., stimulated to create and store components of alkaloid metabolism) opium poppy cell cultures using pyrosequencing followed by MS analysis was described in another study (Desgagne-Penix et al. 2010). The researchers found 1004 proteins mediating linkages between transcripts, enzymes and pathway components in the alkaloid metabolic network. Previously undescribed enzymes that might be involved in sanguinarine biosynthesis were also discovered. While work using cell cultures is valuable, studying the connections between BIA profile and the proteome in whole plant tissues is crucial, as these relationships are more intricate in comparison to cell cultures. Moreover, extraction from the plant remains the most successful means of generating significant amounts of BIAs for commercial purposes (Ozber and Facchini, 2022). The same research team performed another LC-MS/MS study on the overall metabolome and transcriptome of eight different varieties of opium poppy (Desgagne-Penix et al. 2012). The eight cultivars were selected to represent a wide genetic diversity and contain a range of alkaloid content and composition. The results revealed significant differences among the cultivars in terms of their transcript and metabolite profiles, highlighting distinct pathways and regulatory mechanisms that influence alkaloid biosynthesis in European cultivars.

In other work, Onoyovwe et al. (2013) used whole stem and latex from cv. Roxanne for shotgun proteomics to examine total protein extracts but did not compare the results with lines having different BIA profiles. Pathak et al. (2013) investigated papaverine production in opium poppy by transcriptomic analysis of a high papaverine opium poppy line in comparison with a wild-type counterpart and revealed some unknown steps in the biosynthesis pathway. In addition, analysis of the transcriptome datasets of 10 opium poppy varieties was performed to search for transcription factors involved in the biosynthetic pathway of BIAs (Agarwal et al., 2015). Many of the identified transcription factors were found to be from the WRKY, MYB, and bHLH families and were important for the regulation of BIA production in *P. somniferum*. Several of those transcription factors were also observed to have differential expression only in certain tissues, implying an important tissue-specific regulation of alkaloid production.

In 2019, Zhao et al. performed the first comprehensive analysis of the complete transcriptome (55,114 high-quality transcripts) of *P. somniferum* by examining Illumina transcriptomes from 33 poppy samples representing various tissues, growth stages, and varieties. These data establish a foundation for transcriptomic analysis of the opium

poppy, potentially aiding in the identification of splice variants and non-coding RNAs that play roles in regulating the biosynthesis of BIAs.

Another study examined the grouping of genes in the BIA pathway of opium poppy in order to explore the relationships between gene expression, copy number variation, and alkaloid production. The researchers discovered that the absence of a T6ODM gene group resulted in higher levels of thebaine and lower levels of morphine production. Additionally, the deletion of 11 genes in the noscapine pathway caused a deficiency in noscapine production (Li et al., 2020b).

An investigation of how opium poppy responds to drought stress at its initial stage of germination was conducted by transcriptome and proteome analysis. This study provided information on critical genes and proteins that significantly change their expression according to environmental stimuli and how they are associated with drought stress (Kundrátová et al., 2021).

Most recently, a study by Aykanat and Türktaş (2024) examined the proteomic profiles of three registered opium poppy cultivars in stem and capsule, resulting in 1202 differentially expressed proteins. Enrichment analysis for the DEP indicated that the morphine-rich cultivar showed photosynthesis pathway activity among the top significant enrichment pathways, while noscapine-rich cultivar activity was related to the translation pathway. These findings suggest that while photosynthesis plays a critical role in BIA biosynthesis, different processes are involved in morphine and noscapine biosynthesis, indicating organ and cultivar-dependent variation in protein expression in mature poppy.

1.3. Aim of the Study

The key alkaloids found in opium, such as morphine, codeine, thebaine, noscapine, and papaverine, are exclusive to the opium poppy plant, making it a plant of significant therapeutic and economic importance among the many medicinal plants known today (Carlin et al., 2020). Because of its unique metabolic profile, *P. somniferum* is the only model system for unraveling BIA metabolism (Lee et al., 2013). Examination of the biological and molecular processes involved in the BIA biosynthetic pathway is crucial for scientific advancement. Progress in transcriptomics, proteomics, as well as metabolomics studies has made it possible to identify metabolic pathways and elucidate their connection to gene expression profiles in a number of plant species. Although an

organism's protein content vastly exceeds its genome or transcriptome content, proteomic studies in this field are considerably less common compared to the numerous transcriptome studies that have been done. The literature offers limited information on the protein profiles of opium poppy cultivars, and studies focusing on the connection between MS-based proteomics and BIA profiles of tissue samples from various opium poppy varieties are not adequate. Consequently, in spite of the extensive research on identifying the players in the BIA pathway in opium poppy, there is still a lack of understanding regarding the biochemical and genetic control of BIA metabolism, accumulation, and transport.

This work aimed to evaluate the proteome profiles of the BIA pathway in the tissues (capsule, stem, and roots) of opium poppy utilizing mass spectrometry technologies, focusing on three Turkish *P. somniferum* cultivars with varying alkaloid content profiles. These lines are the morphine-accumulator Ofis 2, the noscapine-accumulator Ofis NM, and the thebaine-accumulator TMO T (Figure 1.2).

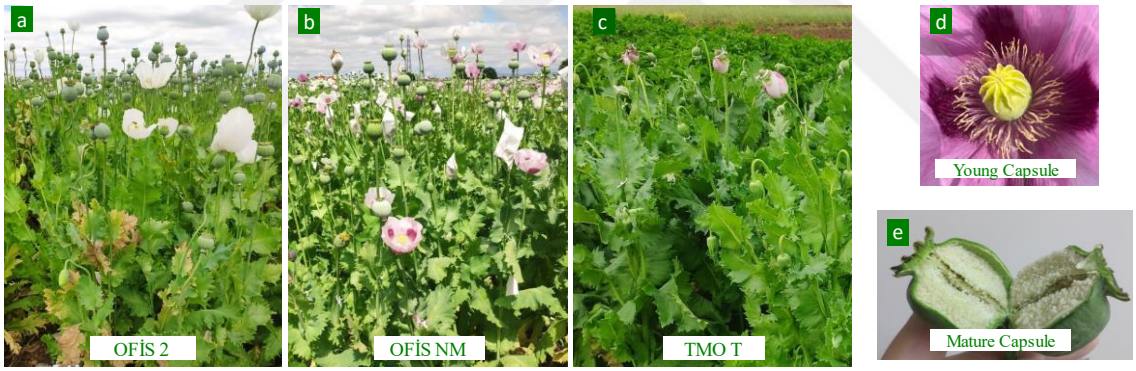

Figure 1.2. Turkish opium poppy lines with differential alkaloid content profiles collected from opuim poppy fields of TMO (Bolvadin, Afyon). (a) morphine-accumulator Ofis 2, (b) noscapine-accumulator Ofis NM, (c) thebaine-accumulator TMO T. Two developmental stages of the opium poppy capsule: (d) young capsule and (e) mature capsule.

An overall end-to-end workflow of the study is presented in Figure 1.3. The method involved protein extraction from opium poppy tissue samples, followed by peptide digestion, TMT labeling, and MS analysis together with BIA quantification of dry poppy capsules via TLC/HPLC. This was complemented by protein identification and quantification which was used for differential expression analysis. By comparison of the protein and BIA profiles of these lines and tissues, the links between alkaloid content and protein expression were investigated for differentially expressed biosynthetic and

regulatory pathway components in opium poppy. This research can provide knowledge for more targeted breeding of opium poppy and manipulation of BIA production.

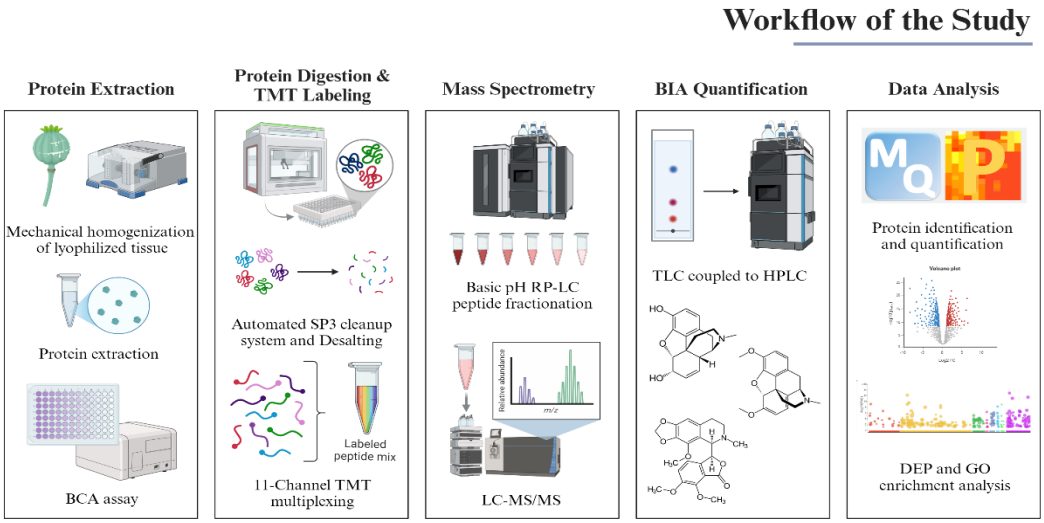

Figure 1.3. End-to-end workflow of the study.

CHAPTER 2

MATERIALS AND METHODS

2.1. Biological Materials

The opium poppy cultivars used in this research were the morphine-rich Ofis 2, the noscapine-rich Ofis NM, and the thebaine-rich TMO T. All materials were supplied by the Turkish Grain Board (TMO). The plants were cultivated for 120 days in standard soil at TMO under normal agronomic conditions until the capsules reached maturity. The plants were grown in a field making use of a block layout, with a distance of 10 cm between each plant and 45 cm between rows. Each cultivar had approximately 25 plants in each block. To prevent any potential influences from the edges, three replicates from each cultivar were chosen for collection within each block.

2.2. Collection of Plant Tissues

The mature organs of opium poppy plants were collected from three replicates of plants 30 days after flowering. Fully developed roots were gathered from the plants and cleaned. Two stem samples were processed in two different ways. Primary stems were gathered in 5 cm lengths from young capsules and served as the initial sample type. Furthermore, the main stems were cut into one mm segments and soaked in water for 1 h to remove the latex, as described by Li et al. (2020). Thus, the second sample category consisted of these soaked stems that did not contain latex. The collection of immature capsules occurred while the plant was in bloom. The fully developed capsules were collected 30 days after flowering. All organs were used for the proteome analysis. In addition, mature dried capsules were collected towards the end of the growing period (approximately 60 d after flowering) to determine the BIA metabolome profiles of each cultivar. The samples were freeze-dried before further analysis.

2.3. Protein Extraction from Plant Tissue

Opium poppy tissues were ground to a powder using a tissue lyser (TissueLyser II, QIAGEN). The powdered tissue was then stored at -20°C. Protein extraction was performed via TCA/acetone protein precipitation followed by phenol extraction as described by Brajkovic et al. (2023). For protein precipitation, pre-chilled (-20°C) precipitation solution (10% TCA, 90% acetone) was added to the powdered tissue at a ratio of at least 3x volume precipitation solution (approximately 1.5 mL). Proteins were then precipitated overnight at -20°C. The samples were centrifuged at 15,000 g for five min at 4°C to separate the protein pellet from the supernatant following precipitation. The supernatant was discarded after centrifugation to separate the protein pellet. The pellet was rinsed with 1 mL pre-chilled acetone. Excess TCA was eliminated through centrifugation at 15,000 g for five min at 4°C. The washing steps were repeated at least twice to remove the remaining TCA. After the last wash, the remaining acetone was taken out and the protein pellet was allowed to dry at room temperature (RT) under the fume hood. The dried pellet was stored at -80°.

Total proteins were resolubilized using SDS in the following manner. The dry powdered tissue was first resuspended in 750 µL of SDS extraction buffer which included 4% SDS, 0.15 M Tris-HCl (pH 8.8), 1 mM EDTA, and 2 mM PMSF. The samples were then incubated at 60°C for 1 h at 450 rpm and vortexed periodically until the pellet was completely resolubilized. Immediately after the incubation, the samples were centrifuged at 15,000 g for 10 min at RT. The resulting supernatant containing the extracted proteins was transferred to a new 2 mL Eppendorf tube. Any residual pellet left over from the previous centrifugation step was extracted again. This was achieved by adding 0.25 mL SDS extraction buffer to the pellet and vortexing the mixture well. The tubes were centrifuged once again at 15,000 g for 10 min at RT. The supernatant from this additional extraction step was transferred to the same Eppendorf tube to consolidate the protein extract before the phenol extraction step.

Protein extraction was performed via the phenol method. The protein extracts were mixed with an equivalent volume of TE-buffered phenol (approximately 750 µL). The two ingredients were mixed by vortexing for 1-2 min to form a milky white emulsion. The mixture was centrifuged for 5 min at 15,000 g at RT. The samples were handled carefully to avoid disruption of the separated phases. The yellow (lower) phenol layer in the mixture was separated and was transferred into new Eppendorf tubes. Each tube

received 900 µL of 0.1 M ammonium acetate in methanol, which was vortexed for 30 seconds. Following this, the samples were left at 20°C overnight to precipitate the proteins extracted with phenol.

For further precipitation of phenol-extracted proteins, the samples were centrifuged at 15,000 g for 10 min at 4°C. The protein pellets were subsequently rinsed with 1 mL of 0.1 M ammonium acetate in methanol, accompanied by 10 s of vortexing. The samples underwent centrifugation at 15,000 g for 5 min at 4°C, after which the supernatant was discarded. The pellets were subsequently rinsed with 1 mL of 80% acetone and vortexed for 10 s. They were centrifuged a second time at 15,000 g for 5 min at 4°C, discarding the supernatant. This washing process was repeated twice to remove any remaining contaminants. The supernatant was discarded after the final centrifugation, and protein pellets were air-dried at RT for 1 h to complete the purification.

2.4. Protein Resolubilization and BCA Assay

The dry protein pellet was resuspended in 250 µL of lysis buffer (40 mM Tris-HCl pH 7.6, 4% SDS). The samples were subjected to sonication using a Diagenode Bioruptor with a cycle of 30 s on/off for a total of 25 cycles (300 s duration) to shear any remaining DNA and heated for 10 min at 95°C. Following this, 100% TFA (trifluoroacetic acid) was added to achieve a final concentration of 1%, and the mixture was incubated for 1 min. By lowering the pH, TFA strong acid helps in breaking down protein aggregates and promoting the solubilization of proteins in the solution. NMM (N-methylmorpholine) was then added to reach a final concentration of 2%. NMM is a weak base that helps to bring the pH back to a near-neutral range, ensuring that the proteins remain in a solubilized and stabilized state without being denatured by excessive acidity. The samples were subsequently centrifuged at 21,100 g for 1 h at 4°C to exclude any insoluble component. The supernatant was moved to a fresh Eppendorf tube, and the protein concentration was quantified utilizing the Bicinchoninic Acid Assay (BCA) method (Walker, 2009). The lysate was stored at -20°C.

In BCA method, bovine serum albumin (BSA) standards were prepared to achieve final concentrations ranging from 25 µg/mL to 2000 µg/mL. The samples were prepared by diluting protein lysates with ddH_2O at a ratio of 1:10. Reagent A and Reagent B (Pierce BCA Protein Assay Kit) were combined in a 50:1 ratio for BCA working reagent. The

BSA standards and diluted samples (10 µL each) were introduced to a 96-well plate, and 200 µL of the BCA working reagent was added to each well. The plate was incubated at 37°C for 30 min, and the absorbance was measured at 562 nm using a spectrophotometer following the incubation. The protein concentrations of the lysates were determined through comparison of their absorbance values to the standard curve constructed from the BSA standards mentioned above.

2.5. Tryptic Digestion via SP3 and Desalting

A total of 200 µg of protein lysate from each opium poppy sample was processed utilizing a Bravo Agilent pipetting system including Sera-Mag Carboxylate-Modified Magnetic Beads as a protein aggregation system according to Mikulášek et al. (2021). Firstly, SP3 magnetic beads were mixed in 1:1 ratio (120 µL of Sera-Mag A + 120 µL Sera-Mag B with 50 mg/mL concentration) by vortex. Then 4x (960 µL) distilled water was added to the beads and mixed. The tube with the beads was placed on the magnet and the beads were allowed to settle for 2 min. The supernatant was discarded, and the beads were rinsed with 5x (1200 µL) distilled water. The beads were stored in 0.5x (120 µL) distilled water at 4°C.

The volume of lysate required for 200 µg protein was calculated according to the protein concentrations from the BSA assay. The lysates were combined with 10 µL pre-washed magnetic beads in a 1:5 ratio of protein to beads. Protein precipitation was induced using ethanol at a final concentration of 70%. The beads, containing the aggregated proteins, were separated from the supernatant containing non-protein compounds by magnetic capture. The beads were washed three times with 80% ethanol (1 mL per well), followed by a final wash with 100% acetonitrile (500 µL per vial) to eliminate any remaining ethanol. For reduction and alkylation of the proteins, 100 µL of reduction and alkylation buffer including 200 mM HEPPS (pH 8.5), 55 mM CAA, 10 mM TCEP, and 2 mM $CaCl_2$ was mixed with the samples at 37°C for 1 h at 1200 rpm. An overnight enzymatic digestion was performed using 5 µg of trypsin at 37°C at 800 rpm and, the resulting tryptic digest was acidified with 2% formic acid (150 µL per well).

The acidified digest was subjected to desalting utilizing HLB desalting plates, containing 10 mg of N-vinylpyrrolidone-divinylbenzene porous particles (30 µm). Peptide elution was performed with 200 µL of a solvent comprised of 70% acetonitrile

and 0.1% formic acid via spinning at 200 rpm for 1 min and centrifugation at 1000 rpm for 1 min. Then, 4 µL aliquots were taken from each sample, and peptide concentration was determined with BSA assay as described above (Walker, 2009). The eluates were completely dried using a speed-vac for about 3 h and stored at -80°C until TMT labeling.

2.6. 11-Channel TMT Multiplexing

TMT labeling of the peptide samples was done according to the manufacturer's protocol with modification. The batch placement of opium poppy samples in 11-channel TMT multiplexing (Table 2.1) was organized to minimize possible bias, variability, and batch effects. Stock TMT solution was prepared by addition of 16 µL of dry ACN to 0.5 mg of TMT reagent. Vortexing was applied for 30-60 s followed by centrifugation at 1000 rpm for 1 min. Labeling of the protein digests was performed by diluting 200 µg of protein digest in 200 µl of solvent A (200 mM HEPPS buffer). Then, 5 µl of each TMT stock solution (TMT11 Label Reagents, Thermo Scientific) was added to each peptide sample and mixed well with a pipette. The reaction mixture was incubated at 20°C with shaking at 400 rpm for 1 h in a Thermomixer to complete the labeling reaction. In order to stop the reaction, 2 µL of solvent B (5% hydroxylamine) was added to each sample with further incubation at 20°C and 400 rpm for 15 min. The resulting samples were then centrifuged to spin down the peptides.

All of the differential TMT-labeled samples (i.e., three cultivars of the same tissue type with three biological replicates + two reference samples) were combined into one reaction vessel (i.e., five batch/vessel for five tissues in total), and acidification was done through the addition of 20 µL of solvent D (10% formic acid). Then, 20 µL of solvent C (10% ACN and 10% formic acid) was added to the reaction wells, and the samples were incubated at 20°C for 5 min with shaking on the Thermomixer at 400 rpm. Labeled samples were pooled together and dried in a Speedvac. The dried sample was then stored at -80°C for further analysis.

Table 2.1. Distribution of opium poppy samples across five batches utilizing TMT labeling prior to MS. R1-R3 represents the biological replicates, whereas two reference samples (REF) consist of a pooled mixture of equal amount of peptide from all the individual samples.

	Tissue	Channel 1	Channel 2	Channel 3	Channel 4	Channel 5	Channel 6	Channel 7	Channel 8	Channel 9	Channel 10	Channel 11
TMT Batch 1	Root	REF	Ofis2_R1	Ofis2_R2	Ofis2_R3	TMOT_R1	TMOT_R2	TMOT_R3	OfisNM_R1	OfisNM_R2	OfisNM_R3	REF
TMT Batch 2	Stem w/o Latex	REF	Ofis2_R1	Ofis2_R2	Ofis2_R3	TMOT_R1	TMOT_R2	TMOT_R3	REF	OfisNM_R1	OfisNM_R2	OfisNM_R3
TMT Batch 3	Stem w Latex	REF	Ofis2_R1	Ofis2_R2	Ofis2_R3	REF	TMOT_R1	TMOT_R2	TMOT_R3	OfisNM_R1	OfisNM_R2	OfisNM_R3
TMT Batch 4	Mature Capsule	REF	REF	Ofis2_R1	Ofis2_R2	Ofis2_R3	TMOT_R1	TMOT_R2	TMOT_R3	OfisNM_R1	OfisNM_R2	OfisNM_R3
TMT Batch 5	Young Capsule	REF	Ofis2_R1	Ofis2_R2	Ofis2_R3	TMOT_R1	REF	TMOT_R2	TMOT_R3	OfisNM_R1	OfisNM_R2	OfisNM_R3

2.7. Basic Reverse Phase Peptide Fractionation

TMT-labeled peptides (100 µg in total) were divided into six fractions utilizing basic reversed-phase liquid chromatography (bRP-LC). Peptides were dissolved in 100 µL of solvent A (25 mM ammonium formate in ddH_2O, pH 10). The samples were vortexed and centrifuged for total resolubilization before applying on the columns.

bRP fractionation was done on an AssayMap pipetting system. The platform was primed using sequential solvent injections: isopropanol, acetonitrile (ACN), solvent B containing 25 mM ammonium formate in 50% ACN at a flow rate of 50 µL/min. Before sample loading, the columns (XBridge BEH130 C18, 130 Å, 3.5 µm, 4.6 mm x 250 mm) were washed with bRP solvent A for equilibration. Samples were loaded at a flow rate of 5 µL/min and the flow-through was collected. After the loading step, the columns were washed with 50 µL of bRP solvent A at a flow rate of 5 µL/min, and the resulting wash fraction was combined with the flow through.

A gradient elution was performed with increasing percentage of ACN in solvent B. The following concentrations were used for six fractions: 5%, 7.5%, 10%, 12.5%, 15% and 17.5% ACN. The flow rate for elution was set at 5 µL/min for each fraction. For elution wash, 80% isopropanol was used to remove any traces of bound particles from the columns at a flow rate of 50 µL/min. The obtained fractions were then immediately subjected to formic acid to a final concentration of 0.1%. A pooling strategy was adopted to reduce the number of fractions. For the full proteome, 3 µg of each fraction (~70 µl) was mixed into 48 fractions in a new MS plate.

2.8. Liquid Chromatography - Mass Spectrometry (LC-MS/MS)

This study utilized a Thermo Scientific Orbitrap Eclipse Tribrid mass spectrometer, coupled with a Vanquish Neo liquid chromatography system, to analyze peptides labeled with TMT for full proteome analysis based on an optimized protocol (Brajkovic et al., 2023). The peptides were injected onto an Acclaim PepMap 100 C18 column (2 µm particle size, 1 mm internal diameter, 150 mm length), which facilitated their separation.

Peptide separation occurred over a 25-min gradient at a flow rate of 50 µL/min, beginning with 4% solvent B and increasing to 32% B. To ensure thorough rinsing and re-equilibration of the column, the system was washed with 90% solvent B and then equilibrated at 1% solvent B. The mobile phases used included solvent A, consisting of 0.1% formic acid (FA) and 3% dimethyl sulfoxide (DMSO) in water, and solvent B, comprising 0.1% FA and 3% DMSO in acetonitrile.

The MS system was operated in a fast, data-dependent MS3 mode. Ionization was achieved using a spray voltage of 3.5 kV and vaporizer temperature of 125°C, with aid from sheath gas (32 units) and auxiliary gas (5 units). Full-scan MS1 data were collected every 1.2 s over a mass-to-charge range of 360 to 1600 m/z, with a resolution of 60,000 in profile mode on the Orbitrap. The automatic gain control (AGC) target was set to 4e5 with a maxIT of 50 ms for MS1. Precursor ions to undergo MS/MS scans were selected based on carrying a charge state between 2 and 6, a peptide-like isotope pattern as determined by MIPS, and an intensity > 1e4. A quadrupole isolation window of 0.6 Th was used for MS2 scans. The TMT-labeled peptides were fragmented by higher-energy collision dissociation (HCD) with a normalized collision energy (NCE) of 32%. MS2 spectra were acquired in rapid scan mode in the ion trap, using an AGC target of 1.2e4 and a maxIT of 40 ms. Once fragmented, precursor ions were excluded from further scans for 50 s across all charge states.

Sequential MS3 scan was performed to detect TMT reporter ions after the preceding MS/MS scan. An MS3 quadrupole isolation window of 1.2 was used to isolate a new set of precursor ions. A procedure similar to the MS2 scan was applied on the isolated precursors for their HCD fragmentation. In parallel within the ion trap, synchronous precursor selection was used to select the eight most intense fragment ions from the MS2 scans for isolation. Fragment ions within a mass range of 400 to 2000 Th

and outside the precursor exclusion window (-50 Th to +5 Th) were selected. Further HCD of the selected top 10 fragment ions was performed using an NCE of 55%. At a resolution of 50,000, an MS3 spectrum was acquired at a mass range of 100 to 1000 Th in centroid mode in the Orbitrap. The MS3 AGC target was set to 1e5 charges, with a maxIT of 86 ms.

2.9. Thin Layer Chromatography (TLC) and High-Pressure Liquid Chromatography (HPLC)

The BIA analysis of opium poppy dry capsules was conducted following TMO's standard proprietary protocol, which is briefly outlined below and was optimized for tissue samples. All collected tissues were dried at 60 °C for 48 h and subsequently ground into a powder. Four biological replicates were used for each tissue-cultivar combination. Preliminary analysis of the samples was performed using thin layer chromatography (TLC). An aliquot of the powdered sample was ground in 70% ethanol, centrifuged, and the supernatant was transferred to a flask. The flask was rinsed with ethanol, then heated and stirred at 50-60 °C in a water bath for 30 min. After cooling, the sample was filtered and diluted in ethanol.

Aliquots of each sample were applied to a TLC silica gel plate (5-40 µm) as a 10 mm band. The mobile phase consisted of concentrated ammonia, 96% ethanol, acetone, and toluene (2:6:40:40 V/V/V/V), and samples were run for 15 cm. The plates were dried at 100-105 °C for 15 min, and spots were detected using potassium iodobismuthate solution followed by sulfuric acid (4 g/L). A reference solution containing standard amounts of pure BIAs (morphine hydrochloride, papaverine hydrochloride, codeine phosphate, noscapine hydrochloride in 70% ethanol) was run alongside the test samples. Based on TLC results, the tissue samples were subjected to HPLC analysis for the relevant compounds.

High performance liquid chromatography (HPLC) was performed according to TMO's proprietary protocol, which is briefly described and was optimized for tissue samples. At least four biological replicates were used for each tissue-cultivar combination. Each sample was ground in 50% ethanol and sonicated for 1 h. The aliquot of the supernatant was mixed with ammonium chloride buffer solution (pH 9.5) and

diluted with distilled water. This solution was applied to a chromatography column containing kieselguhr and eluted with iso-propanol and methylene chloride. The eluent was evaporated in a vacuum evaporator at 40 °C and then resuspended in mobile phase (sodium heptanesulfonate monohydrate in water, phosphoric acid, and acetonitrile). The sample and reference solutions were then injected into an HPLC analyzer (Shimadzu LC20-AT) fitted with a precolumn and column (0.25 m length, 4.0 mm diameter) containing octylsilyl silica gel (5 µm) stationary phase. The mobile phase had a flow rate of 1.5 mL/min with spectrophotometric detection at 280 nm. The run time was determined according to the known retention times of the expected BIAs. Reference solutions consisted of appropriate amounts of each BIA dissolved in the mobile phase. The percentage of each BIA in each sample was calculated according to TMO's established methodology.

2.10. Data Analysis

MaxQuant (v2.6.5.0) and its integrated search engine, Andromeda, were utilized for identifying and quantifying peptides and proteins. MS/MS spectra were matched against the UniProt *P. somniferum* sequence database. Quantification relied on the intensity of reporter ions generated during fragmentation, corresponding to each label in the TMT11 set, allowing for direct comparison of protein levels across the samples.

Unless otherwise specified, MaxQuant's default settings were applied. For MaxQuant parameters, proteolytic enzyme was determined as trypsin/P permitting maximum two failed cleavages. N-terminal acetylation and methionine oxidation were regarded as variable modifications, whereas carbamidomethylation of cysteine was implemented as a fixed modification. The target-decoy method with reversed sequences was employed to ascertain the false discovery rate (FDR) for peptide spectrum matches (PSMs) and proteins. MaxQuant research was conducted with an FDR threshold of 1% at the PSM level.

Further processing and analysis of the MaxQuant output were carried out in Perseus (v1.6.14). Reverse hits, contaminants and proteins only identified by site were filtered out. The protein intensities were logarithmically transformed (log2) to normalize the data. Missing value imputation was performed by replacing the missing values from

normal distribution to simulate low-abundance proteins. Proteins were then filtered based on valid values by setting the minimum value to 2 in at least one group (i.e., a protein was only retained if it had non-missing values in two replicates of one cultivar for a single tissue).

DEP analysis was done using Amica Proteomics (v3.0.1) tool (https://bioapps.maxperutzlabs.ac.at/app/amica) in order to compare protein abundance between the opium poppy samples, taking into consideration significant differences at FDR ≤ 0.05 and FC ≥ 1.5. Principal component analysis (PCA), volcano plots, and heatmaps were constructed to show significant changes in expression for proteins with the most drastic fold changes that were statistically significant. Replicates that consistently deviated from the other replicates of the same tissue due to sample preparation errors (e.g., low protein/peptide amount and quality) were excluded from the data.

DEPs identified from the pairwise comparisons between opium poppy cultivars (Ofis NM, Ofis 2, and TMO T) were subjected to Gene Ontology (GO) and Kyoto Encyclopedia of Genes and Genomes (KEGG) pathway enrichment analyses. GO enrichment analysis was performed to categorize DEPs based on their associated biological processes, molecular functions, and cellular components, while KEGG analysis identified metabolic and signaling pathways associated with the DEPs. For GO enrichment, g-Profiler tool (https://biit.cs.ut.ee/gprofiler) was utilized, using a significance threshold of adjusted p-value ≤ 0.05. The p-value was adjusted with the Benjamini-Hochberg procedure for multiple comparison correction. KEGG pathway enrichment was conducted using the DAVID (Database for Annotation, Visualization & Integrated Discovery) functional annotation tool (https://davidbioinformatics.nih.gov), with FDR ≤ 0.05.

CHAPTER 3

RESULTS and DISCUSSION

3.1. Protein Quantification by BCA Assay Across Different Opium Poppy Cultivars and Tissues

Results of the BCA assay which yielded the concentration (µg/µl) and total amount (µg) of protein extracted from each opium sample are presented in Table 3.1 with a gradient color bar indicating the protein amounts from lowest (red) to highest (green). The concentration values were calculated from the BSA standard curve in Figure 3.1 with the equation y = 0.4853x + 0.0963.

Table 3.1. Protein quantification results from the BCA assay for five different tissues across three opium poppy cultivars.

Cultivar	Tissue	Replicate	AV	c(µg/µl)	Total protein (µg)	Cultivar	Tissue	Replicate	AV	c(µg/µl)	Total protein (µg)
Ofis 2	root	1	0.184	1.81	451.78	TMO T	mature capsule	1	0.145	0.99	248.30
Ofis 2	root	2	0.169	1.50	374.51	TMO T	mature capsule	2	0.193	1.99	498.15
Ofis 2	root	3	0.231	2.78	693.90	TMO T	mature capsule	3	0.195	2.02	505.87
Ofis 2	stem w/ latex	1	0.191	1.94	485.27	TMO T	young capsule	1	0.769	14.05	3512.77
Ofis 2	stem w/ latex	2	0.131	0.72	178.76	TMO T	young capsule	2	0.453	7.50	1875.00
Ofis 2	stem w/ latex	3	0.147	1.03	258.60	TMO T	young capsule	3	0.852	15.77	3943.63
Ofis 2	stem w/o latex	1	0.104	0.16	39.67	Ofis NM	root	1	0.578	9.93	2481.45
Ofis 2	stem w/o latex	2	0.104	0.15	37.09	Ofis NM	root	2	0.742	13.29	3323.72
Ofis 2	stem w/o latex	3	0.109	0.25	62.85	Ofis NM	root	3	0.513	8.59	2146.61
Ofis 2	mature capsule	1	0.423	6.87	1716.67	Ofis NM	stem w/ latex	1	0.889	16.33	4083.56
Ofis 2	mature capsule	2	0.516	8.81	2202.03	Ofis NM	stem w/ latex	2	0.877	16.09	4021.74
Ofis 2	mature capsule	3	0.358	5.52	1379.26	Ofis NM	stem w/ latex	3	0.796	14.42	3604.47
Ofis 2	young capsule	1	0.665	11.89	2972.90	Ofis NM	stem w/o latex	1	0.625	10.88	2721.00
Ofis 2	young capsule	2	0.841	15.55	3886.52	Ofis NM	stem w/o latex	2	0.614	10.67	2666.91
Ofis 2	young capsule	3	0.721	13.06	3266.20	Ofis NM	stem w/o latex	3	0.908	16.72	4178.86
TMO T	root	1	0.143	0.96	240.57	Ofis NM	mature capsule	1	0.191	2.06	514.95
TMO T	root	2	0.176	1.63	408.00	Ofis NM	mature capsule	2	0.240	3.07	766.72
TMO T	root	3	0.231	2.78	693.90	Ofis NM	mature capsule	3	0.273	3.76	940.61
TMO T	stem w/ latex	1	0.192	1.96	490.42	Ofis NM	young capsule	1	0.630	11.18	2793.81
TMO T	stem w/ latex	2	0.178	1.67	418.30	Ofis NM	young capsule	2	0.788	14.45	3611.40
TMO T	stem w/ latex	3	0.141	0.91	227.69	Ofis NM	young capsule	3	0.607	10.69	2671.82
TMO T	stem w/o latex	1	0.147	1.03	258.60						
TMO T	stem w/o latex	2	0.140	0.90	225.12						
TMO T	stem w/o latex	3	0.267	3.52	879.35						

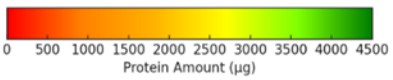

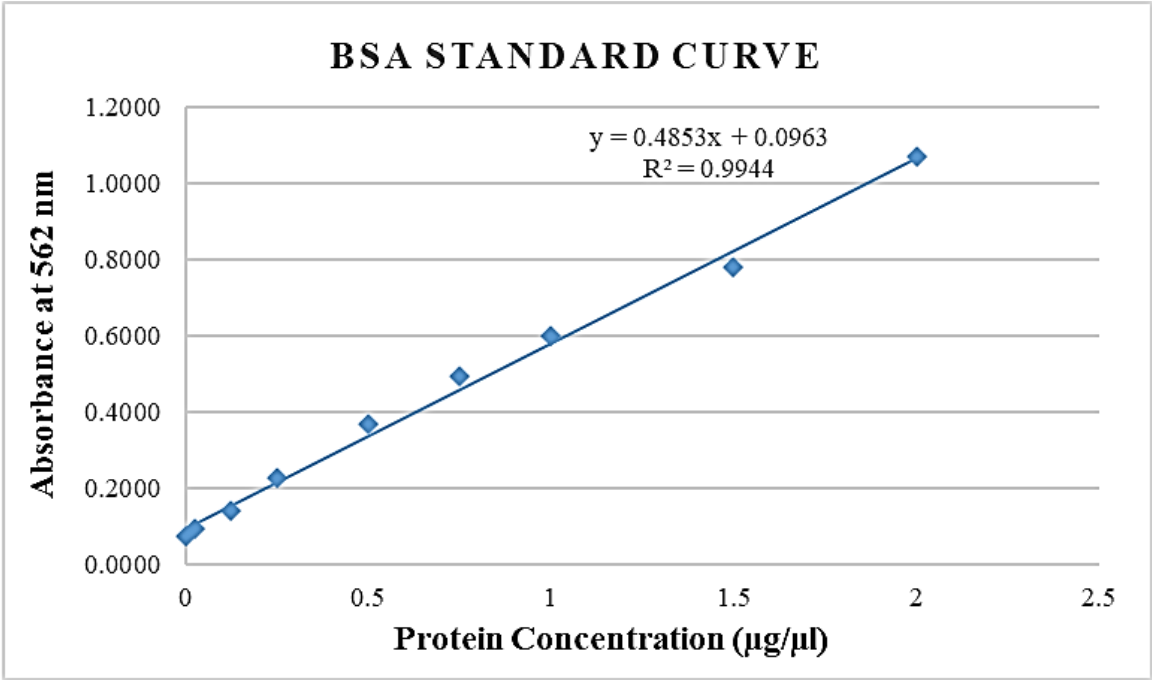

Figure 3.1. BSA standard curve for protein concentration calculations.

In root samples, Ofis NM showed significantly higher protein amounts (~2650 µg) compared to Ofis 2 (~506 µg) and TMO T (~447 µg). This might suggest that the roots of Ofis NM have a higher natural protein content or easier extractability, possibly due to differences in root tissue composition or protein expression. Ofis 2 and TMO T, however, showed significantly lower yields, which could suggest that the extraction process was less effective for these cultivars. This could arise from tougher tissue structure in the roots that resists homogenization and/or the presence of secondary metabolites or other interfering substances that inhibit protein extraction. Roots tend to have lower protein extraction yields compared to other tissues (Rodrigues et al., 2012; Viana et al., 2020).

For stem samples, protein amounts were significantly higher in stems with latex (Ofis 2: ~307 µg Ofis NM: ~3902 µg TMO T: ~378 µg) compared to stems without latex (Ofis 2: ~46 µg Ofis NM: ~3188 µg TMO T: ~241 µg) across all three cultivars. Latex is a complex fluid that contains a variety of proteins, including enzymes, defense-related proteins, and storage proteins. These additional proteins present in latex are likely to contribute to the total protein content in the stems with latex (Nessler et al., 1985). In addition, the presence of latex may facilitate the homogenization process, making it easier to break down the tissue and release proteins. Its fluid structure may help distribute the

extraction buffer more evenly, potentially improving the efficiency of protein solubilization. Again, protein amounts of Ofis NM cultivar in both stems with and without latex were much higher than Ofis 2 and TMO T. The fact that the stems of Ofis NM were less woody and were thinner compared to Ofis 2 and TMO T lines could be related to the more efficient extraction of proteins. Less fibrous tissues might be easier to homogenize and break down during the extraction process, allowing for more complete disruption of cells and better release of proteins into the extraction buffer, resulting in higher measured protein amounts compared to cultivars with more fibrous tissues (Singh et al., 2015). Another explanation for the higher protein content of Ofis NM in stems and roots might be that the Ofis NM line was at a slightly different developmental stage compared to Ofis 2 and TMO T during the sample collection. Developmental stage can impact protein expression levels. Plant organs in a more active growth phase may exhibit higher protein synthesis (Mergner et al., 2020a; Mergner et al., 2020b).

Consistent with this, total protein amounts of young capsules were consistently higher (Ofis 2: ~3374 µg Ofis NM: ~3025 µg TMO T: ~3110 µg) than those of mature capsules (Ofis 2: ~1765 µg Ofis NM: ~740 µg TMO T: ~417 µg) in all cultivars. Young capsules also resulted in higher protein yields overall compared to other tissues. In opium poppy, young capsules are expected to exhibit high protein content due to their vital role in alkaloid biosynthesis, active growth, latex production, and defense against environmental threats . The specific demands of these processes lead to increased synthesis of enzymes, structural proteins, and defense-related proteins, which might cause young capsules to be protein-rich compared to other tissues. Protein accumulation might reflect the multifunctional role of young capsules in supporting both the plant's growth, BIA metabolism and its defense strategies. Mature capsules might have less need for new protein production, as their role shifts towards maintaining existing structures and supporting seed maturation and dispersal (Aykanat and Türktaş, 2024, Li et al., 2018).

Based on the protein quantification analysis comparisons, it is clear that different cultivars and tissues of opium poppy have unique properties that can affect protein yield, such as cellular structure, presence of interfering substances, developmental stage, or tissue-specific protein composition (e.g., presence of latex). Optimizing the extraction protocol for diverse types of tissue and cultivars (e.g., adjusting buffer composition and using more effective homogenization methods) could help improve consistency and accuracy of the MS analysis.

3.2. Quality Assessment of Protein Digestion and TMT Labeling

The quality and efficiency of tandem mass tag (TMT) labeling across the selected tissues of the opium poppy cultivars were investigated to assess the reliability and comprehensiveness of the proteomic analysis. Figure 3.2(a) represents the TMT labeling efficiency vs. TMT label site graphs, which illustrate the percentage of peptides successfully labeled at different modification sites across the tissue types analyzed, including mature capsules, young capsules, stems with and without latex, and roots. The TMT labeling sites were lysine residues, peptide N-termini, carbamidomethyl cysteines (Carba-Cys), and oxidized methionines (Ox-Met). In all five tissues of interest, the majority of peptides showed high labeling efficiency at primary binding sites (i.e., lysine residues, N-termini) and Carba-Cys (~98-99%), indicating that the TMT labeling was successful for nearly every peptide in the sample. High percentages of labeled carbamidomethyl cysteines also indicate a near-complete reduction and alkylation during protein digestion. On the other site, TMT labeling efficiency of oxidized methionines was the lowest across all tissue types (~ 45-70%) as expected. Methionine oxidation is a variable modification across proteins, and not all peptides contain methionine residues. This could explain the variable and lower labeling efficiency of the samples at this peptide modification site (Bettinger et al., 2019).

Miscleavage refers to the failure of trypsin enzyme to fully cleave a peptide at its expected cleavage sites, lysine and arginine, resulting in peptides that contain one or more missed cleavage sites. For example, a two-miscleavage peptide means that there are two sites of that peptide where cleavage did not occur, generating a longer peptide fragment than anticipated. This could occur due to factors like enzyme inefficiency, suboptimal digestion conditions, or structural hindrances in the protein (Burkhart et al., 2012; Lin et al., 2020).

In Figure 3.2(b), the total number of peptides with a particular number of miscleavages (e.g., 0, 1, 2 on the x-axis) as determined by LC-MS/MS analysis for each opium poppy tissue is illustrated. The large number of peptides with 0 missed cleavage sites (>80,000) indicates that the digestion was very effective for the majority of the peptides. A relatively small number of peptides exhibited one missed cleavage, and very few show two missed cleavages. This further confirms efficient digestion by trypsin, as only a minor fraction of peptides was incompletely cleaved. This result suggest that the

enzymatic digestion process was optimized and worked well for each tissue/cultivar combination. Efficient digestion enhances peptide identification and quantification by producing peptides that are readily detected and quantified by LC-MS/MS, which is critical for the accuracy and precision of the analysis (Burkhart et al., 2012).

The box plots in Figure 3.2(c) provide a visual representation of the relative abundance of peptides across different opium poppy cultivars in the 11-channel TMT multiplexing (see Table 2.1) for each tissue. The intensity of the reporter ions for each channel is proportional to the relative abundance of the peptides or proteins in the corresponding opium poppy sample. Variation of median intensities and spread is expected between the channels of different opium poppy cultivars, since they are likely to have distinct protein expression profiles, which naturally causes variation in intensity levels across channels. However, the channels also displayed a minor degree of variability within the biological replicates of the same cultivar. For instance, channels 6 to 8 of stems with latex samples belong to the TMO T cultivar but the first replicate (channel 6) shows a noticeably lower median intensity compared to other replicates. This might have been caused by technical errors such as uneven sample loading and labeling efficiency issues during the TMT labeling or sample loss due to problems in the previous extraction/protein degradation steps.

Mature capsules:

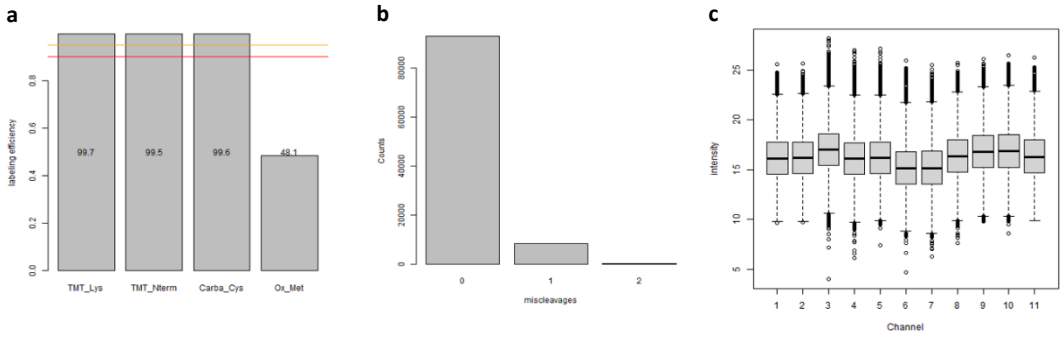

(Cont. on the next page)

Figure 3.2. Assessment of TMT labeling efficiency and data quality for opium poppy tissues: (a) Bar plot showing the TMT labeling efficiency across four modification types - lysine, Nterm, Carba_Cys, and Ox_Met. Red line represents a minimum acceptable threshold for labeling efficiency, whereas yellow line indicates an optimal efficiency level (b) Histogram representing the frequency of peptide miscleavages by trypsin. (c) Box plot displaying the intensity distribution across 11-TMT channels (Table 2.1). Each channel shows a median intensity, with variation in range of the data indicated by outliers.

Young capsules:

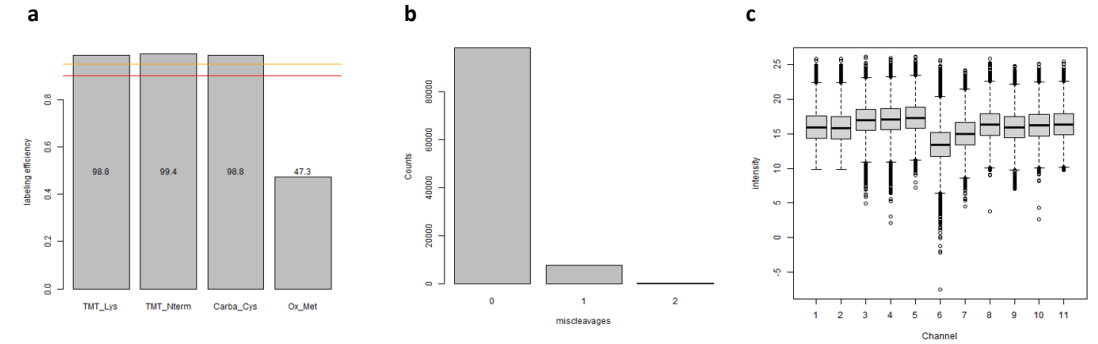

Stems without latex:

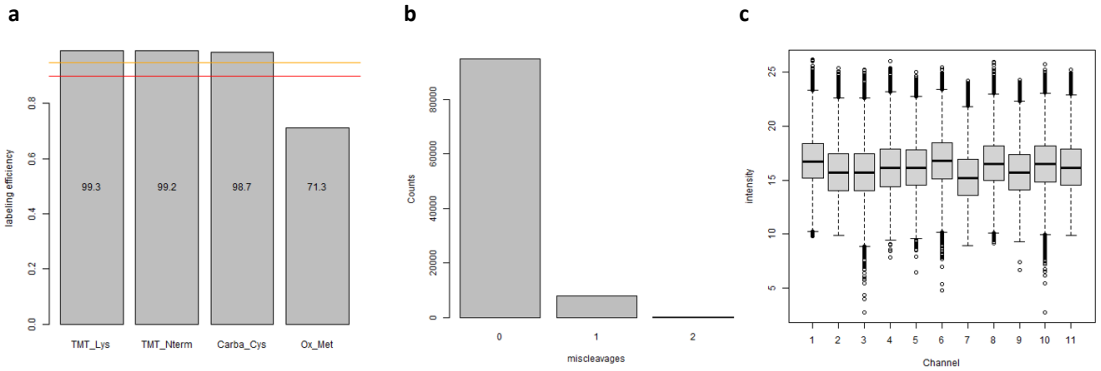

Stems with latex:

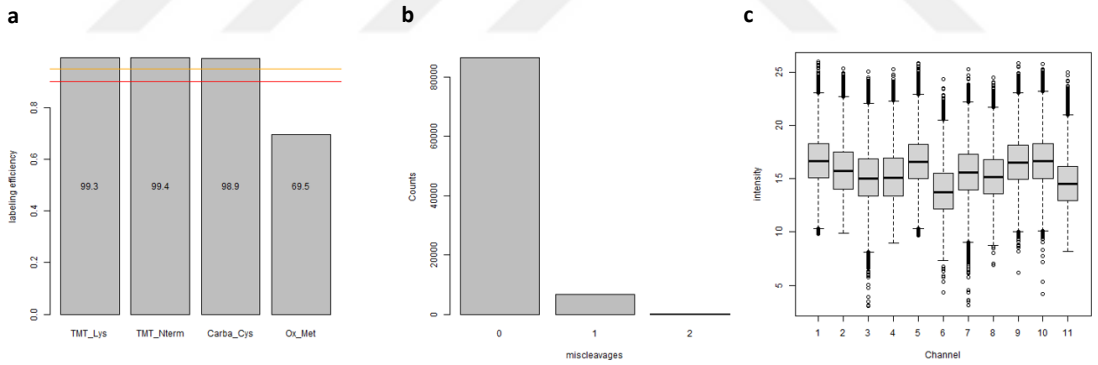

Roots:

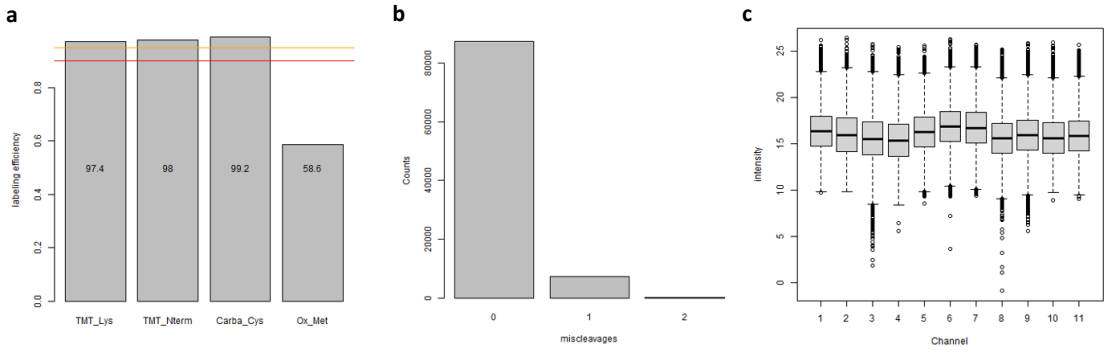

Figure 3.2. (cont.)

3.3. Protein and Peptide Identification of Opium Poppy Cultivars

The LC-MS/MS analysis identified the peptides and proteins from five tissues of *P. somniferum* across three cultivars: Ofis 2, Ofis NM, and TMO T, utilizing TMT11plex labeling. Biological replicates and reference pool samples were included in each tissue type to ensure reliability and reproducibility across the five TMT11 batches. The data were examined in terms of identified protein and peptide counts along with the average counts for each tissue across the three cultivars as presented in Table 3.2. The LC-MS/MS analysis identified a total of 8166 proteins.

Table 3.2. Protein and peptide identifications of opium poppy cultivars Ofis 2, Ofis NM and TMO T for five different tissues: mature capsules, young capsules, stems with latex, stems without latex, and roots, respectively.

Tissue	Channel 1	Channel 2	Channel 3	Channel 4	Channel 5	Channel 6	Channel 7	Channel 8	Channel 9	Channel 10	Channel 11
Mature Capsule	REF	REF	Ofis2_R1	Ofis2_R2	Ofis2_R3	TMOT_R1	TMOT_R2	TMOT_R3	OfisNM_R1	OfisNM_R2	OfisNM_R3
Protein IDs	7352	7351	7366	7355	7354	7302	7318	7349	7362	7363	7341
Peptide IDs	51161	51151	51344	51201	51241	50665	50698	51164	51298	51296	51129

Tissue	Channel 1	Channel 2	Channel 3	Channel 4	Channel 5	Channel 6	Channel 7	Channel 8	Channel 9	Channel 10	Channel 11
Young Capsule	REF	Ofis2_R1	Ofis2_R2	Ofis 2_R3	TMOT_R1	REF	TMOT_R2	TMOT_R3	OfisNM_R1	OfisNM_R2	OfisNM_R3
Protein IDs	7979	7980	8001	7994	8006	7774	7948	7991	7971	7990	7994
Peptide IDs	57422	57427	57609	57561	57817	54379	57137	57613	57401	57587	57651

Tissue	Channel 1	Channel 2	Channel 3	Channel 4	Channel 5	Channel 6	Channel 7	Channel 8	Channel 9	Channel 10	Channel 11
Stem w/o Latex	REF	Ofis2_R1	Ofis2_R2	Ofis 2_R3	TMOT_R1	TMOT_R2	TMOT_R3	REF	OfisNM_R1	OfisNM_R2	OfisNM_R3
Protein IDs	7059	6974	6981	6998	7012	7047	6983	7053	6974	7032	7004
Peptide IDs	47607	46915	46883	47134	47224	47502	46882	47575	46833	47322	47175

Tissue	Channel 1	Channel 2	Channel 3	Channel 4	Channel 5	Channel 6	Channel 7	Channel 8	Channel 9	Channel 10	Channel 11
Stem w/ Latex	REF	Ofis2_R1	Ofis2_R2	Ofis2_R3	REF	TMOT_R1	TMOT_R2	TMOT_R3	OfisNM_R1	OfisNM_R2	OfisNM_R3
Protein IDs	7153	7095	7055	7007	7154	6827	7092	7052	7137	7135	6958
Peptide IDs	47242	46569	46115	45725	47240	43915	46511	46357	46914	46945	45391

Tissue	Channel 1	Channel 2	Channel 3	Channel 4	Channel 5	Channel 6	Channel 7	Channel 8	Channel 9	Channel 10	Channel 11
Root	REF	Ofis2_R1	Ofis2_R2	Ofis 2_R3	TMOT_R1	TMOT_R2	TMOT_R3	OfisNM_R1	OfisNM_R2	OfisNM_R3	REF
Protein IDs	7250	7196	7182	7169	7243	7247	7248	7203	7233	7148	7232
Peptide IDs	50500	49863	49682	49647	50341	50470	50458	49982	50330	49717	50324

Tissue	Average Protein #	Average Peptide #
Mature Capsule	7346	51122
Young Capsule	7966	57236
Stem without Latex	7010	47186
Stem with Latex	7060	46265
Root	7213	50119

Young capsules displayed the highest protein and peptide counts, with averages of 7966 proteins and 57,236 peptides. These elevated counts indicate a highly active proteome, reflecting the intensive metabolic demands of young capsules. In contrast, mature capsules had lower but still substantial protein composition, with an average of 7346 proteins and 51,122 peptides across the three cultivars. The difference in protein counts between young and mature capsules was statistically significant (p-value = 1.92×10^{-12}, paired t-test). This indicates a stable proteome profile for the mature capsules, which might suggest that as the capsule develops, its metabolic activity shifts from growth-focused biosynthesis to maintenance and storage functions. Young capsules are a primary site for alkaloid biosynthesis and other secondary metabolites, which are critical for the plant's defense and development (Li et al., 2018). Therefore, the high proteomic complexity in this tissue aligns with its role in supporting robust biosynthetic pathways during the developmental stage. While mature capsules are less metabolically demanding than young capsules, the relatively high counts still reflect ongoing physiological activities, potentially related to maturation processes and sustained secondary metabolite storage (Aykanat and Türktaş, 2024, Li et al., 2018).

Among the analyzed tissues, opium poppy stem, both with and without latex, exhibited the lowest average protein and peptide counts, with latex-free stems averaging 7010 proteins and 47,186 peptides, and latex-including stems averaging 7060 proteins and 46,625 peptides across the three cultivars. Several factors might have contributed to the comparatively lower protein and peptide identifications in stems, including the structural characteristics of opium poppy stems and technical challenges related to protein extraction and identification. Opium poppy stems contain a significant amount of lignin, cellulose, and other rigid cell wall components, which can hinder efficient protein extraction. These structural molecules might create a dense matrix that can sequester or shield proteins, making them less accessible during the extraction process (Kocabaş et al., 2020; Marriott et al., 2016). The difficulty in breaking down these complex cell walls without damaging proteins often results in suboptimal protein yields from stem samples. Additionally, proteins bound within the cell wall matrix may be more resistant to solubilization, leading to incomplete protein recovery and lower representation of structural or wall-associated proteins in the final proteomic data. This technical limitation can potentially underrepresent the actual number of proteins present in stem tissues. Furthermore, certain latex-associated compounds in latex-containing stems, such as

alkaloids, may interfere with downstream processing steps in MS, impacting protein identification and quantification. The presence of latex can complicate sample preparation, as latex components can precipitate or clog filters, thereby reducing the quality of the extracted protein sample (Weid et al., 2004). This adds a layer of technical complexity, especially in stems with latex, where these issues can further reduce protein yields and influence the identification process. Roots showed moderate levels of protein and peptide identifications, averaging 7250 proteins and 50,119 peptides across the three opium poppy cultivars. Positioned between the higher values observed in capsules and the lower values in stems, the moderate counts in root tissues might suggest a functional role in maintaining core physiological processes that sustain the plant.

Protein and peptide counts within each tissue type (mature capsules, young capsules, stems with latex, stems without latex, and roots) showed minimal variation across the three cultivars with consistency between the biological replicates. Consistent protein and peptide identifications across cultivars and replicates provide confidence in the precision of the observed proteomic patterns, suggesting that these patterns are not merely artifacts of experimental variation. Also, this consistency in protein identification numbers suggests that the core proteomic composition of each tissue is relatively stable across cultivars, indicating conserved tissue-specific functions. However, while the number of identified proteins remains consistent across cultivars, it is likely that the expression levels of specific proteins vary between them. These variations in protein abundance can reflect cultivar-specific adaptations and are likely associated with phenotypic differences, such as variations in alkaloid content or resistance to environmental stressors. Overall, these data highlight the diversity of protein expression profiles across different opium poppy tissues and reflect the functional specialization of each tissue, which is discussed in detail in the following analysis.

3.4. Alkaloid Profiles of Opium Poppy Dried Capsules

The BIA profiles of dried capsules were obtained via HPLC analysis (Table 3.3). Consistent with literature information (Yazici and Yılmaz, 2021), morphine was the dominant alkaloid in all three cultivars, though its proportion varies depending on the cultivar's specialization. Ofis 2 has the highest morphine content (1.72%), consistent with its classification as a morphine-rich cultivar. TMO T was highest in thebaine production (0.52%) and contains a considerable amount of morphine (1.07%). Ofis NM, identified

as a noscapine-rich cultivar, has the highest noscapine proportion (0.1%) but still retains significant morphine levels (0.88%). Thebaine levels are minimal in Ofis 2 and Ofis NM, while papaverine remains a minor component across all cultivars but highest in Ofis NM. These data underscore that morphine biosynthesis is central to all cultivars, while specialization into noscapine or thebaine production reflects cultivar-specific metabolic divergence.

Table 3.3. Alkaloid composition (%) in the dry capsules of three opium poppy cultivars: Ofis 2 (morphine-rich), TMO T (thebaine-rich), and Ofis NM (noscapine-rich). Percentages represent the relative abundance of four major alkaloids.

	Morphine (%)	Thebaine (%)	Noscapine (%)	Papaverine (%)
Ofis 2	1.72	0.04	0.03	0.01
TMO T	1.07	0.52	0.08	0.01
Ofis NM	0.88	0.06	0.1	0.03

3.5. Principal Component Analysis (PCA) of Opium Poppy Cultivars

Principal component analysis (PCA) was performed on the opium poppy tissue samples comprising the biological replicates of three cultivars (Ofis NM, Ofis 2, and TMO T) and two reference samples (i.e., mixture of samples) based on the protein expression data of around 7,000 proteins. The PCA plots in Figure 3.3 display the distribution of tissue-specific proteomic profiles between the three cultivars, each enriched in different alkaloids: Ofis 2 (morphine), Ofis NM (noscapine), and TMO T (thebaine). The first two principal components (PC1 and PC2) captured the most variance among the data. Component 1 accounted for the majority of the variance in all of the tissues, ranging from 36.86% to 68.47%, while Component 2 added additional differentiation, capturing between 13.99% and 30.04%. Except for young capsules and latex-free stems, a clear separation between the cultivars is visible along the primary component axes, while the biological replicates of the same cultivar tend to be clustered together. These results indicate distinct proteomic profiles that might be associated with the dominant alkaloid in each cultivar or with other cultivar-specific differences in the samples. The clustering of replicates from different cultivars in young capsules but a more distinct separation in mature capsules might reflect a biological transition from shared early-stage growth activities to specialized secondary metabolism and alkaloid production.

a) Mature Capsules:

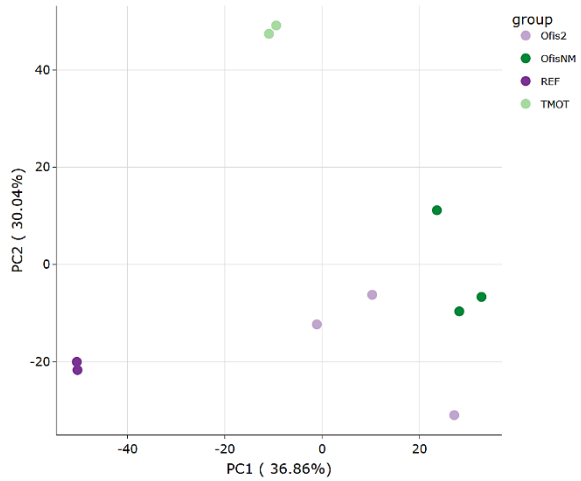

b) Young Capsules:

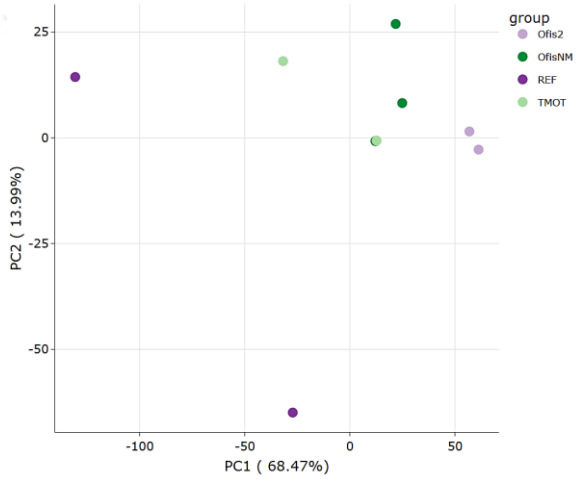

c) Stems without Latex:

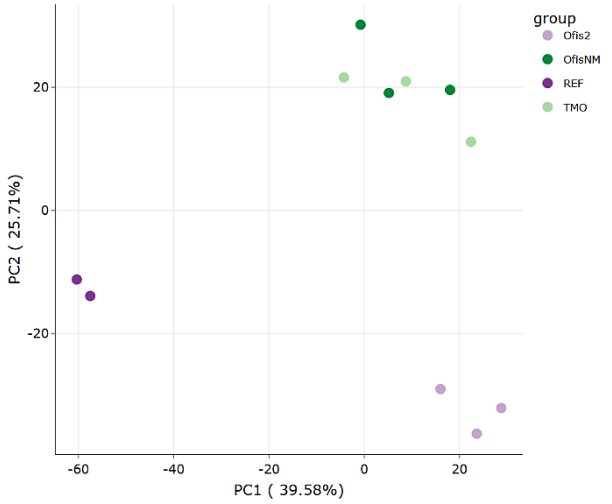

(Cont. on the next page)

Figure 3.3. PCA of protein profiles across 3 opium poppy cultivars in (a) mature capsules, (b) young capsules, (c) stems without latex, (d) stems with latex, and (e) roots.

d) Stems with Latex:

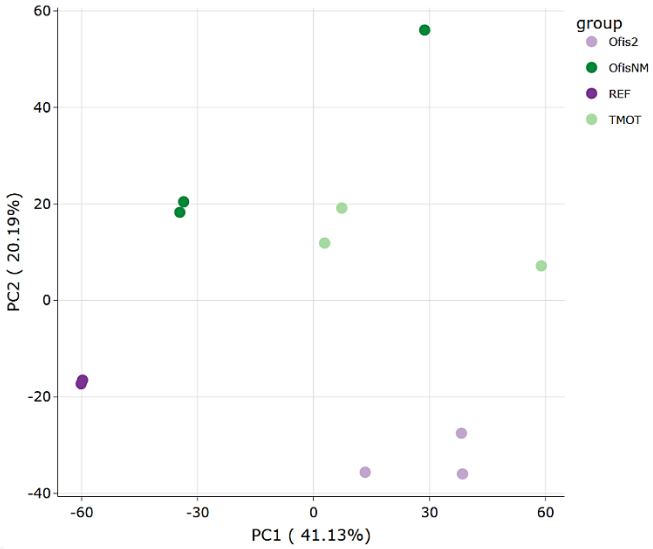

e) Roots:

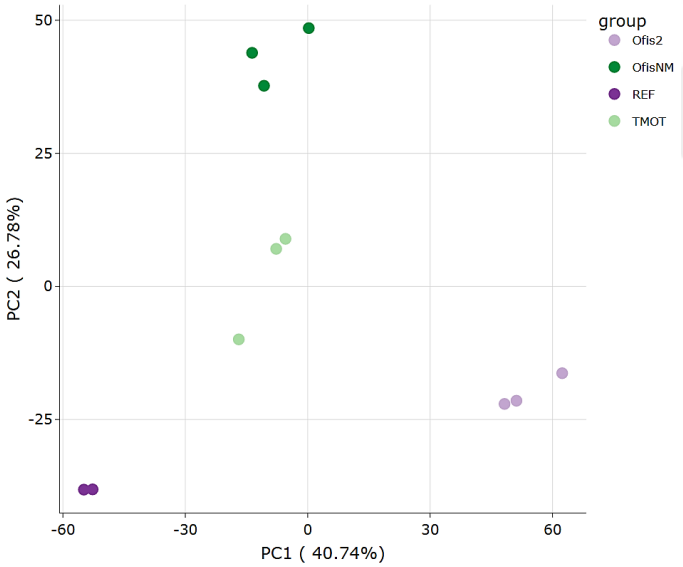

Figure 3.3. (cont.)

3.6. Differential Protein Expression of Opium Poppy Cultivars

Among the 8166 proteins identified by LC-MS/MS analysis, differential protein expression across the three opium poppy cultivars was examined for each of the five target tissues to compare their cultivar-specific proteome profiles. Proteins satisfying the criteria of FDR ≤ 0.05 and a fold change (FC) ≥ 1.5 were classified as differentially expressed proteins (DEPs) and illustrated with the volcano plots in Figure 3(4-8).

Mature Capsules:

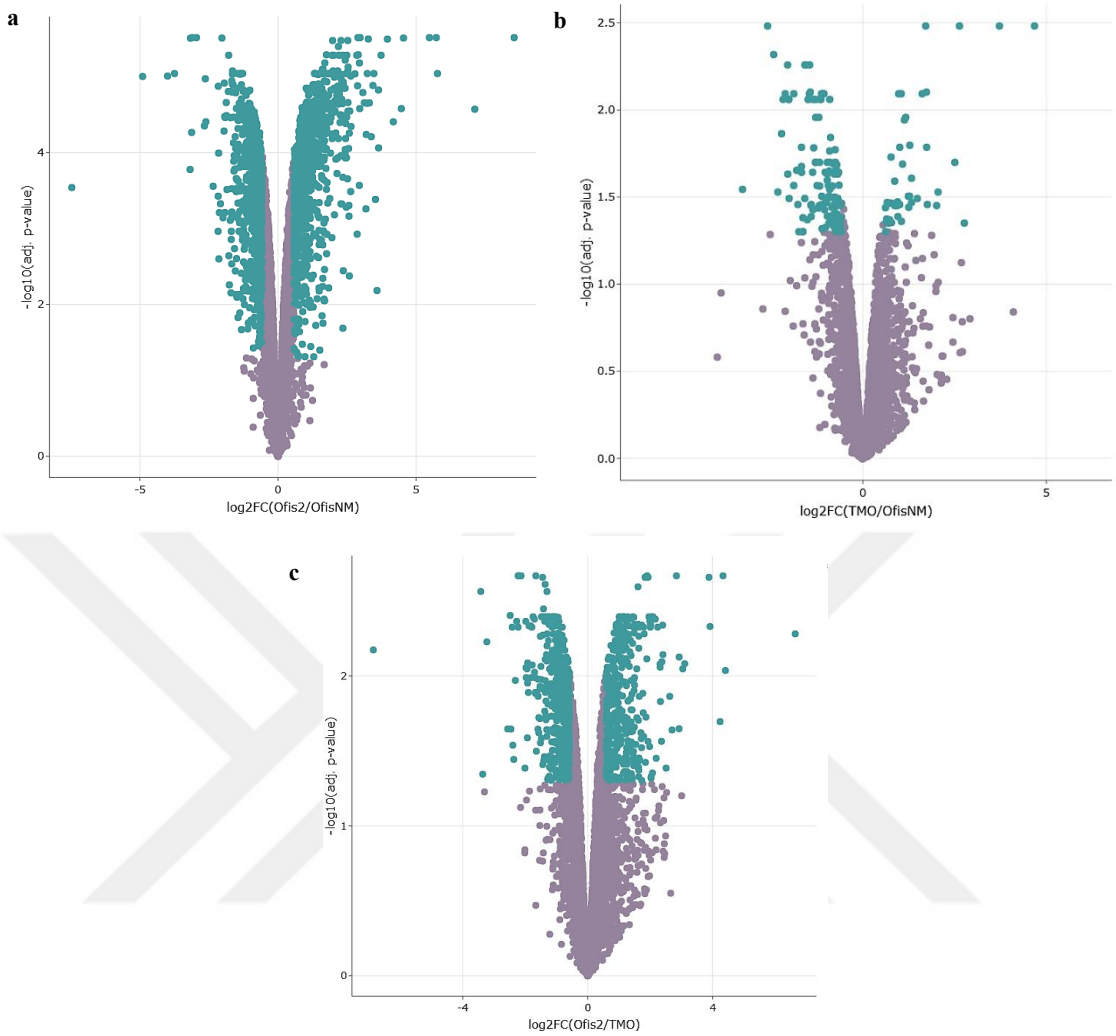

Figure 3.4. Volcano plots comparing differentially expressed proteins across the mature capsules of three opium poppy cultivars: comparison between (a)Ofis NM and Ofis 2, (b) Ofis NM and TMO T, (c) TMO T and Ofis 2 with the x-axis representing the difference (log2FC) in protein abundance and the y-axis representing the statistical significance (-log p-value). Proteins differentially expressed in each comparison are shown in cyan, whereas proteins with non-significant differences are shown in purple (FDR:0.05).

Mature capsules of opium poppy exhibited the highest differential expression levels among all the tissues, with distinct clusters of up- and down-regulated proteins in each pairwise cultivar comparison. Morphine-rich Ofis 2 cultivar showed a robust proteomic profile with a larger number of significantly differentially expressed proteins in both comparisons with noscapine-rich Ofis NM and thebaine-rich TMO T. The total number of DEPs in comparison of Ofis NM with TMO T mature capsules were lower than the other pairwise comparisons.

Young Capsules:

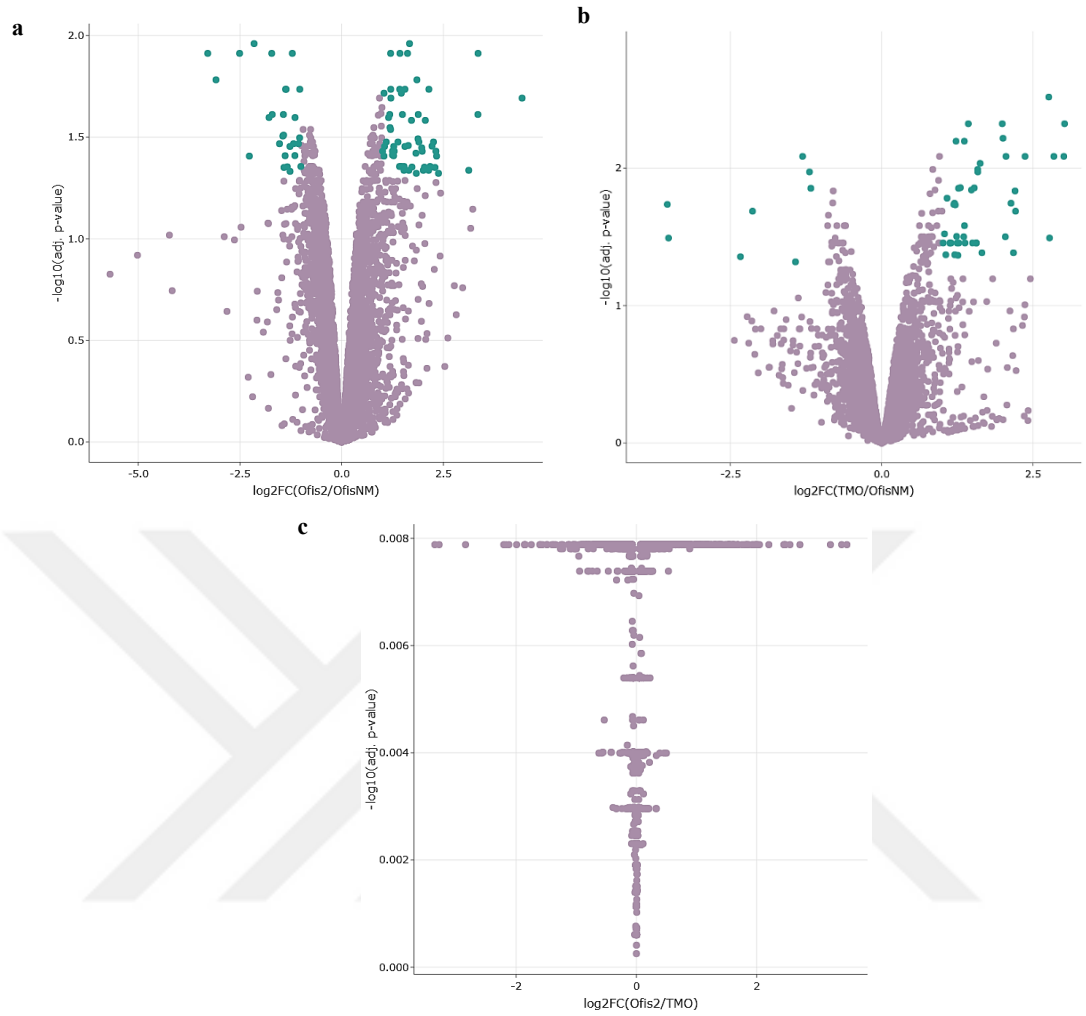

Figure 3.5. Volcano plots comparing differentially expressed proteins across the young capsules of three opium poppy cultivars: comparison between (a)Ofis NM and Ofis 2, (b) Ofis NM and TMO T, (c) TMO T and Ofis 2 with the x-axis representing the difference (log2FC) in protein abundance and the y-axis representing the statistical significance (-log p-value). Proteins differentially expressed in each comparison are shown in cyan, whereas proteins with non-significant differences are shown in purple (FDR:0.05).

Young capsules showed less differential expression between the cultivars compared to mature capsules. Most proteins are within the non-significant range, with only a few showing significant fold changes. In contrast to the mature capsules where Ofis 2 exhibited strong differential regulation, a substantial number of DEPs were observed in Ofis NM young capsules compared to Ofis 2 and TMO T. Comparisons of TMO T and Ofis 2 young capsules resulted in no DEPs indicating a balanced expression profile between these two cultivars at this developmental stage.

Latex-included Stems:

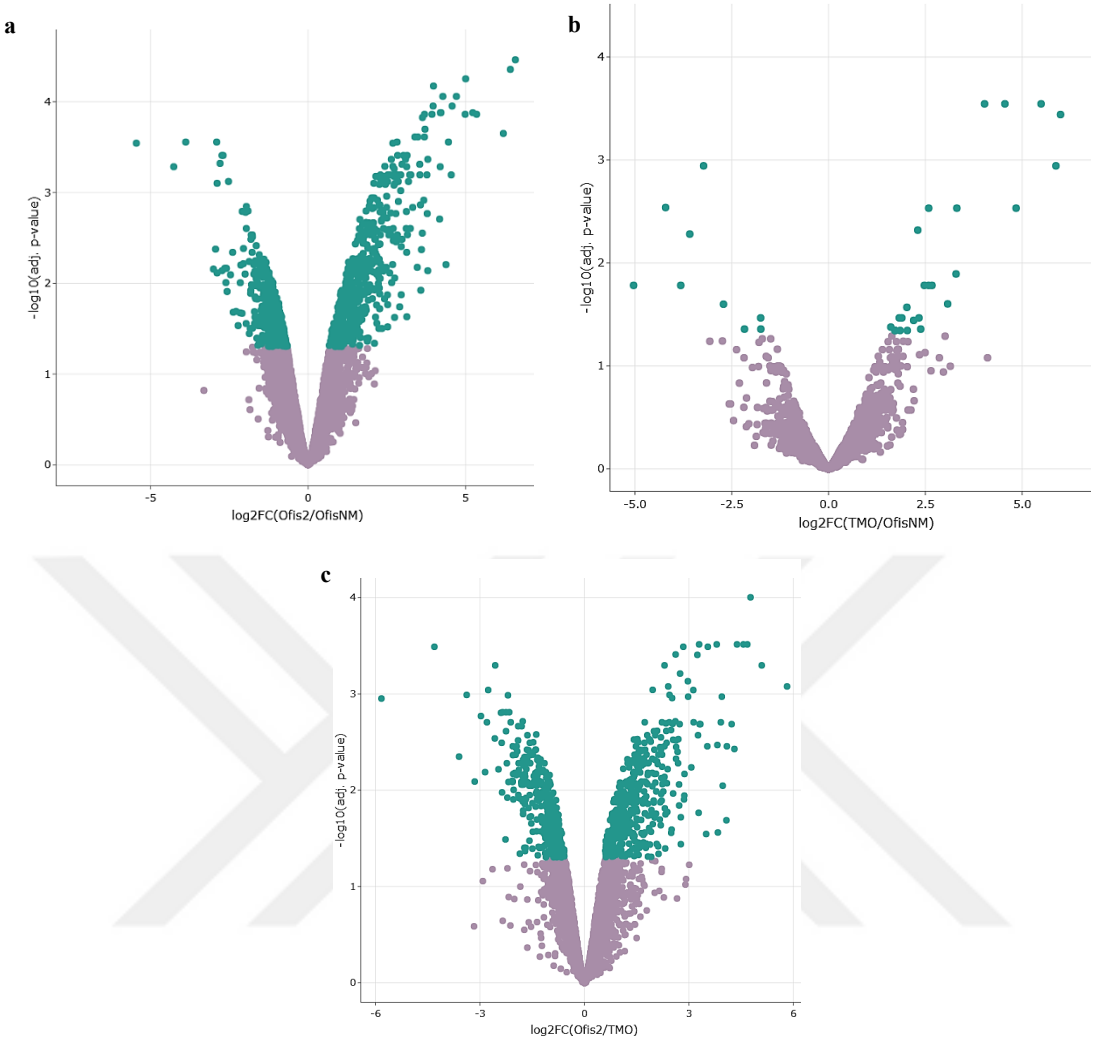

Figure 3.6. Volcano plots comparing differentially expressed proteins across the latex-included stems of three opium poppy cultivars: comparison between (a)Ofis NM and Ofis 2, (b) Ofis NM and TMO T, (c) TMO T and Ofis 2 with the x-axis representing the difference (log2FC) in protein abundance and the y-axis representing the statistical significance (-log p-value). Proteins differentially expressed in each comparison are shown in cyan, whereas proteins with non-significant differences are shown in purple (FDR:0.05).

Latex-including stems provided higher numbers of DEPs, both up-regulated and down-regulated, compared to latex-free stems. The presence of latex in stems might be correlated with increased metabolic complexity, likely driven by the need to produce, transport, and store alkaloids and other secondary metabolites. Similar to the mature capsules, latex-including stems of Ofis 2 showed a larger number of significant DEPs compared to Ofis NM and TMO T. In contrast, the number of DEPs in the comparison of TMO T and Ofis NM stems with latex was lower and more balanced in terms of up- and down-regulated proteins.

Similar to other tissues, the number of DEPs in pairwise comparison of Ofis 2 with both Ofis NM and TMO T was highest. However, the largest protein expression difference between Ofis NM and TMO T was also obtained in roots compared to other four tissues.

Latex-free Stems:

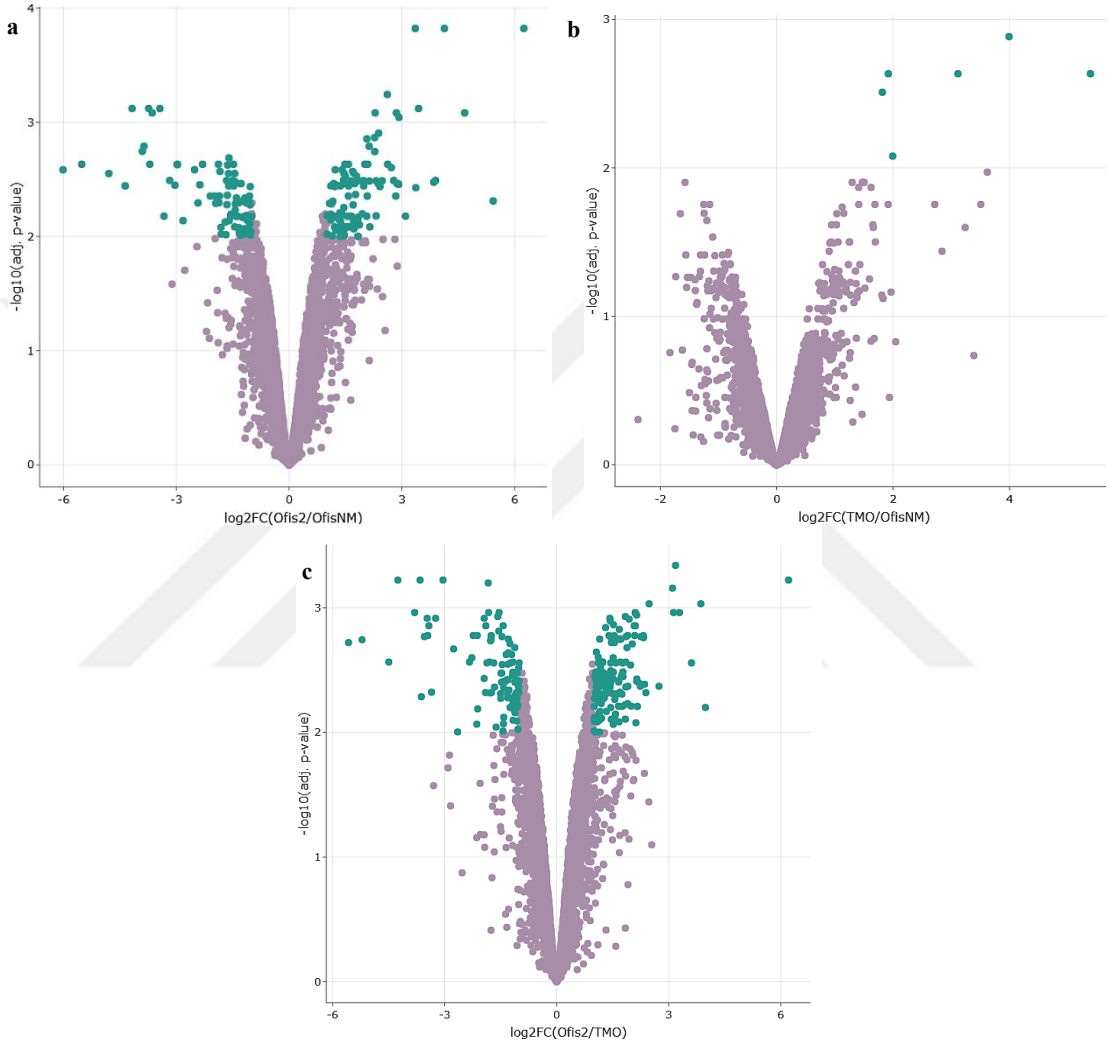

Figure 3.7. Volcano plots comparing differentially expressed proteins across the latex-free stems of three opium poppy cultivars: comparison between (a)Ofis NM and Ofis 2, (b) Ofis NM and TMO T, (c) TMO T and Ofis 2 with the x-axis representing the difference (log2FC) in protein abundance and the y-axis representing the statistical significance (-log p-value). Proteins differentially expressed in each comparison are shown in cyan, whereas proteins with non-significant differences are shown in purple (FDR:0.05).

Roots:

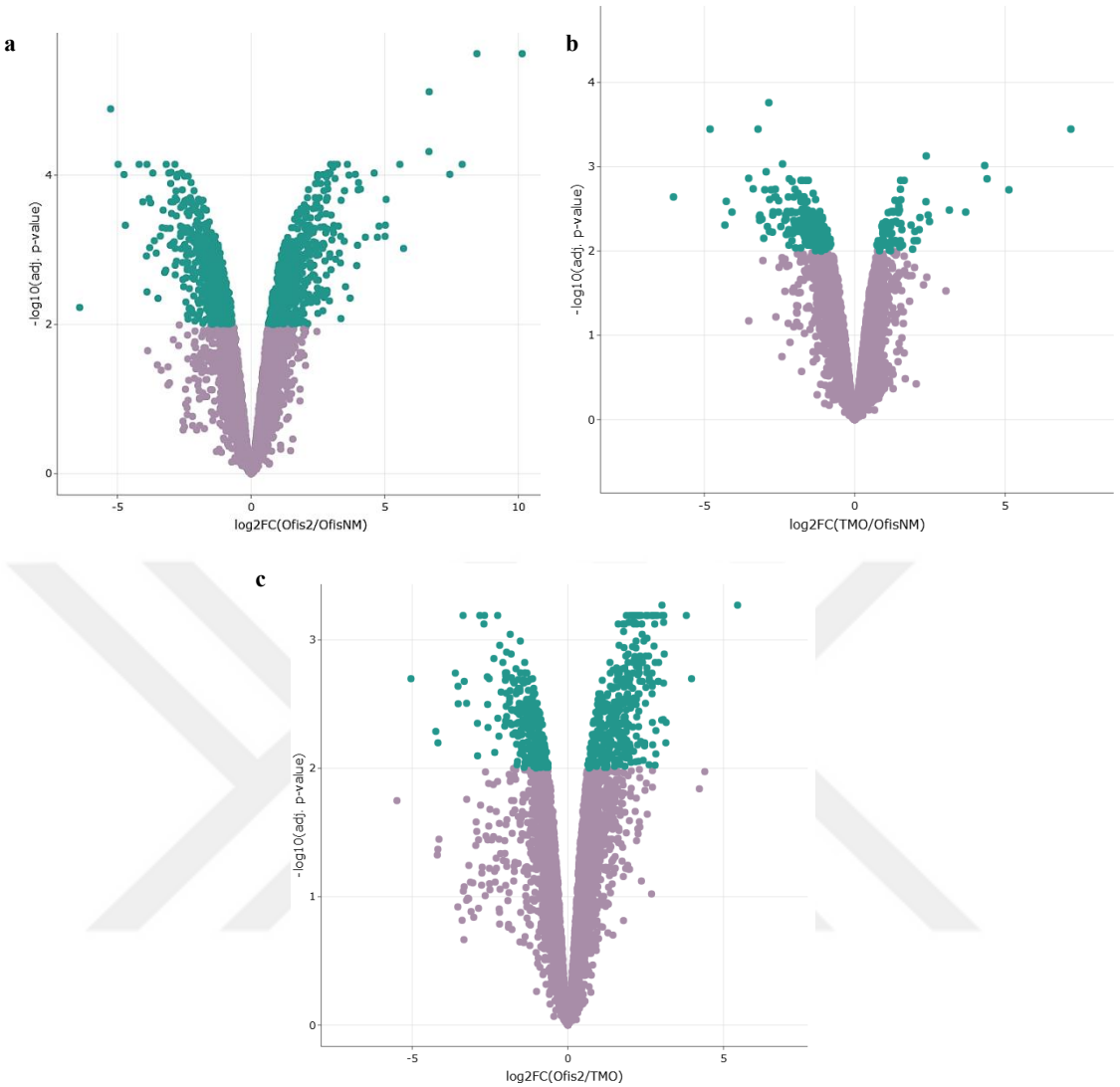

Figure 3.8. Volcano plots comparing differentially expressed proteins across the roots of three opium poppy cultivars: comparison between (a)Ofis NM and Ofis 2, (b) Ofis NM and TMO T, (c) TMO T and Ofis 2 with the x-axis representing the difference (log2FC) in protein abundance and the y-axis representing the statistical significance (-log p-value). Proteins differentially expressed in each comparison are shown in cyan, whereas proteins with non-significant differences are shown in purple (FDR:0.05).

The hierarchical clustering heatmap of protein expression in mature capsules (Figure 3.9) highlighted overall differences among Ofis 2, Ofis NM, and TMO T cultivars. Ofis 2 formed a distinct cluster, indicating a unique protein expression profile that diverges significantly from both TMO T and Ofis NM. Conversely, TMO T and Ofis NM clustered together, suggesting a higher similarity in their protein expression patterns.

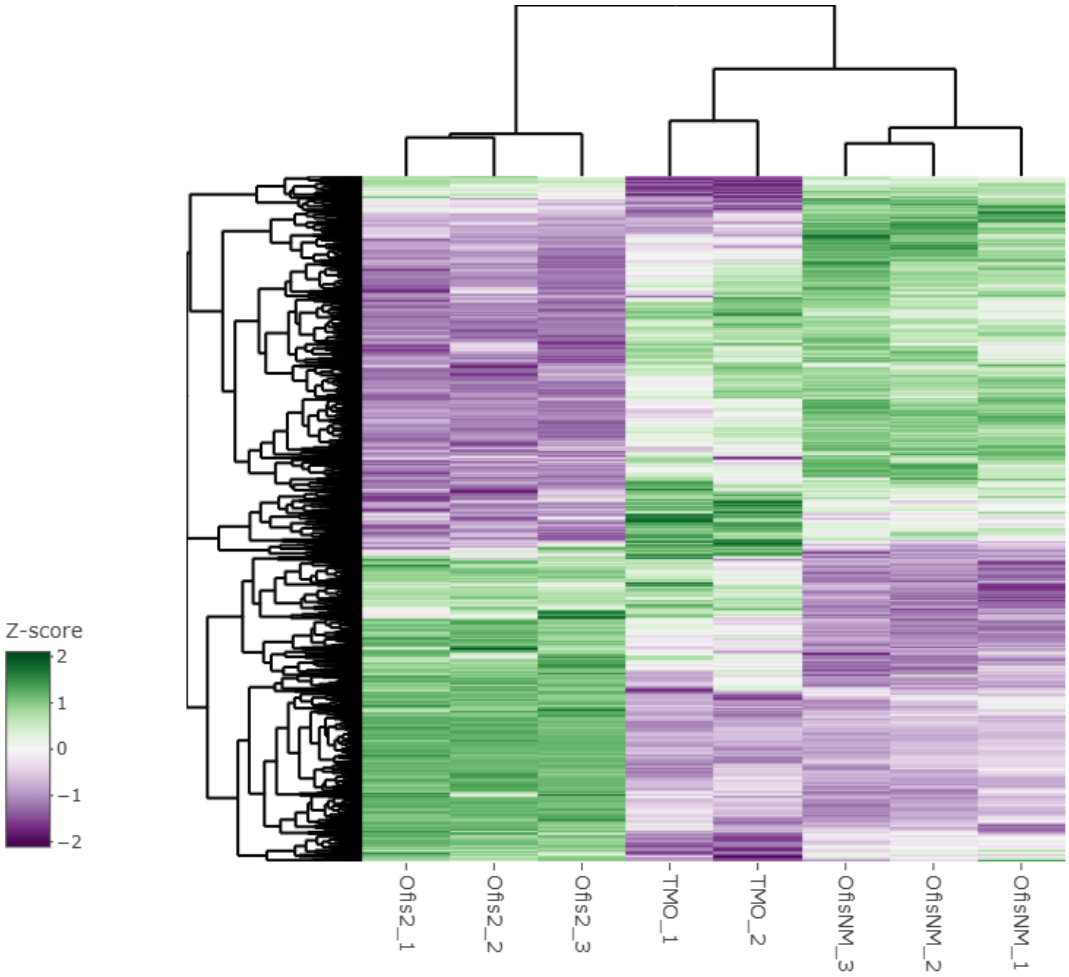

Figure 3.9 Heatmap representation of the protein abundances across mature capsules of three opium poppy cultivars: Ofis 2, Ofis NM, and TMO T. The rows represent individual proteins, while the columns represent biological replicates of each cultivar. Colors indicate an increase of protein expression level from purple to green.

Upset plots and Euler diagrams in Figure 3.10 summarize the number of DEPs identified across the pairwise comparisons of the opium poppy cultivars for the five target tissues. The intersection of two comparison sets that does not overlap with the third set represents proteins uniquely differentially expressed in one cultivar for a specific tissue. For example, in the mature capsules, the intersection of the "Ofis 2 v. TMO T" set with the "TMO T v. Ofis NM" set contains 60 proteins that are uniquely differentially expressed in TMO T mature capsules. These areas highlight cultivar-specific proteomic differences, providing insight into unique biological features or adaptations of the cultivars in specific tissues.

The central intersection in each diagram, on the other side, represents proteins that are consistently differentially expressed across all three pairwise comparisons, highlighting shared proteomic changes. Mature capsules have the largest number of cultivar-specific DEPs (2066 proteins in total) compared to other tissues, suggesting a more distinct proteomic profile in this tissue for each cultivar, followed by roots and latex-including stems. Young capsules and latex-free stems have lower numbers of DEPs, indicating less differentiation between cultivars for these organs. Overall, these comparisons reflected the complexity and variability in proteomic expression among tissues and cultivars of opium poppy, influenced by both tissue function and cultivar-specific traits.

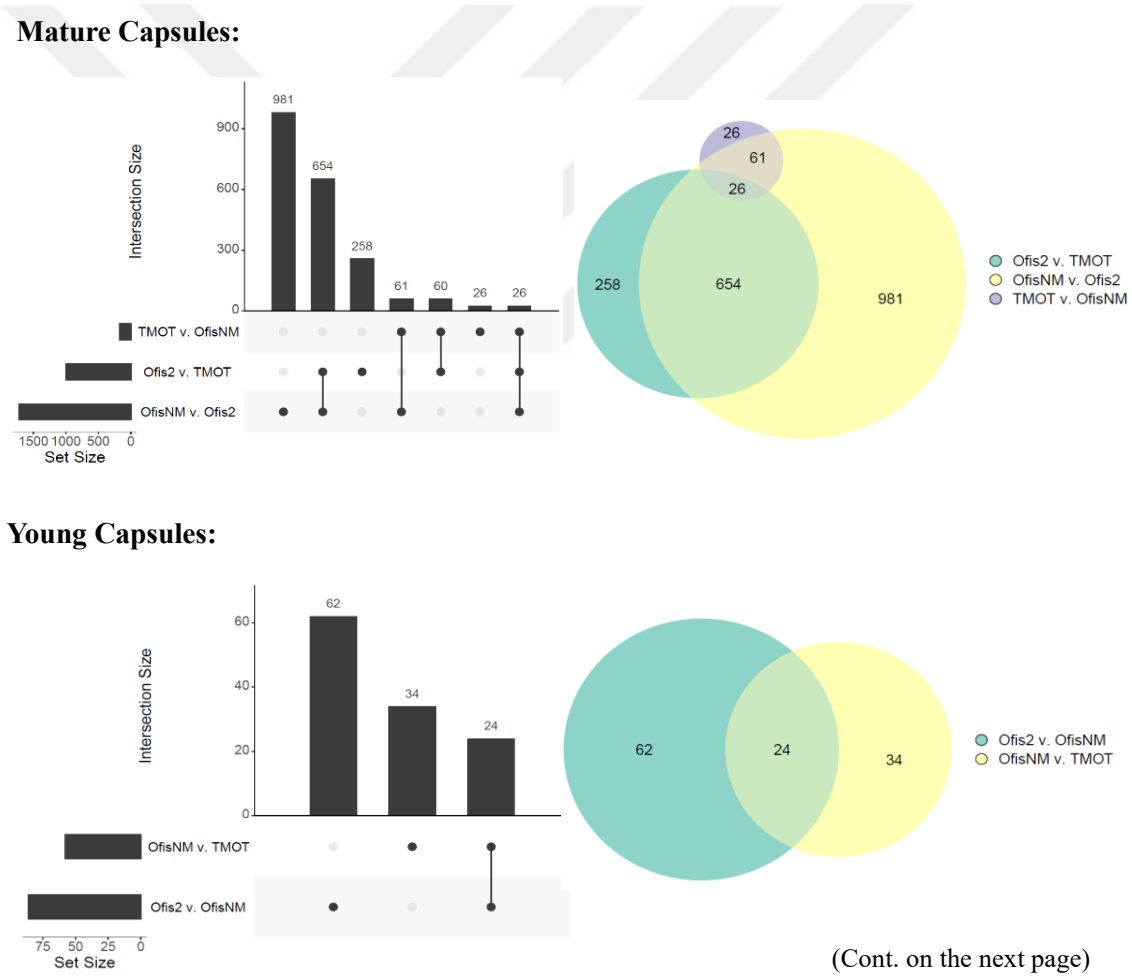

(Cont. on the next page)

Figure 3.10. Differentially expressed proteins across three Papaver somniferum cultivars (Ofis NM, Ofis 2, and TMO T). The data was visualized using Upset plots (left) and Euler diagrams (right) for five tissues: mature capsules, young capsules, latex-included stem, latex-free stems, and roots, respectively (FDR: 0.05).

Latex-included Stems:

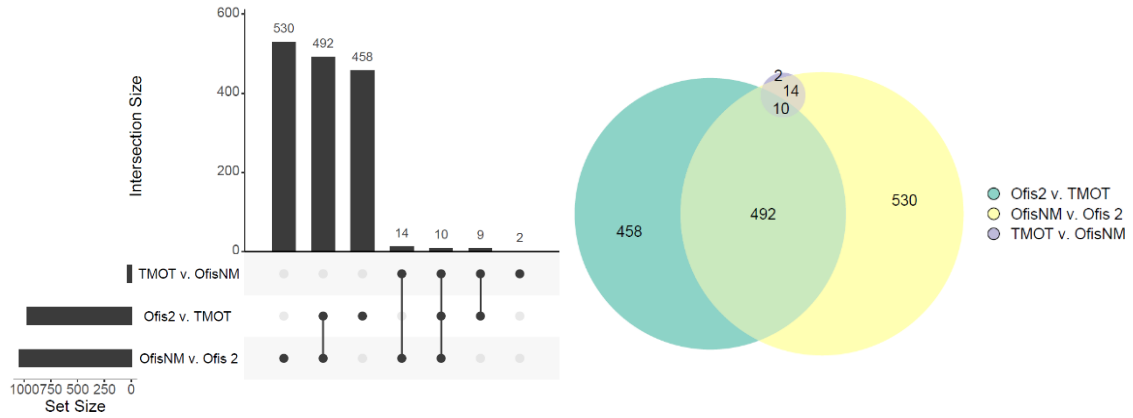

Latex-free Stems:

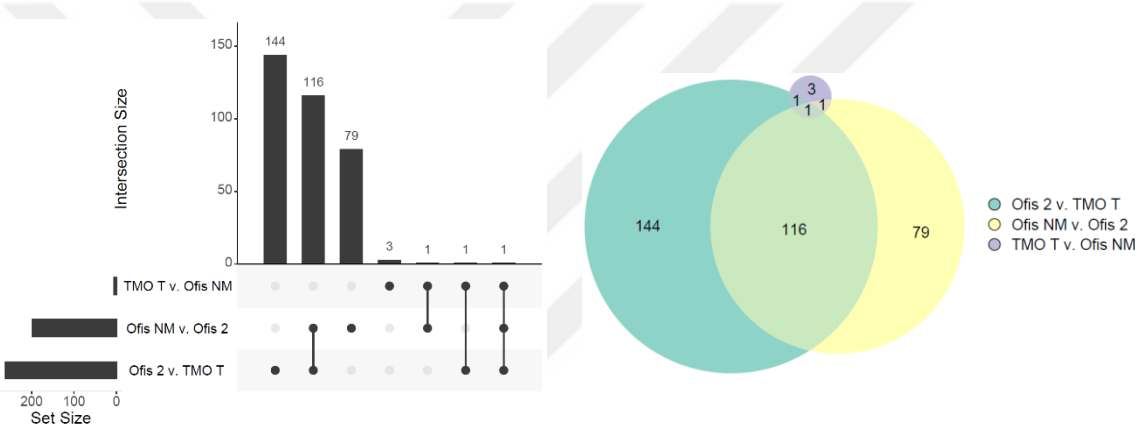

Roots:

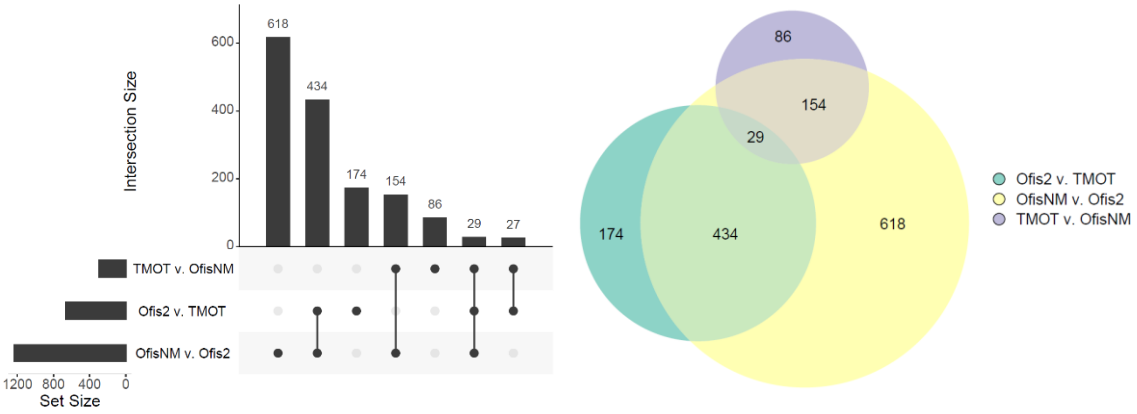

Figure 3.10. (cont.)

3.7. Functional Annotation of Differentially Expressed Proteins by Gene Ontology (GO) and Pathway Enrichment Analyses

Following the identification of DEPs in each pairwise comparison among the three opium poppy cultivars (Ofis NM, Ofis 2, and TMO T) for five tissues of interest, Gene Ontology (GO) and Kyoto Encyclopedia of Genes and Genomes (KEGG) pathway enrichment analyses were performed. These analyses provided insights into the molecular functions, biological processes and cellular components associated with the DEPs to identify key metabolic or signaling pathways that might be cultivar-specific in opium poppy.

3.7.1. GO Enrichment Analysis of DEPs across Cultivars

GO enrichment analyses of differentially expressed proteins in the three opium poppy cultivars (Ofis NM, Ofis 2, and TMO T) for the target tissues are represented in Figure 3.11-13.

a) Mature Capsules – Ofis NM v. Ofis 2:

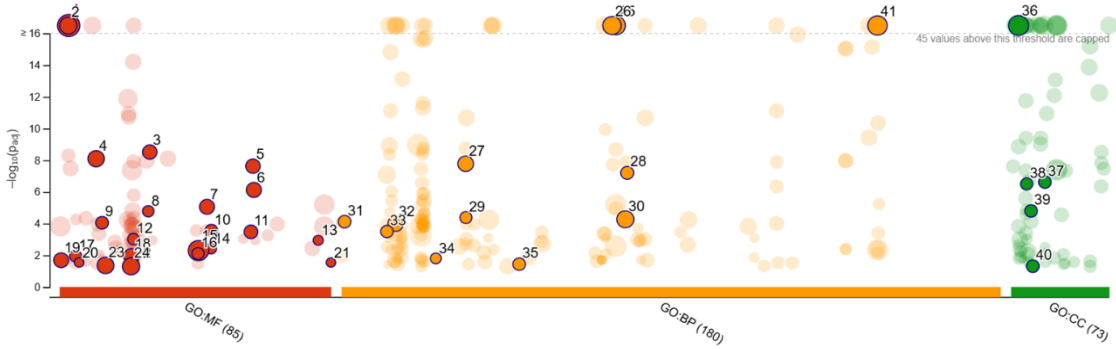

ID	Source	Term ID	Term Name	p_{adj} (query_1)
1	GO:MF	GO:0003824	catalytic activity	5.825×10^{-48}
2	GO:MF	GO:0003735	structural constituent of ribosome	1.123×10^{-20}
3	GO:MF	GO:0019843	rRNA binding	3.042×10^{-9}
4	GO:MF	GO:0005525	GTP binding	8.002×10^{-9}
5	GO:MF	GO:0051287	NAD binding	2.357×10^{-8}

(Cont. on the next page)

Figure 3.11. GO enrichment analysis of DEPs in mature capsules of (a) Ofis NM v. Ofis 2, (b) Ofis 2 v. TMO T, and (c) TMO T v. Ofis NM. The plot displays enriched Gene Ontology (GO) terms across three GO domains: molecular function (MF, red), biological process (BP, orange), and cellular component (CC, green). Each circle represents a GO term, with the x-axis categorizing the terms and the y-axis indicating their statistical significance (-log10 adjusted p-value). The size of the circles corresponds to the number of proteins associated with each GO term, and the terms with the highest significance are labeled with IDs for reference. The accompanying table lists the top significantly enriched GO terms, along with their adjusted p-values.

25	GO:BP	GO:0044281	small molecule metabolic process	2.167×10^{-62}
26	GO:BP	GO:0043603	amide metabolic process	3.189×10^{-34}
27	GO:BP	GO:0015979	photosynthesis	1.674×10^{-8}
28	GO:BP	GO:0045454	cell redox homeostasis	6.255×10^{-8}
29	GO:BP	GO:0015995	chlorophyll biosynthetic process	4.127×10^{-5}
36	GO:CC	GO:0005737	cytoplasm	2.548×10^{-101}
37	GO:CC	GO:0033178	proton-transporting two-sector ATPase complex, c...	2.398×10^{-7}
38	GO:CC	GO:0009654	photosystem II oxygen evolving complex	3.108×10^{-7}
39	GO:CC	GO:0019898	extrinsic component of membrane	1.583×10^{-5}
40	GO:CC	GO:0030120	vesicle coat	4.824×10^{-2}

b) Mature Capsules – Ofis 2 v. TMO T:

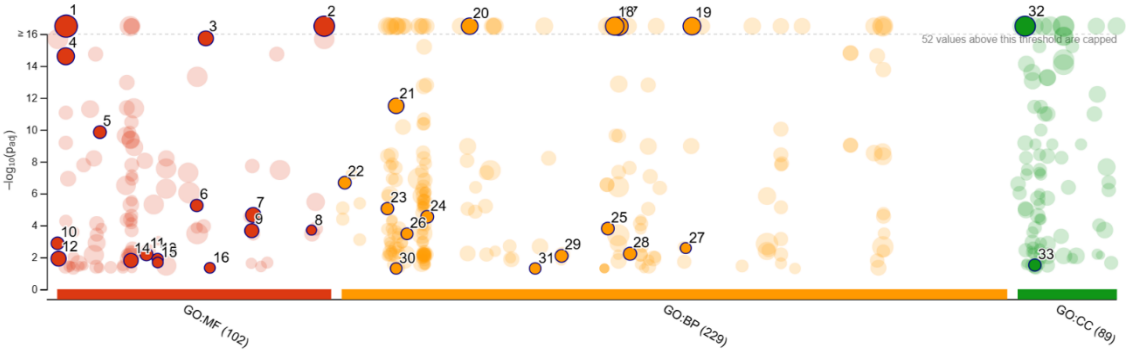

ID	Source	Term ID	Term Name	p_{adj} (query_1)
1	GO:MF	GO:0003824	catalytic activity	4.021×10^{-60}
2	GO:MF	GO:1901363	heterocyclic compound binding	8.883×10^{-20}
3	GO:MF	GO:0045182	translation regulator activity	1.844×10^{-16}
4	GO:MF	GO:0003735	structural constituent of ribosome	2.447×10^{-15}
5	GO:MF	GO:0008483	transaminase activity	1.403×10^{-10}
17	GO:BP	GO:0044281	small molecule metabolic process	4.847×10^{-71}
18	GO:BP	GO:0043603	amide metabolic process	5.793×10^{-38}
19	GO:BP	GO:0051641	cellular localization	5.480×10^{-34}
20	GO:BP	GO:0016192	vesicle-mediated transport	7.958×10^{-21}
21	GO:BP	GO:0006457	protein folding	3.152×10^{-12}
32	GO:CC	GO:0005737	cytoplasm	1.054×10^{-158}
33	GO:CC	GO:0015629	actin cytoskeleton	3.041×10^{-2}

c) Mature Capsules – TMO T v. Ofis NM:

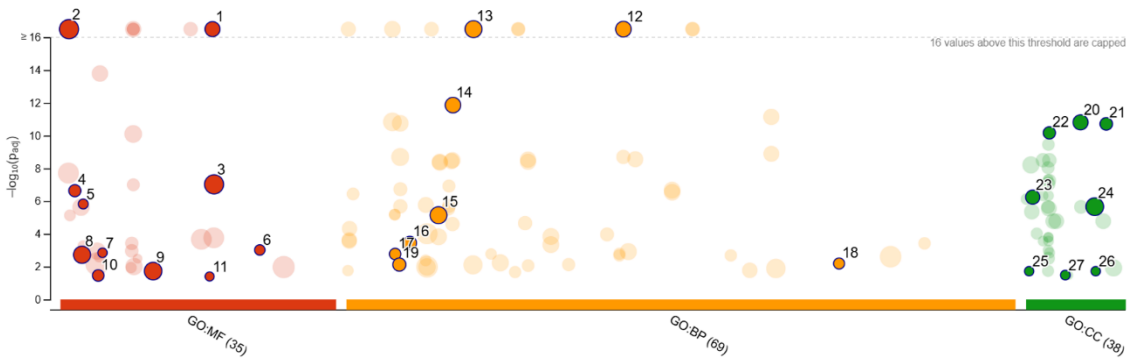

(Cont. on the next page)

Figure 3.11. (cont.)

ID	Source	Term ID	Term Name	p_{adj} (query_1)
1	GO:MF	GO:0046527	glucosyltransferase activity	5.117×10^{-34}
2	GO:MF	GO:0003723	RNA binding	1.678×10^{-23}
3	GO:MF	GO:0046914	transition metal ion binding	9.485×10^{-8}
4	GO:MF	GO:0004097	catechol oxidase activity	2.316×10^{-7}
5	GO:MF	GO:0004612	phosphoenolpyruvate carboxykinase (ATP) activity	1.500×10^{-6}
12	GO:BP	GO:0044042	glucan metabolic process	1.608×10^{-31}
13	GO:BP	GO:0016071	mRNA metabolic process	7.445×10^{-17}
14	GO:BP	GO:0010629	negative regulation of gene expression	1.379×10^{-12}
15	GO:BP	GO:0009820	alkaloid metabolic process	7.264×10^{-6}
16	GO:BP	GO:0006888	endoplasmic reticulum to Golgi vesicle-mediated t...	3.629×10^{-4}
20	GO:CC	GO:0048046	apoplast	1.550×10^{-11}
21	GO:CC	GO:0098797	plasma membrane protein complex	1.928×10^{-11}
22	GO:CC	GO:0030658	transport vesicle membrane	6.805×10^{-11}
23	GO:CC	GO:0005681	spliceosomal complex	5.723×10^{-7}
24	GO:CC	GO:0071944	cell periphery	2.182×10^{-6}

Figure 3.11. (cont.)

Molecular function (MF) analysis of DEPs from comparison of morphine-rich Ofis 2 mature capsules with noscapine-rich Ofis NM (Figure 3.11a) revealed significant enrichment in catalytic activity, ribosomal structural functions, and several binding activities, such as rRNA, GTP, and NAD binding. These functions suggest differences in protein synthesis, enzymatic activity, and energy-related metabolic pathways between the two cultivars. For biological processes (BP), photosynthesis and amide metabolic processes emerged as significantly enriched terms, which may contribute to differential growth or capsule development traits. The enrichment of chlorophyll biosynthetic processes also suggests cultivar-specific regulation of photosynthetic machinery.

The cytoplasm was the most significant cellular component (CC) term for the Ofis NM v. Ofis 2 mature capsule comparison. A majority of the DEPs identified in the comparison are localized in or associated with cytoplasmic processes. The cytoplasm serves as the primary site for numerous key cellular activities, including protein synthesis, energy metabolism, and enzymatic reactions, which aligns with the highly enriched molecular function (MF) and biological process (BP) terms. Notably, the enrichment of the "photosystem II oxygen evolving complex" further supports the differentiation of photosynthetic activity.

Comparison of Ofis 2 and TMO T mature capsules (Figure 3.11b) identified enrichment of similar GO terms except photosynthesis. Molecular functions such as structural constituent of ribosomes and heterocyclic compound binding were significantly enriched, suggesting variations in protein synthesis, enzymatic activity and secondary metabolite interactions.

The observed differences of Ofis 2 mature capsules with Ofis NM and TMO T may be attributed to their distinct metabolic and regulatory pathways tuned to distinct strategies for alkaloid biosynthesis in a broad aspect. Catalytic activity, being the most significantly enriched molecular function (MF), highlights the significant participation of enzymes in biochemical reactions within the capsules, including alkaloid biosynthesis. The significant alteration of catalytic activity in Ofis 2 is likely linked to the metabolic demand for enzymes involved in the production of high amounts of morphine.

In the comparison of Ofis NM and TMO T (Figure 3.11c), the GO analysis emphasized the enrichment of molecular functions such as glucosyltransferase activity and RNA binding, whereas biological process enrichment pointed to metabolic pathways related to mRNA processing, glucan metabolism, and ATP-dependent activities. These findings point to differences in carbohydrate metabolism and transcriptional regulation between these two cultivars. Interestingly, alkaloid metabolic processes also appeared significantly enriched, reflecting the role of specialized metabolism in differentiating these cultivars.

When there is significant overall variation between the cultivars, the pathway-specific differences may become less detectable because the biological variance between the samples overshadows the specific metabolic shifts related to BIA production. This can result in the appearance of more generalized processes, such as translation or enzyme activity, while specific pathways like alkaloid metabolism might not be as clearly highlighted. The number of DEPs in the pairwise comparison of Ofis NM and TMO T was lower than that in the comparison of Ofis 2 with Ofis NM and TMO T. As a result of this greater divergence between Ofis 2 and the other cultivars, the direct differences in alkaloid metabolic pathways might have been masked by the broader, more pronounced variations in other metabolic activities which are not directly associated with alkaloid pathways. Conversely, the lower number of DEPs in the Ofis NM v. TMO T comparison might have prioritized the differentiation of the proteome directly involved in the biosynthesis of noscapine and thebaine.

The GO enrichment terms obtained from young capsules did not show strong enrichment patterns and were excluded from the results, consistent with the initially low number of DEPs identified in this group. Young capsules might exhibit less pronounced proteomic changes in this developmental stage, resulting in weaker GO term associations.

a) Stems with Latex – Ofis NM v. Ofis 2:

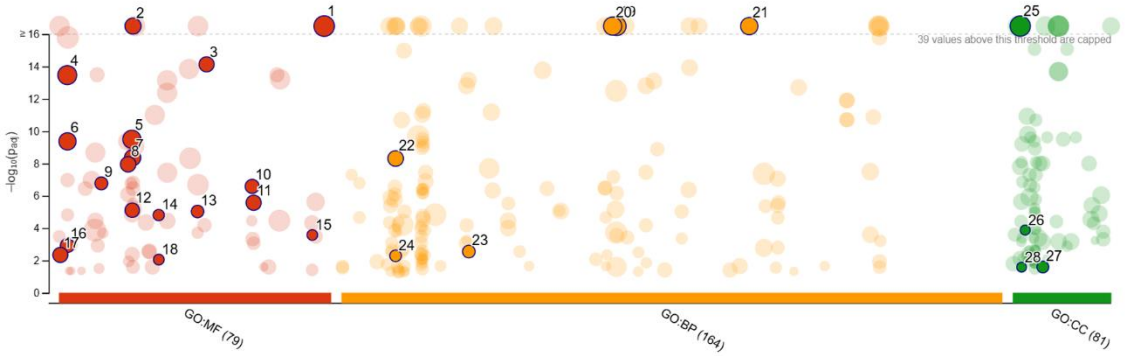

ID	Source	Term ID	Term Name	p_{adj} (query_1)
1	GO:MF	GO:1901363	heterocyclic compound binding	1.584×10^{-22}
2	GO:MF	GO:0016874	ligase activity	1.603×10^{-22}
3	GO:MF	GO:0045182	translation regulator activity	7.359×10^{-15}
4	GO:MF	GO:0003723	RNA binding	3.403×10^{-14}
5	GO:MF	GO:0016817	hydrolase activity, acting on acid anhydrides	3.168×10^{-10}
6	GO:MF	GO:0003735	structural constituent of ribosome	4.292×10^{-10}
19	GO:BP	GO:0044281	small molecule metabolic process	1.085×10^{-49}
20	GO:BP	GO:0043604	amide biosynthetic process	4.640×10^{-29}
21	GO:BP	GO:0070727	cellular macromolecule localization	1.972×10^{-19}
22	GO:BP	GO:0006457	protein folding	4.913×10^{-9}
23	GO:BP	GO:0016226	iron-sulfur cluster assembly	2.812×10^{-3}
24	GO:BP	GO:0006450	regulation of translational fidelity	5.159×10^{-3}
25	GO:CC	GO:0005737	cytoplasm	2.090×10^{-106}
26	GO:CC	GO:0008540	proteasome regulatory particle, base subcomplex	1.317×10^{-4}
27	GO:CC	GO:0032040	small-subunit processome	2.536×10^{-2}
28	GO:CC	GO:0005802	trans-Golgi network	2.599×10^{-2}

(Cont. on the next page)

Figure 3.12. GO enrichment analysis of DEPs in latex-included stems of (a) Ofis NM v. Ofis 2, (b) Ofis 2 v. TMO T, and (c) TMO T v. Ofis NM. The plot displays enriched Gene Ontology (GO) terms across three GO domains: molecular function (MF, red), biological process (BP, orange), and cellular component (CC, green). Each circle represents a GO term, with the x-axis categorizing the terms and the y-axis indicating their statistical significance (-log10 adjusted p-value). The size of the circles corresponds to the number of proteins associated with each GO term, and the terms with the highest significance are labeled with IDs for reference. The accompanying table lists the top significantly enriched GO terms, along with their adjusted p-values.

b) Stems with Latex – Ofis 2 v. TMO T:

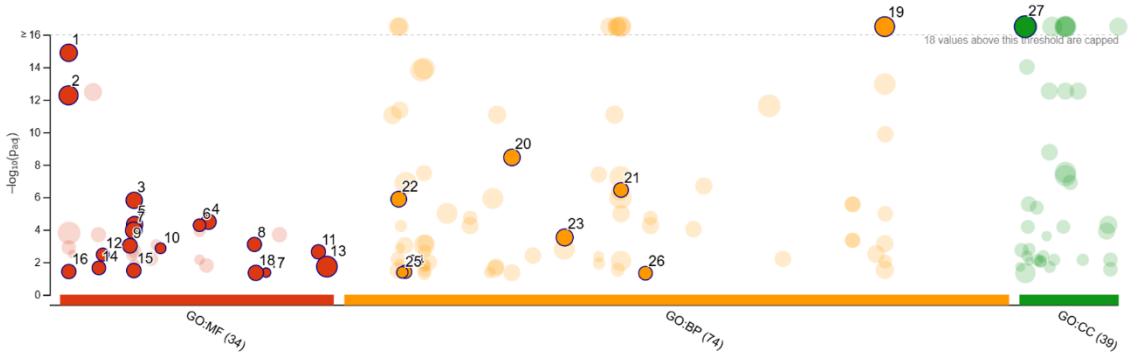

ID	Source	Term ID	Term Name	p_{adj} (query_1)
1	GO:MF	GO:0003735	structural constituent of ribosome	1.291×10^{-15}
2	GO:MF	GO:0003723	RNA binding	5.315×10^{-13}
3	GO:MF	GO:0016853	isomerase activity	1.555×10^{-6}
4	GO:MF	GO:0045182	translation regulator activity	3.236×10^{-5}
5	GO:MF	GO:0016874	ligase activity	4.774×10^{-5}
19	GO:BP	GO:1901566	organonitrogen compound biosynthetic process	7.545×10^{-26}
20	GO:BP	GO:0022613	ribonucleoprotein complex biogenesis	3.541×10^{-9}
21	GO:BP	GO:0044282	small molecule catabolic process	3.558×10^{-7}
22	GO:BP	GO:0006457	protein folding	1.319×10^{-6}
23	GO:BP	GO:0034660	ncRNA metabolic process	2.981×10^{-4}
24	GO:BP	GO:0006779	porphyrin-containing compound biosynthetic pro...	3.904×10^{-2}
25	GO:BP	GO:0006635	fatty acid beta-oxidation	4.231×10^{-2}
26	GO:BP	GO:0046148	pigment biosynthetic process	4.721×10^{-2}
27	GO:CC	GO:0005622	intracellular anatomical structure	1.043×10^{-58}

c) Stems with Latex – TMO T v. Ofis NM:

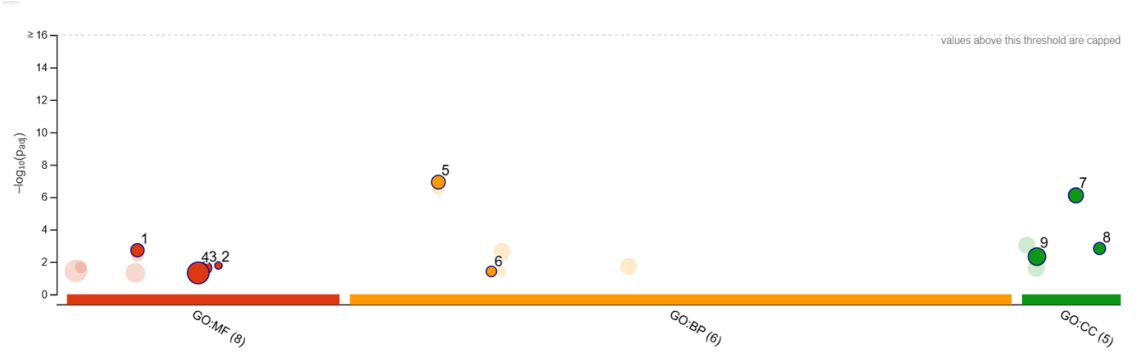

ID	Source	Term ID	Term Name	p_{adj} (query_1)
1	GO:MF	GO:0016682	oxidoreductase activity, acting on diphenols and r...	1.904×10^{-3}
2	GO:MF	GO:0046863	ribulose-1,5-bisphosphate carboxylase/oxygenase...	1.671×10^{-2}
3	GO:MF	GO:0043022	ribosome binding	2.359×10^{-2}
4	GO:MF	GO:0036094	small molecule binding	4.791×10^{-2}
5	GO:BP	GO:0009698	phenylpropanoid metabolic process	1.188×10^{-7}
6	GO:BP	GO:0019253	reductive pentose-phosphate cycle	3.865×10^{-2}
7	GO:CC	GO:0048046	apoplast	7.817×10^{-7}
8	GO:CC	GO:0098552	side of membrane	1.486×10^{-3}
9	GO:CC	GO:0009536	plastid	4.721×10^{-3}

Figure 3.12. (cont.)

In the GO enrichment of DEPs from comparison of latex-including stems (Figure 3.12), biological processes (BP) of amide metabolic process, organonitrogen compound biosynthetic process, cellular macromolecule localization and ribonucleoprotein complex biogenesis were highlighted along with the molecular function (MF) terms such as heterocyclic compound binding, ligase activity, translation regulator activity, structural constituent of ribosome and RNA binding. The most enriched cellular components were cytoplasm and intracellular anatomical structure. Latex biosynthesis and storage rely heavily on intracellular organelles like plastids (for precursor synthesis), the endoplasmic reticulum (for protein processing and lipid metabolism), and vacuoles (for storage of secondary metabolites like alkaloids) (Gracz-Bernaciak et al., 2021). The enrichment of this term might suggest that these organelles are actively engaged in processes that are critical for latex production and storage, such as alkaloid biosynthesis and transport.

Enrichment of organonitrogen compound biosynthetic process likely reflects the biosynthesis of nitrogen-containing secondary metabolites, such as alkaloids, which are produced and transported in the stems. Also, alkaloids are derived from amino acid precursors and involve complex enzymatic pathways that integrate nitrogen into their structure (Gracz-Bernaciak et al., 2021). The enrichment of this process in latex-including stems emphasizes metabolic specialization, particularly in relation to secondary metabolism and nitrogen usage. The BP of "phenylpropanoid metabolic process" and "reductive pentose-phosphate cycle" and the CC of "plastid" were also enriched in the comparison of TMO T and Ofis NM, suggesting active secondary metabolism and photosynthesis similar to mature capsules. The phenylpropanoid metabolic process involves the conversion of phenylalanine into a wide array of secondary metabolites, such as flavonoids, lignins, and other aromatic compounds. Plastids house the shikimate pathway, which provides precursors for both phenylpropanoids (via phenylalanine and cinnamic acid) and benzylisoquinoline alkaloids (via tyrosine and dopamine) (Dixon et al., 2002; Facchini et al., 2007). Thus, metabolic flux through phenylpropanoid biosynthesis can influence the availability of precursors like tyrosine and phenylalanine, which are critical for BIA biosynthesis. In addition, environmental factors that activate the phenylpropanoid pathway (e.g., cinnamic acid production) may also upregulate alkaloid biosynthesis as part of a coordinated defense response (Dixon et al., 2002).

GO enrichment analysis of DEPs both in capsules and latex-including stems of opium poppy cultivars showed a possible relationship between the term "photosynthesis"

and alkaloid biosynthesis. Light is a key environmental factor that influences the biosynthesis and accumulation of certain secondary metabolites in plants, including alkaloids (Thoma et al., 2020). Research has demonstrated that enhancing photosynthetic efficiency can lead to increased production of alkaloids such as morphine and thebaine in opium poppy (Kara, 2021). For instance, the application of the plant growth regulator triacontanol has been reported to elevate morphine content while enhancing photosynthetic activity (Srivastava and Sharma, 1990). Similarly, treatment with a consortium of endophytes has been shown to simultaneously improve morphine and thebaine levels and photosynthetic performance in poppy plants (Ray et al., 2019). In other research, the term photosynthesis was shown to be the most abundant term in the GO analysis of opium poppy stems (Aykanat & Türktaş, 2024). As supported by the literature, the findings in this study suggest a link between high photosynthetic assimilation rates and alkaloid biosynthesis, with the energy generated through photosynthesis likely supporting the metabolic demands of alkaloid production. The GO enrichment terms determined in the latex-free stems (Figure 3.13), on the other hand, showed weaker enrichment patterns with lower significance values, in agreement with the low number of DEPs identified in this group. All of the three pairwise comparisons revealed enrichment of similar GO terms.

a) Stems without Latex – Ofis NM v. Ofis 2:

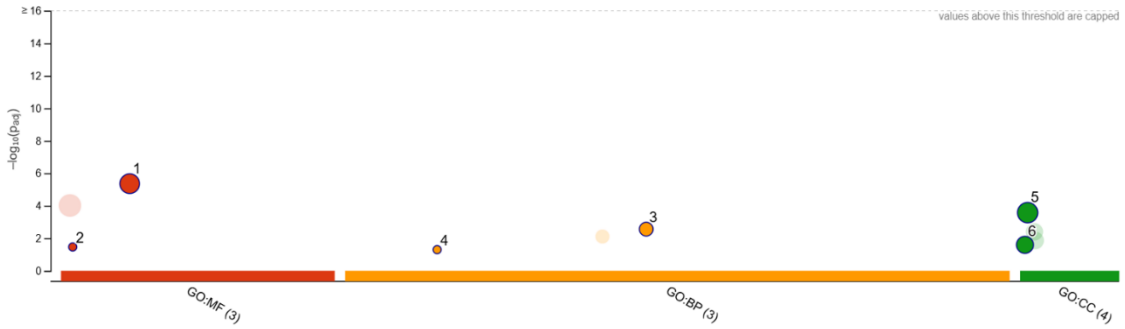

(Cont. on the next page)

Figure 3.13. GO enrichment analysis of DEPs in latex-free stems of (a) Ofis NM v. Ofis 2, (b) Ofis 2 v. TMO T, and (c) TMO T v. Ofis NM.The plot displays enriched Gene Ontology (GO) terms across three GO domains: molecular function (MF, red), biological process (BP, orange), and cellular component (CC, green). Each circle represents a GO term, with the x-axis categorizing the terms and the y-axis indicating their statistical significance (-log10 adjusted p-value). The size of the circles corresponds to the number of proteins associated with each GO term, and the terms with the highest significance are labeled with IDs for reference. The accompanying table lists the top significantly enriched GO terms, along with their adjusted p-values.

ID	Source	Term ID	Term Name	p_{adj} (query_1)
1	GO:MF	GO:0016491	oxidoreductase activity	4.344×10^{-6}
2	GO:MF	GO:0003973	(S)-2-hydroxy-acid oxidase activity	3.429×10^{-2}
3	GO:BP	GO:0046148	pigment biosynthetic process	2.738×10^{-3}
4	GO:BP	GO:0009854	oxidative photosynthetic carbon pathway	4.978×10^{-2}
5	GO:CC	GO:0005737	cytoplasm	2.640×10^{-4}
6	GO:CC	GO:0005576	extracellular region	2.521×10^{-2}

b) Stems without Latex – Ofis 2 v. TMO T:

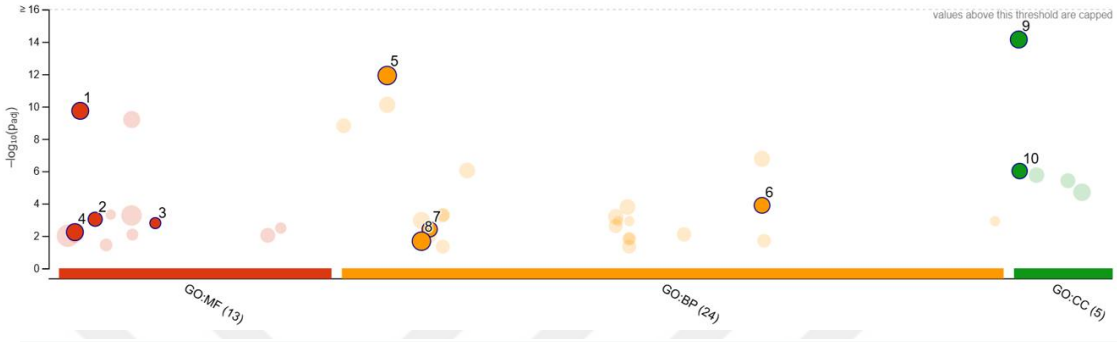

ID	Source	Term ID	Term Name	p_{adj} (query_1)
1	GO:MF	GO:0004553	hydrolase activity, hydrolyzing O-glycosyl compou...	1.839×10^{-10}
2	GO:MF	GO:0005507	copper ion binding	9.237×10^{-4}
3	GO:MF	GO:0030570	pectate lyase activity	1.609×10^{-3}
4	GO:MF	GO:0004175	endopeptidase activity	5.805×10^{-3}
5	GO:BP	GO:0005975	carbohydrate metabolic process	1.204×10^{-12}
6	GO:BP	GO:0071555	cell wall organization	1.285×10^{-4}
7	GO:BP	GO:0009653	anatomical structure morphogenesis	3.902×10^{-3}
8	GO:BP	GO:0009056	catabolic process	2.105×10^{-2}
9	GO:CC	GO:0005576	extracellular region	7.172×10^{-15}
10	GO:CC	GO:0005618	cell wall	9.692×10^{-7}

c) Stems without Latex – TMO T v. Ofis NM:

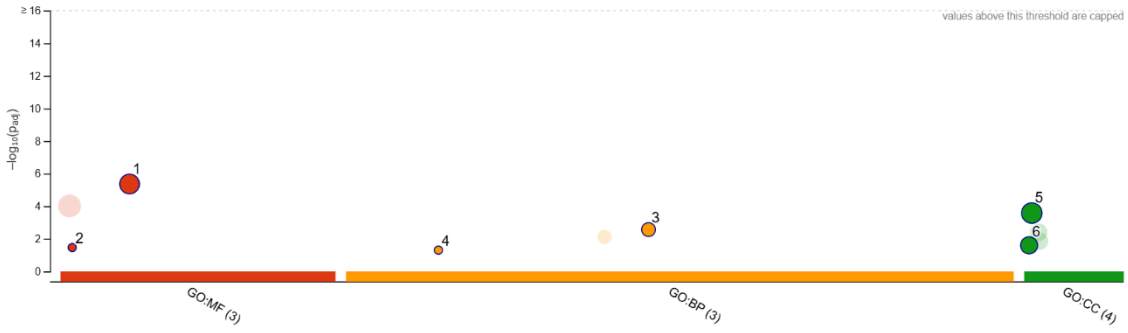

ID	Source	Term ID	Term Name	p_{adj} (query_1)
1	GO:MF	GO:0016491	oxidoreductase activity	4.344×10^{-6}
2	GO:MF	GO:0003973	(S)-2-hydroxy-acid oxidase activity	3.429×10^{-2}
3	GO:BP	GO:0046148	pigment biosynthetic process	2.738×10^{-3}
4	GO:BP	GO:0009854	oxidative photosynthetic carbon pathway	4.978×10^{-2}
5	GO:CC	GO:0005737	cytoplasm	2.640×10^{-4}
6	GO:CC	GO:0005576	extracellular region	2.521×10^{-2}

Figure 3.13. (cont.)

In contrast to latex-including stems, DEPs across latex-free stems of different opium poppy cultivars were enriched in molecular function (MF) terms such as "oxidoreductase activity, acting on diphenols", "S-2-hydroxy-acid oxidase activity", "hydrolase activity, hydrolyzing O-glycosyl compounds", and "pectate lyase activity", alongside biological process (BP) terms like "carbohydrate metabolic process", “oxidative photosynthetic carbon pathway”, "cell wall organization", and "pigment biosynthetic process".

The removal of latex may have shifted the enrichment of cultivar-specific differentiation in the cellular activities of the remaining stem tissues, leading to an increased emphasis on the mentioned GO terms. For instance, carbohydrate metabolism is essential for synthesizing cell wall components like cellulose and hemicellulose, which provide mechanical strength and flexibility to the stems. Hydrolase (on O-glycosyl compounds) and pectate lyase (pectin degradation) activities also suggest dynamic cell wall remodeling of opium poppy stems in a cultivar-specific way, consistent with the cellular component (CC) terms "extracellular region" and "cell wall” (Gilbert, 2010). Furthermore, plants use oxidoreductase enzymes to respond to environmental stress, including wounding, infection, and oxidative damage (Sharma et al., 2012).

Oxidoreductases, such as polyphenol oxidases, play a key role in generating reactive oxygen species (ROS) and other signaling molecules, which can trigger the activation of stress-related metabolic pathways, including biosynthesis of alkaloids serving as chemical defenses against herbivores and pathogens (Waszczak et al., 2018). Enhanced oxidoreductase activity could facilitate the diversion of precursors like tyrosine into specific branches of the BIA biosynthetic pathway, leading to higher production of different alkaloids depending on the cultivar's genetic and environmental context (Winzer et al, 2015).

3.7.2. KEGG Pathway Enrichment Analysis of DEPs across Cultivars

KEGG pathway enrichment analyses of DEPs between the three opium poppy cultivars (Ofis NM, Ofis 2, and TMO T) for the target tissues are represented in Figure 3.14-16.

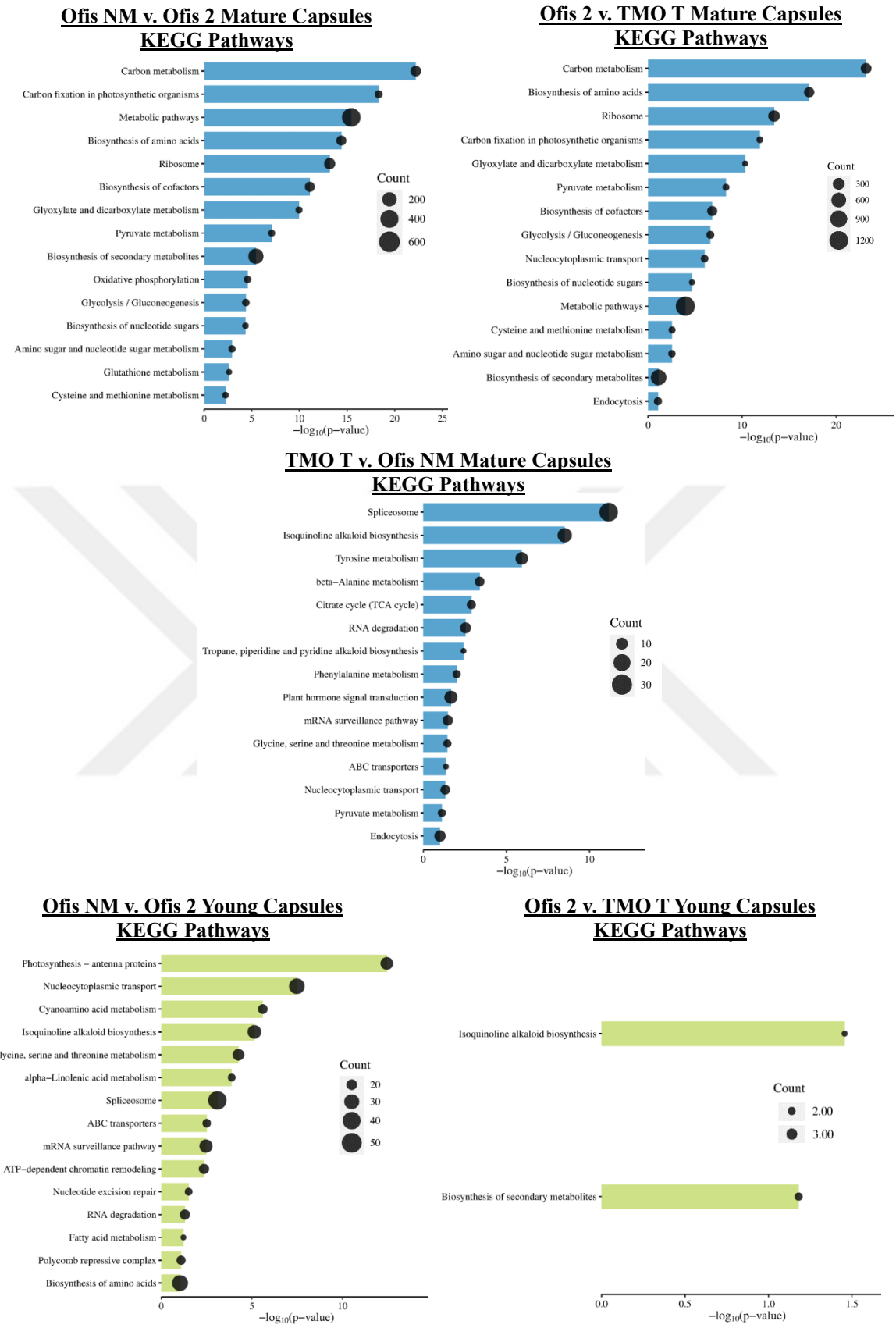

Figure 3.14. KEGG pathway enrichment analysis of DEPs in mature capsules of opium poppy across pairwise comparisons of three cultivars (Ofis NM, Ofis 2, and TMO T). The x-axis shows the -log(p-value) indicating the significance of pathway enrichment, while the bubble size represents the number of DEPs contributing to each pathway.

In the comparison of morphine-rich Ofis 2 with noscapine-rich Ofis NM and thebaine-rich TMO T cultivars, distinct patterns emerge between young and mature capsules regarding KEGG pathway enrichment. In young capsules, despite the low number of DEPs, the BIA biosynthesis pathway showed significant enrichment. This might suggest that even at an early stage of capsule development, the biosynthetic pathways for alkaloid production become cultivar-specialized.

Particularly in the comparison of Ofis 2 and TMO T young capsules, three DEPs are exclusively enriched in the BIA biosynthesis pathway. It could be hypothesized that alkaloid biosynthesis is one of the earliest diverging pathways between these two cultivars at that early stage in capsule development. In mature capsules, the pathway enrichment became broader and more significant, including more general metabolic pathways such as carbon metabolism, amino acid biosynthesis, and biosynthesis of secondary metabolites. This represents a higher degree of cultivar-specific cellular activity in mature capsules, possibly reflecting metabolic divergence and further specialization during development.

In contrast, KEGG pathway enrichment comparison between Ofis NM and TMO T young capsules did not show any significant results. The lack of significant KEGG pathway enrichment in young capsules when comparing Ofis NM (noscapine-accumulator) and TMO T (thebaine-accumulator) might suggest that, at the early developmental stage, differentiation between these two cultivars at the protein expression level is minimal. In mature capsules, on the other hand, BIA biosynthesis was highly enriched in contrast to pairwise comparisons of Ofis 2 (morphine accumulator). This aligns with the fact that morphine and thebaine are structurally and biosynthetically very closely related alkaloids within the morphinan branch of BIA biosynthesis. Both morphine and thebaine share many upstream biosynthetic steps, and their divergence occurs only at the final steps of alkaloid production as opposed to divergence of the noscapine branch earlier in the pathway. Enrichment of tyrosine metabolism, which is a key precursor in BIA biosynthesis, in mature capsules of TMO T v. Ofis NM also shows the cultivar-specific differentiation of capsules in terms of producing precursors required for downstream alkaloid biosynthesis during maturation.

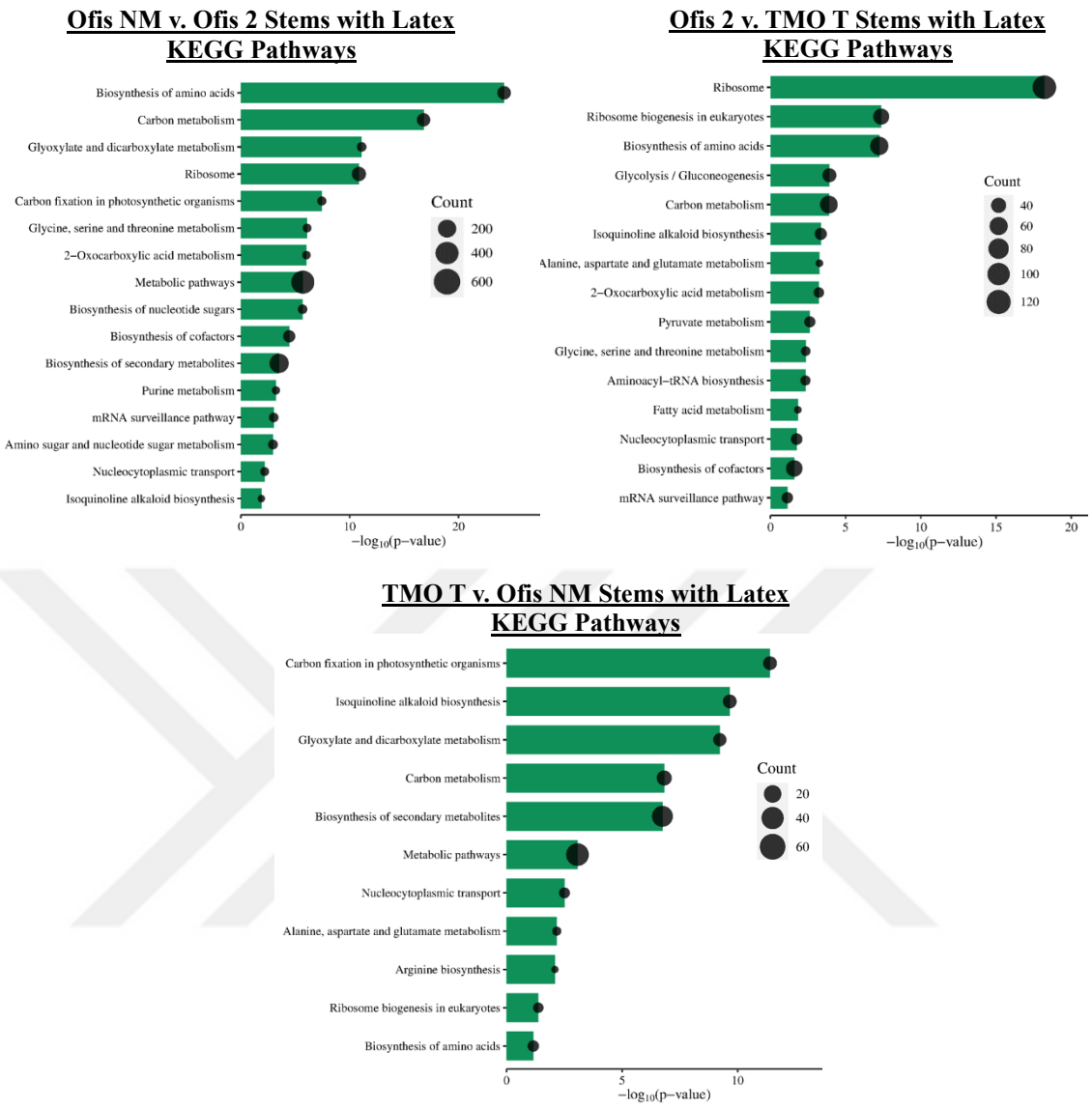

Figure 3.15. KEGG pathway enrichment analysis of DEPs in latex-included stems of opium poppy across pairwise comparisons of three cultivars (Ofis NM, Ofis 2, and TMO T). The x-axis shows the -log(p-value) indicating the significance of pathway enrichment, while the bubble size represents the number of DEPs contributing to each pathway.

In agreement with the results of GO enrichment analysis, KEGG pathway enrichment of DEPs across the three cultivars of latex-including stems highlighted metabolic pathways of carbon metabolism, ribosome, biosynthesis of secondary metabolites and amino acids, as well as BIA biosynthesis. The prominence of pathways like biosynthesis of secondary metabolites and specifically BIAs was consistent with the biological role of latex in plant defense. The enrichment of ribosome pathways suggested differential protein synthesis in stems, likely to meet the biosynthetic demands of alkaloid-producing enzymes.

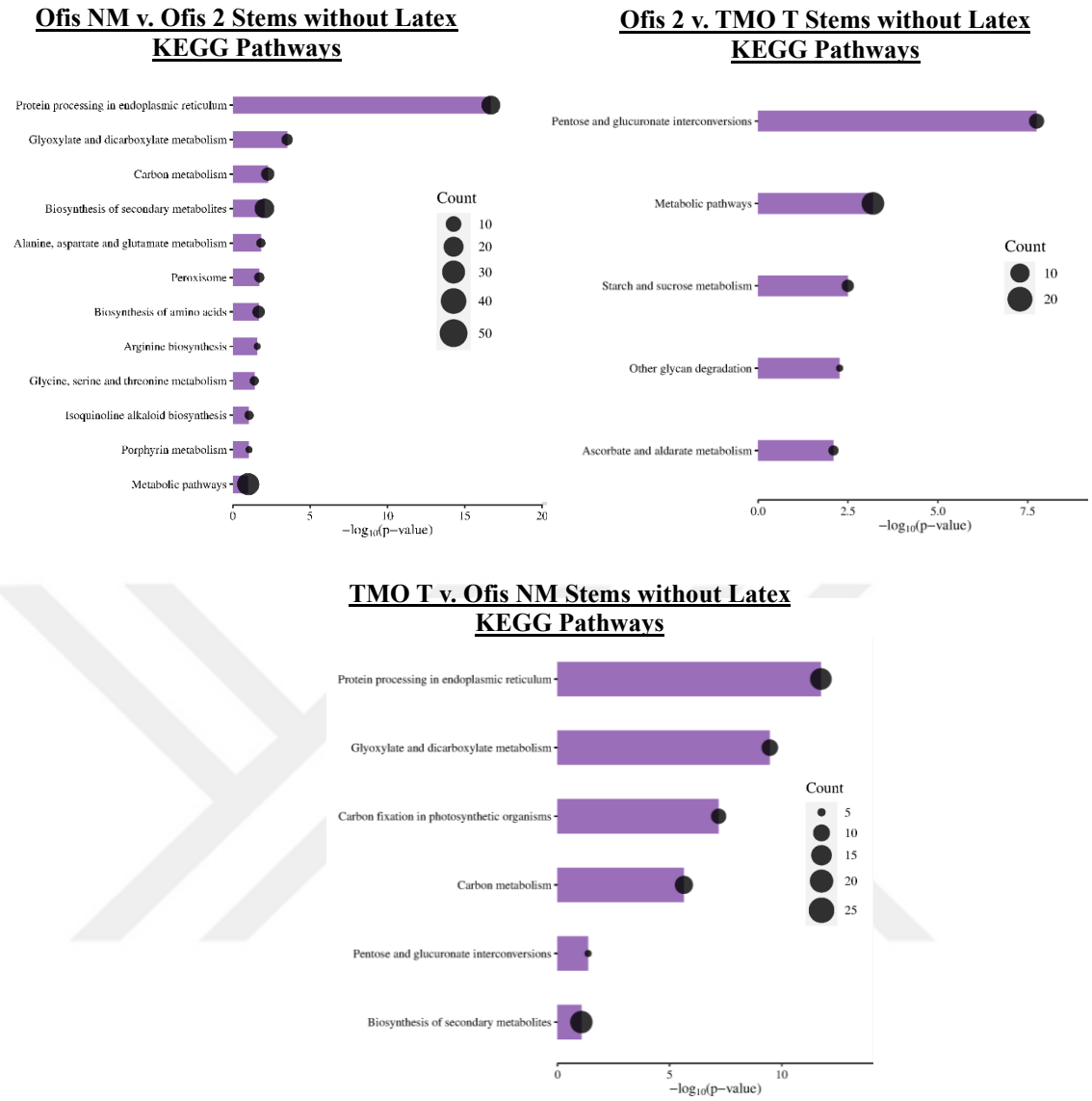

Figure 3.16. KEGG pathway enrichment analysis of DEPs in latex-included stems of opium poppy across pairwise comparisons of three cultivars (Ofis NM, Ofis 2, and TMO T). The x-axis shows the -log(p-value) indicating the significance of pathway enrichment, while the bubble size represents the number of DEPs contributing to each pathway.

DEPs between latex-free stems of cultivars, however, were enriched in pathways such as “protein processing in ER”, “glyoxylate and dicarboxylate metabolism”, “starch and sucrose metabolism” and “pentose and glucuronate interconversions”. The enrichment of these pathways in latex-free stems underscores their role in maintaining energy balance, carbon storage, and structural support in plants. Glyoxylate and dicarboxylate metabolism facilitates the conversion of stored lipids into carbohydrates, providing a crucial energy source for non-photosynthetic tissues like stems (Maurino &

Engqvist, 2015). Starch and sucrose metabolism reflects the stem's function as a carbohydrate reservoir, enabling sugar storage and translocation to energy-demanding tissues of opium poppy. Meanwhile, the pentose and glucuronate interconversions pathway contributes to cell wall biosynthesis and remodeling, essential for the stem's structural integrity and support. These metabolic activities align with the fundamental roles of stems in resource allocation, energy management, and mechanical support within the plant (Pilatzke-Wunderlich and Nessler, 2001).

3.7.3. Differential Expression of Proteins Involved in BIA Pathway

The DEPs with the greatest fold changes that are known to be involved in the BIA metabolism of opium poppy were further investigated in the mature capsules and latex-included stems across three opium poppy cultivars as represented in Figure 3.17 and Figure 3.18, respectively.

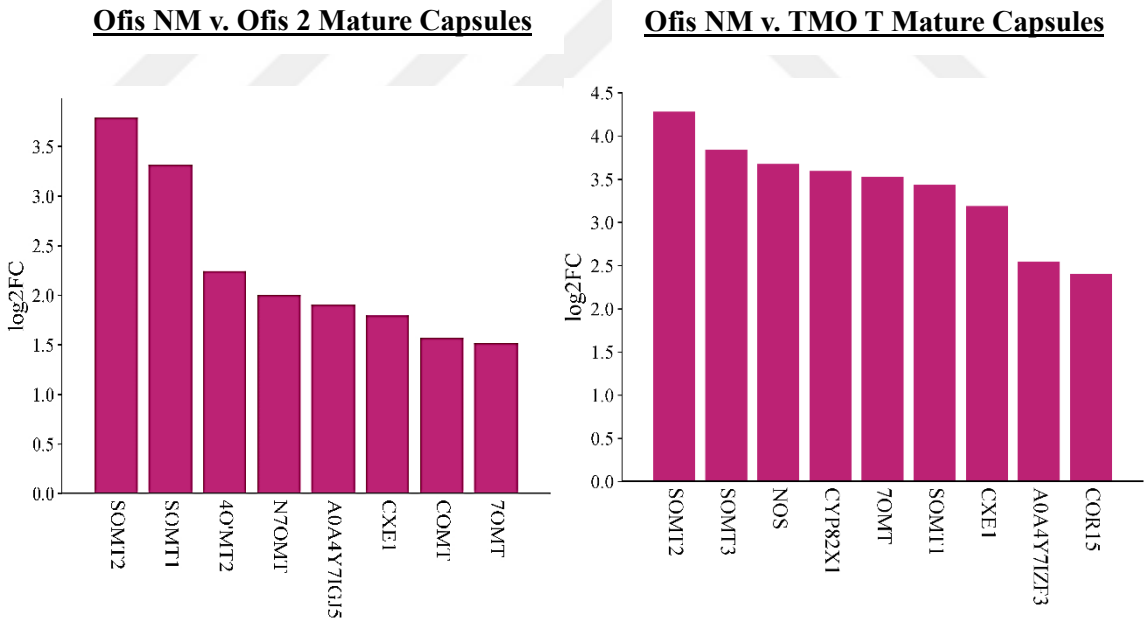

(Cont. on the next page)

Figure 3.17. Bar plots representing top differentially expressed proteins involved in the BIA metabolism of opium poppy mature capsules across pairwise comparisons of three cultivars (Ofis NM, Ofis 2, and TMO T). The x-axis shows the names of DEPs, and the y-axis shows the difference (log2FC) in protein abundance (FDR: 0.05). Proteins up-regulated in the first cultivar of each comparison are shown as pink in the upper graphs, while those down-regulated are shown as cyan in the lower graph.

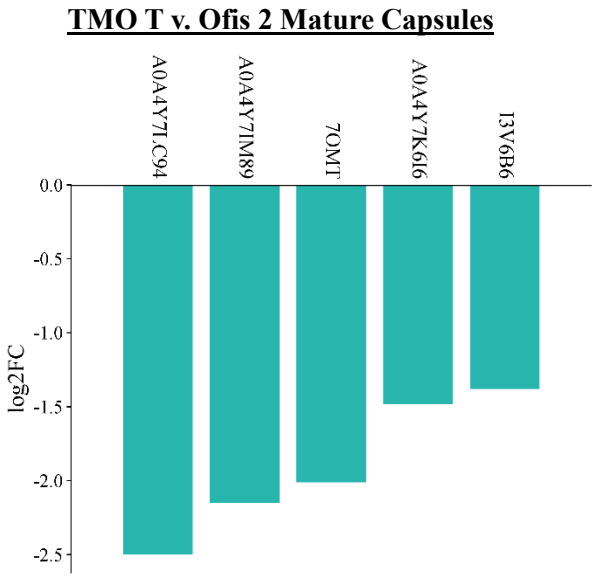

Figure 3.17. (cont.)

In the comparison between mature capsules of Ofis NM with Ofis 2 and TMO T, DEPs associated with the noscapine branch of BIA biosynthesis, such as SOMT1 (scoulerine 9-O-methyltransferase 1), SOMT2 (3-O-acetyl-4'-O-demethylpapaveroxine 4'-O-methyltransferase OMT2), and SOMT3 (3-O-acetyl-4'-O-demethylpapaveroxine 4'-O-methyltransferase OMT3), were significantly up-regulated in Ofis NM. SOMT1 enzyme is involved in the methylation of (S)-scoulerine into (S)-tetrahydrocolumbamine, which is essential in the early step of noscapine biosynthesis. OMT2 and OMT2 form a heterodimer and catalyze the conversion of 3-O-acetyl-4'-O-demethylpapaveroxine to 3-O-acetylpapaveroxine (Dang & Facchini, 2012; Li et al., 2018; Park et al., 2018). Therefore, the higher expression of these enzymes strongly aligns with the accumulation of noscapine alkaloid in Ofis NM (Figure 3.19).

CYP82X1 (1-hydroxy-13-O-acetyl-N-methylcanadine 8-hydroxylase), CXE1 (3-O-acetylpapaveroxine carboxylesterase) and NOS (noscapine synthase) were also up-regulated in Ofis NM compared to TMO T and Ofis 2, underscoring the enhanced metabolic flux toward the noscapine biosynthesis pathway in Ofis NM. CYP82X1 facilitates hydroxylation reactions essential for transforming intermediates like 1-hydroxy-13-O-acetyl-N-methylcanadine into key noscapine precursors, while CXE1 is involved in deacetylating intermediates such as 3-O-acetylpapaveroxine, further driving

the pathway forward to noscapine (Dang and Facchini, 2012; Dang and Facchini, 2014). NOS (noscapine synthase) catalyzes the final step in noscapine biosynthesis, forming the noscapine alkaloid (Dang and Facchini, 2015; Li et al., 2018). This coordinated up-regulation reflects the cultivar's specialization in noscapine production, distinguishing it from Ofis 2 and TMO T which prioritize morphine and thebaine biosynthesis, respectively.

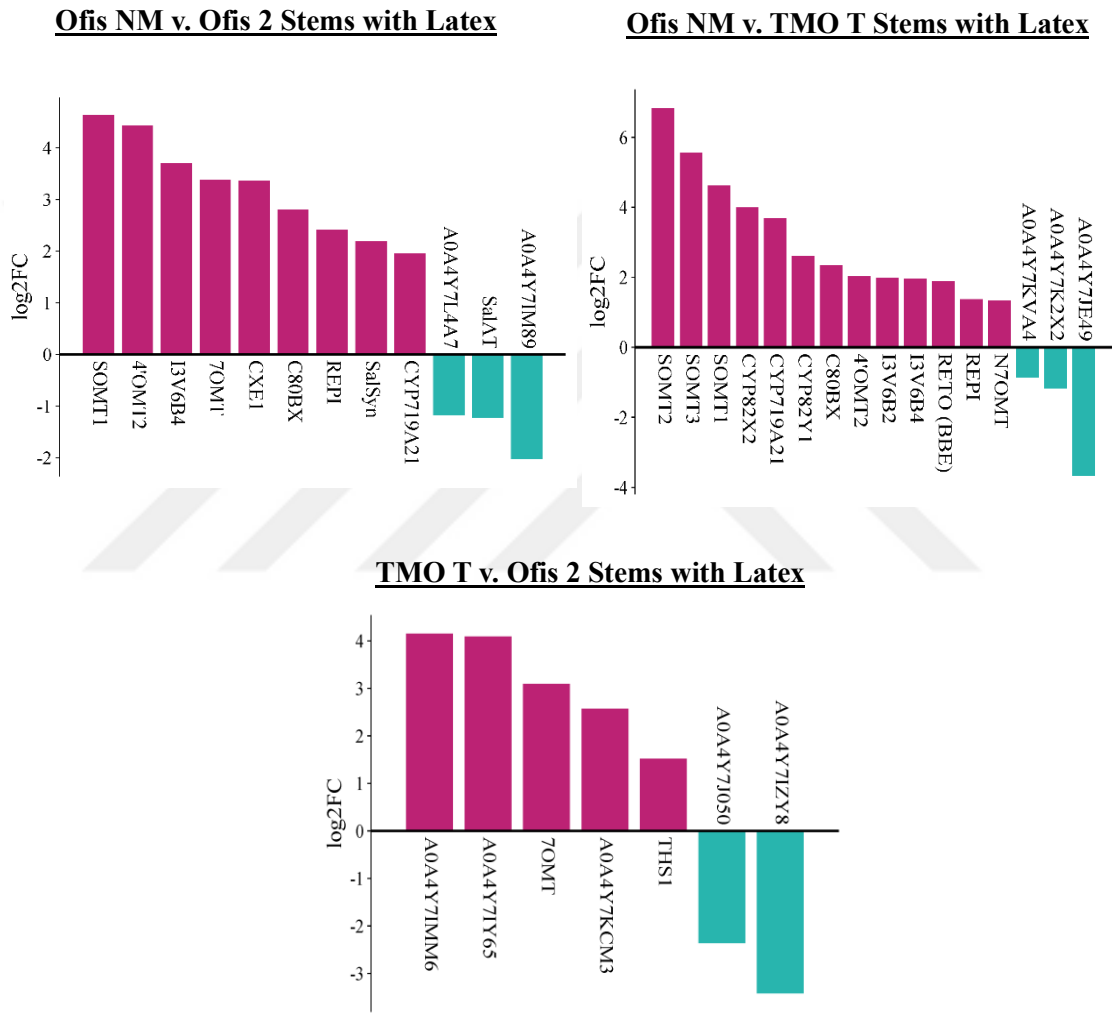

Figure 3.18. Bar plots representing top differentially expressed proteins involved in the BIA metabolism of opium poppy latex-included stems across pairwise comparisons of three cultivars (Ofis NM, Ofis 2, and TMO T). The x-axis shows the names of the DEPs and the y-axis shows the difference (log_2FC) in protein abundance (FDR: 0.05). Proteins up-regulated in the first cultivar of each comparison are shown as pink at the upper part, while those down-regulated are shown as cyan at the bottom.

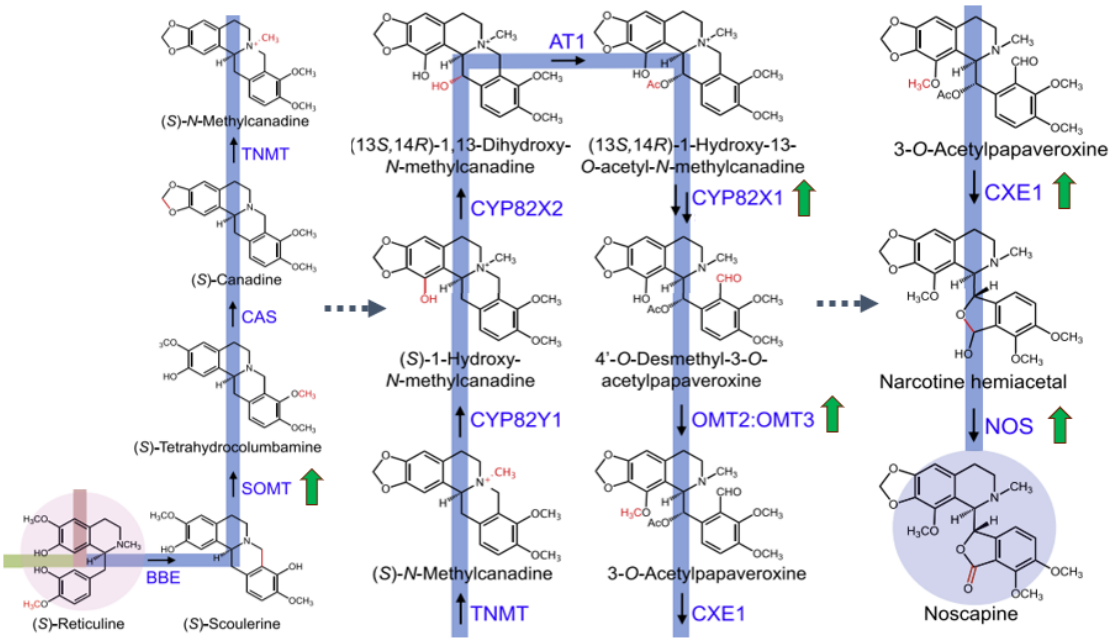

Figure 3.19. Differential expression of enzymes in the noscapine branch of the BIA pathway. Green arrows represents the enzymes upregulated in mature capsules of Ofis NM compared to either Ofis 2 or TMO T.

4'OMT2 (3'-hydroxy-N-methyl-(S)-coclaurine 4'-O-methyltransferase 2) enzyme catalyzes the methylation of (S)-3'-hydroxy-N-methylcoclaurine, forming (S)-reticuline, a crucial intermediate in the biosynthesis of morphine, noscapine, and other BIAs in opium poppy (Morishige et al., 2020). It is also involved in the papaverine branch of the BIA pathway by converting (S)-coclaurine into (S)-norreticuline (Desgagné-Penix & Facchini, 2012; Pathak et al., 2013; Ziegler et al., 2005). N7OMT (norreticuline 7-O-methyltransferase) also serves in the papaverine branch, catalyzing the methylation of (S)-norreticuline into (S)-tetrahydropapaverine (Pathak et al., 2013, Pienkny et al, 2009). Up-regulation of 4'OMT2 and N7OMT in Ofis NM compared to Ofis 2 was determined as expected, underscoring the cultivar's optimized enzymatic machinery to increase noscapine accumulation, as well as relatively higher papaverine production (Figure 3.20).

7OMT (reticuline 7-O-methyltransferase) is another enzyme of the BIA pathway, but it acts in the opposite direction in both the noscapine and morphine branches, by converting (S)-reticuline to (S)-laudanosine and thereby reducing the availability of precursors for morphine, thebaine and noscapine alkaloids. The enzyme showed up-

regulation in Ofis NM compared to both Ofis 2 and TMO T mature capsules, and also up-regulation in Ofis 2 compared to TMO T. Previous research showed a regulatory effect of 4OMT and 7OMT enzymes as a pair that directs the flux of BIA pathway in different directions (Gurkok et al., 2016; Ounaroon et al., 2003; Weid et al., 2004). Silencing and overexpression of 4′OMT and 7OMT gene expression resulted in varied levels of BIA production in both capsule and stem tissues.

It was previously revealed that silencing of 4'OMT resulted in an increase of morphine, thebaine and noscapine accumulation in capsules, whereas overexpression of 7OMT decreased the amount of noscapine (Gurkok et al., 2016). The up-regulation of 7OMT in Ofis NM compared to Ofis 2 and TMO T can be evaluated as a potential regulatory mechanism that influences the balance of BIA production in mature capsules. This counterintuitive result compared to previous studies could suggest a tissue-specific regulation or feedback mechanism in Ofis NM that compensates for 7OMT activity, ensuring sufficient flux into the noscapine pathway despite competing methylation. Additionally, the higher papaverine levels in Ofis NM might also be a result of the altered flux caused by 7OMT up-regulation, as laudanosine can indirectly divert intermediates to the papaverine branch (Pienkny et al., 2009).

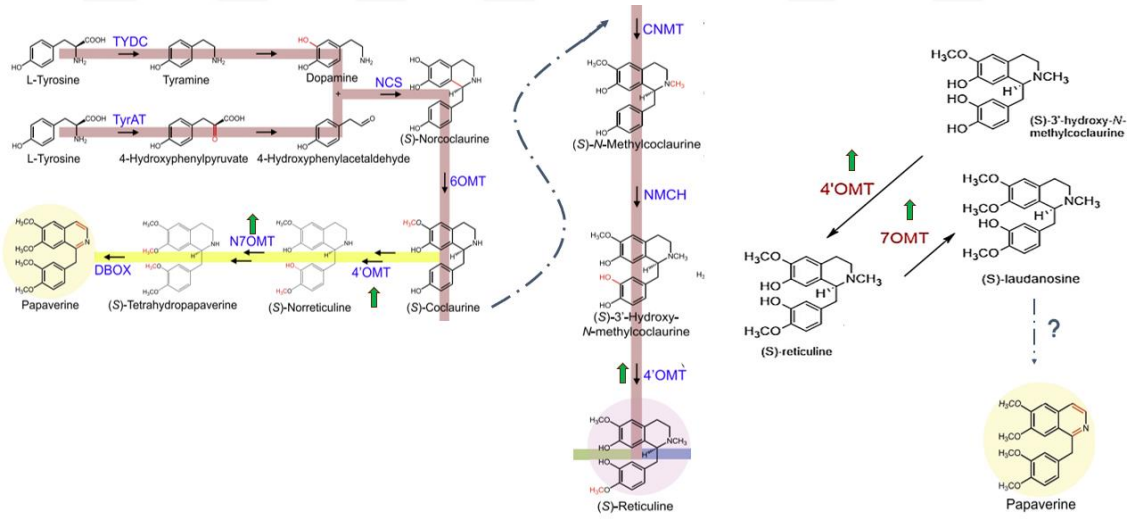

Figure 3.20. Differential expression of enzymes in the papaverine branch of the BIA pathway. Green arrows represents the enzymes upregulated in mature capsules of Ofis NM compared to either Ofis 2 or TMO T.

Interestingly, COR (NADPH-dependent codeinone reductase) which is responsible for conversion of codeinone to codeine and morphinone to morphine was one of the significantly up-regulated proteins in Ofis NM mature capsules compared to TMO

T (Wijekoon and Facchini, 2012) (Figure 3.21). In TMO T, thebaine is the dominant alkaloid, suggesting that the metabolic flux prioritizes the accumulation of thebaine itself rather than its downstream conversion to morphine (Huang and Kutchan, 2000). This restriction step could explain the relatively lower expression of COR15 in TMO T, as thebaine serves as the endpoint of its alkaloid biosynthesis. In contrast, Ofis NM maintains higher COR15 expression despite its noscapine-rich profile, potentially reflecting a more balanced utilization of intermediates like thebaine, allowing for morphine production to coexist with active noscapine synthesis.

The absence of significant differentiation in the downstream morphine branch enzymes except COR (such as SalSyn, SaIR, SalAT, CODM, etc.) among the mature capsules of the three cultivars can be attributed to the consistently higher levels of morphine relative to other alkaloids, such as thebaine and noscapine, across all three cultivars. Morphine is a primary end product in the BIA pathway, and its dominance suggests a strong metabolic preference for its synthesis, likely regulated by a robust enzymatic machinery ensuring its accumulation (Singh et al., 2019). This common prioritization of morphine biosynthesis might minimize the variability in this branch, emphasizing its central role in alkaloid production within these cultivars.

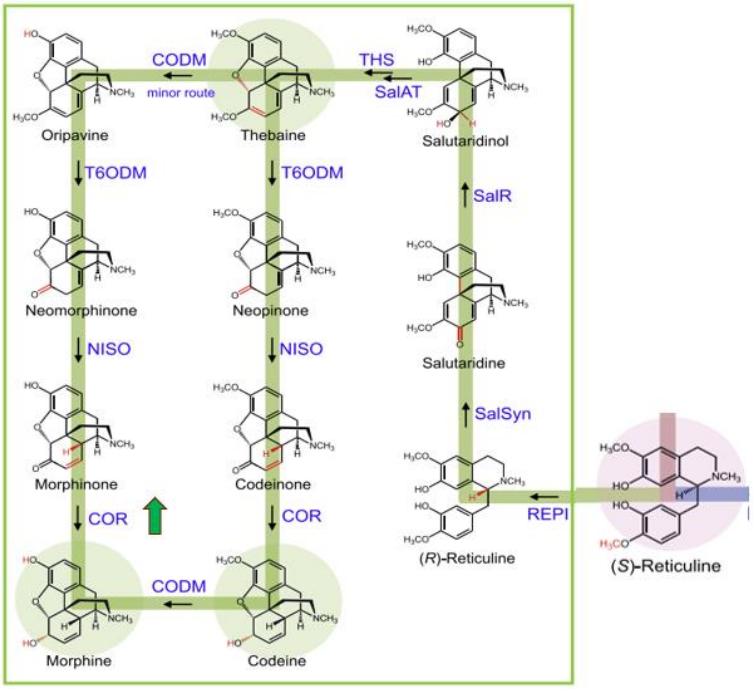

Figure 3.21. Differential expression of enzymes in the morphine branch of the BIA pathway. Green arrows represents the enzymes upregulated in mature capsules of Ofis NM compared to either Ofis 2 or TMO T.

Most of the significantly up-regulated proteins that serve in the noscapine and papaverine branch of the BIA pathway in the mature capsules were also significant in the comparison of latex-including stems of the cultivars. Thus, SOMT1, SOMT2, SOMT3, 4'OMT2, 7OMT and CXE1 enzymes were up-regulated in Ofis NM stems compared to Ofis 2 and/or TMO T. In contrast to mature capsules, BBE (berberine-bridge enzyme) and C80BX ((S)-N-methylcoclaurine 3'-hydroxylase-like protein) were also up-regulated in Ofis NM stems compared to Ofis 2 and TMO T. C80BX hydroxylates (S)-N-methylcoclaurine to (S)-3'-hydroxy-N-methylcoclaurine, a step essential for the synthesis of the key central intermediate (S)-reticuline, while BBE further catalyzes the formation of the berberine bridge in (S)-reticuline to produce (S)-scoulerine which is the starting point of the noscapine branch (Desgagné-Penix et al., 2010; Desgagné-Penix and Facchini, 2012; Yang et al., 2021).

Similar to CYP82X1E, an enzyme which was discussed for the mature capsules, CYP8271, CYP82X2, CYP82Y1, and CYP719A21 are also members of the cytochrome P450 superfamily. All of these proteins were up-regulated in Ofis NM stems compared to Ofis 2 and TMO T and catalyze different oxidation reactions involved in the noscapine branch of the BIA pathway. CYP719A21 catalyzes the formation of a methylenedioxy bridge between the C-4 and C-5 hydroxyl groups of (S)-tetrahydrocolumbamine, converting it into (S)-canadine (Dang and Facchini, 2012; Dang and Facchini, 2014). CYP82Y1 hydroxylates (S)-N-methylcanadine to (S)-1-hydroxy-N-methylcanadine which is further converted to (13S,14R)-1,13-dihydroxy-N-methylcanadine by CYP82X2. Subsequently, CYP82X1 catalyzes the conversion of (13S,14R)-13-O-acetyl-1-hydroxy-N-methylcanadine into (13S,14R)-13-O-acetyl-1,8-dihydroxy-N-methylcanadine by introducing a hydroxyl group at the C-8 position. The consistent up-regulation of noscapine branch enzymes in both the mature capsules and latex-including stems of Ofis NM, compared to Ofis 2 and TMO T, highlights the cultivar's specialized metabolic commitment to noscapine biosynthesis across different tissue types (Dang and Facchini, 2012; Dang and Facchini, 2014).

In contrast to mature capsules, differential expression of proteins downstream of the morphine branch was determined for latex-including stems of the opium poppy cultivars, such as REPI (reticuline epimerase), SalSyn (salutaridine synthase), SalAT (salutaridinol 7-O-acetyltransferase) and THS (thebaine synthase). These enzymes drive the conversion of key intermediates into morphinan alkaloids, including thebaine, codeine

and morphine (Singh et al., 2019). As expected, the expression of SalAT was up-regulated in the morphine-rich Ofis 2 compared to the noscapine-rich Ofis NM. Similarly, THS was up-regulated in thebaine-rich TMO T compared to Ofis 2.

However, since SalSyn (salutaridine synthase) and REPI (reticuline epimerase) are involved in the morphine biosynthesis pathway, their downregulation in Ofis 2 (morphine-rich) and TMO T (thebaine-rich) compared to Ofis NM (noscapine-rich) might seem unexpected. SalSyn and REPI are involved in the early steps of the morphine biosynthesis pathway, converting the common intermediate (S)-reticuline into salutaridine, a precursor for morphinan alkaloids. This up-regulation might act as a mechanism to maintain a balance between the competing pathways of morphine and noscapine production in Ofis NM, allowing production of both without significantly compromising one for the other (Dang and Facchini, 2015; Li et al., 2018).

In addition to the well-characterized enzymes directly involved in the BIA pathway, several proteins (uncharacterized or homology-based evidence) such as cytochrome P450s, allene oxide synthases, and Bet v I/Major latex protein domain-containing proteins, were identified to be differentially expressed among the capsules and stems of the cultivars as represented in the bar plots in Figure 3.17-18.

Cytochrome P450s are highly versatile enzymes capable of catalyzing various oxidation reactions, including hydroxylation, demethylation, and the formation of methylenedioxy bridges. Their significant power to increase the variety of alkaloid structures (by ring formations, expansions, etc.) is critical in the diversity of alkaloid functions. Thus, these unknown P450 proteins could contribute to novel oxidation reactions or pathway branching in the BIA metabolism, specific to alkaloid profiles in each cultivar (Nguyen and Dang, 2021; Williams and De Luca, 2023).

Allene oxide synthases (AOS) have been known to contribute to BIA metabolism by their involvement in the synthesis of jasmonate precursors, which are key signaling molecules and intermediates in plant defense and stress responses (Pauwels et al., 2009). Specifically, AOS catalyzes the conversion of fatty acid hydroperoxides, such as 13-hydroperoxy-octadecatrienoic acid (13-HPOT), into allene oxide, which then undergoes further enzymatic reactions to form jasmonic acid (JA) and its derivatives (Wei, 2010). These jasmonate compounds can act as signaling molecules that regulate the expression of genes involved in the biosynthesis of BIAs by activating several transcription factors

(Huang et al., 2021). A study identified two groups of III WRKY transcription factors, NnWRKY70a and NnWRKY70b, as key activators of BIA biosynthesis in lotus (*Nelumbo nucifera*). Their expression was significantly induced by JA and showed a strong correlation with both the accumulation of BIAs and the activation of genes in the BIA biosynthetic pathway (Li et al., 2022).

Lastly, the bet v I/major latex protein (MLP) domain-containing proteins possess the ability to bind hydrophobic alkaloids in opium poppy, which likely enabled their evolution into enzymes involved in alkaloid biosynthesis (Ban et al., 2018; Dastmalchi, 2021). Among the enzymes contributing to morphine production, norcoclaurine synthase (NCS), thebaine synthase (THS), and neopinone isomerase (NISO) are classified in the MLP/PR10 protein family due to structural similarity (Ozber et al, 2022). Furthermore, rather than directly participating in the enzymatic reactions of BIA biosynthesis, non-catalytic MLP proteins might bind and stabilize hydrophobic alkaloid intermediates, preventing their degradation or facilitating their availability for enzymatic reactions (Dastmalchi, 2021). In addition, these proteins could act as molecular chaperones, helping to transport alkaloid intermediates between different cellular compartments or enzymes in the BIA pathway (Casanal et al., 2013; Ozber et al., 2022).

The uncharacterized proteins may play critical, yet currently underexplored, roles in the cultivar-specific regulation of the BIA pathway in opium poppy. Further functional characterization of these proteins could provide valuable insights into their contributions to metabolic flux and the specialized alkaloid profiles observed in different Turkish opium poppy cultivars.

CHAPTER 4

CONCLUSION

This study provided a comprehensive proteomic analysis of three Turkish opium poppy cultivars, Ofis NM, Ofis 2, and TMO T, each characterized by distinct benzylisoquinoline alkaloid (BIA) profiles: noscapine, morphine, and thebaine, respectively. Through MS-based protein identification and quantification, alongside BIA metabolome analysis, differentiation in the protein composition of Turkish opium poppy cultivars was determined, highlighting tissue- and cultivar-specific regulation of BIA biosynthesis. Among the five tissues of interest, mature capsules exhibited the highest number of significant DEPs (2066 in total). Ofis 2 showed a distinct proteomic profile, diverging significantly from TMO T and Ofis NM, which share a closer relationship in their protein expression patterns. In both mature capsules and latex-including stems, noscapine-accumulator Ofis NM showed significant up-regulation of key enzymes in the noscapine branch compared to TMO T and Ofis 2. GO and KEGG pathway enrichment analyses revealed cultivar-specific variation in biological processes such as biosynthesis of secondary metabolites, ribosome biogenesis, and carbon metabolism, pointing to an integrated metabolic regulation.

This research lays a foundation for exploring BIA biosynthesis and its regulation in opium poppy. Future studies could focus on characterizing unannotated proteins and their roles in pathway branching or metabolite transport. Integrating multi-omics approaches, such as transcriptomics and metabolomics, could uncover gene-protein-metabolite networks underlying BIA accumulation. Techniques like immunohistochemistry or single-cell proteomics could reveal the spatial regulation of alkaloid biosynthesis. Functional studies, including CRISPR-Cas9 or RNA interference, may validate regulatory roles of candidate genes like 7OMT, 4'OMT2, and cytochrome P450s, enabling the manipulation of alkaloid profiles for pharmaceuticals. Additionally, breeding programs could leverage these insights to develop high-yielding cultivars optimized for producing target BIAs, addressing both medicinal and commercial needs.

REFERENCES

Aebersold, R., and M. Mann. 2003. "Mass Spectrometry-Based Proteomics." *Nature* 422 (6928): 198–207.

Agarwal, P., Pathak, S., Lakhwani, D., Gupta, P., Asif, M. H., and Trivedi, P. K. 2015. "Comparative Analysis of Transcription Factor Gene Families from *Papaver somniferum*: Identification of Regulatory Factors Involved in Benzylisoquinoline Alkaloid Biosynthesis." *Protoplasma* 253 (3): 857–71.

Ahmad, P., Abdel Latef, A. A., Rasool, S., Akram, N. A., Ashraf, M., and Gucel, S. 2016. "Role of Proteomics in Crop Stress Tolerance." *Frontiers in Plant Science* 7: 1336.

Allen, R. S., Millgate, A. G., Chitty, J. A., Thisleton, J., Miller, J. A., Fist, A. J., and Larkin, P. J. 2004. "RNAi-Mediated Replacement of Morphine with the Nonnarcotic Alkaloid Reticuline in Opium Poppy." *Nature Biotechnology* 22 (12): 1559–66.

Allen, R. S., Miller, J. A., Chitty, J. A., Fist, A. J., Gerlach, W. L., and Larkin, P. J. 2008. "Metabolic Engineering of Morphinan Alkaloids by Over-Expression and RNAi Suppression of Salutaridinol 7-O-Acetyltransferase in Opium Poppy." *Plant Biotechnology Journal* 6 (1): 22–30.

Altelaar, A. M., Frese, C. K., Preisinger, C., Hennrich, M. L., Schram, A. W., Timmers, H. T. M., and Mohammed, S. 2013. "Benchmarking Stable Isotope Labeling Based Quantitative Proteomics." *Journal of Proteomics* 88: 14–26.

Aslam, B., Basit, M., Nisar, M. A., Khurshid, M., and Rasool, M. H. 2016. "Proteomics: Technologies and Their Applications." *Journal of Chromatographic Science* 55 (2): 182–196.

Ban, Z., Qin, H., Mitchell, A. J., Liu, B., Zhang, F., Weng, J. K., and Wang, G. 2018. "Noncatalytic Chalcone Isomerase-Fold Proteins in *Humulus lupulus* Are Auxiliary Components in Prenylated Flavonoid Biosynthesis." *Proceedings of the National Academy of Sciences* 115 (22): E5223–E5232.

Battle, A., Khan, Z., Wang, S. H., Mitrano, A., Ford, M. J., Pritchard, J. K., and Gilad, Y. 2015. "Impact of Regulatory Variation from RNA to Protein." *Science* 347 (6222): 664–667.

Bettinger, J. Q., Welle, K. A., Hryhorenko, J. R., and Ghaemmaghami, S. 2019. "Quantitative analysis of in vivo methionine oxidation of the human proteome". *Journal of Proteome Research* 19 (2): 624-633.

Bird, D. A., Franceschi, V. R., and Facchini, P. J. 2003. "A tale of three cell types: alkaloid biosynthesis is localized to sieve elements in opium poppy." *The Plant Cell* 15 (11): 2626-2635.

Brajkovic, S., Rugen, N., Agius, C., Berner, N., Eckert, S., Sakhteman, A., Schwechheimer, C., and Kuster, B. 2023. "Getting ready for large-scale proteomics in crop plants." *Nutrients* 15 (3): 783.

Bulut, B., Aydinli, Z., and Türktaş, M. 2020. "MSAP analysis reveals diverse epigenetic statuses in opium poppy varieties with different benzyisoquinoline alkaloid content." *Turkish Journal of Biology* 44 (2): 103-109.

Burkhart, J. M., Schumbrutzki, C., Wortelkamp, S., Sickmann, A., and Zahedi, R. P. 2012. "Systematic and quantitative comparison of digest efficiency and specificity reveals the impact of trypsin quality on MS-based proteomics." *Journal of Proteomics* 75 (4): 1454-1462.

Carlin, M. G., Dean, J. R., and Ames, J. M. 2020. "Opium alkaloids in harvested and thermally processed poppy seeds." *Frontiers in Chemistry* 8: 737.

Casañal, A., Zander, U., Muñoz, C., Dupeux, F., Luque, I., Botella, M. A., ... and Marquez, J. A. 2013. "The strawberry pathogenesis-related 10 (PR-10) Fra a proteins control flavonoid biosynthesis by binding to metabolic intermediates." *Journal of Biological Chemistry* 288 (49): 35322-35332.

Celik, I., Camci, H., Kose, A., Kosar, F. C., Doganlar, S., and Frary, A. 2016. "Molecular genetic diversity and association mapping of morphine content and agronomic traits in Turkish opium poppy (*Papaver somniferum*) germplasm." *Molecular Breeding* 36: 1-13.

Ceylan, O. 2022. "The opium history of Eastern Thrace (1927-1933): Internal and external dynamics." *Belgi Dergisi* (23): 141-167.

Chahl, L. A. 1996. "Experimental and clinical pharmacology: Opioids - mechanisms of action." *Australian Prescriber* 19 (3): 63–65.

Chen, X., and Facchini, P. J. 2013. "Short-chain dehydrogenase/reductase catalyzing the final step of noscapine biosynthesis is localized to laticifers in opium poppy." *The Plant Journal* 77 (2): 173–184.

Cottrell, J. S. 2011. "Protein identification using MS/MS data." *Journal of Proteomics* 74 (10): 1842-1851.

Cox, J., and Mann, M. 2008. "MaxQuant enables high peptide identification rates, individualized ppb-range mass accuracies and proteome-wide protein quantification." *Nature Biotechnology* 26 (12): 1367-1372.

Dang, T. T. T., Chen, X., and Facchini, P. J. 2015. "Acetylation serves as a protective group in noscapine biosynthesis in opium poppy." *Nature Chemical Biology* 11 (2): 104-106.

Dang, T. T. T., and Facchini, P. J. 2012. "Characterization of three O-methyltransferases involved in noscapine biosynthesis in opium poppy." *Plant Physiology,* 159 (2): 618-631.

Dang, T. T. T., and Facchini, P. J. 2014. "CYP82Y1 is N-methylcanadine 1-hydroxylase, a key noscapine biosynthetic enzyme in opium poppy." *Journal of Biological Chemistry* 289 (4): 2013-2026.

Dastmalchi, M. 2021. “Elusive partners: a review of the auxiliary proteins guiding metabolic flux in flavonoid biosynthesis.” *The Plant Journal* 108 (2): 314-329.

Deng, X., Zhao, L., Fang, T., Xiong, Y., Ogutu, C., Yang, D., Vimolmangkang, S., Liu, Y., and Han, Y. 2018. “Investigation of benzylisoquinoline alkaloid biosynthetic pathway and its transcriptional regulation in Lotus.” *Horticulture Research* 5: 29.

Decker, G., Wanner, G., Zenk, M. H., and Lottspeich, F. 2000. “Characterization of proteins in latex of the opium poppy (*Papaver somniferum*) using two-dimensional gel electrophoresis and microsequencing.” *Electrophoresis* 21 (16): 3500–3516.

Desgagné-Penix, I., and Facchini, P. J. 2012. “Systematic silencing of benzylisoquinoline alkaloid biosynthetic genes reveals the major route to papaverine in opium poppy.” *The Plant Journal* 72 (2): 331-344.

Desgagné-Penix, I., Farrow, S. C., Cram, D., Nowak, J., and Facchini, P. J. 2012. “Integration of deep transcript and targeted metabolite profiles for eight cultivars of Opium Poppy.” *Plant Molecular Biology* 79 (3): 295–313.

Desgagne-Penix, I., Khan, M.F., Schriemer, D.C., Cram, D., Nowak, J. and Facchini, P.J. 2010. “Integration of deep transcriptome and proteome analyses reveals the components of alkaloid metabolism in opium poppy cell cultures.” *BMC Plant Biology* 10: 1-17.

Diamond, A., and Desgagné-Penix, I. 2015. “Metabolic Engineering for the production of plant isoquinoline alkaloids.” *Plant Biotechnology Journal* 14 (6): 1319–1328.

Didusch, S., Madern, M., Hartl, M., and Baccarini, M. 2022. “Amica: an interactive and user-friendly web-platform for the analysis of proteomics data.” *BMC Genomics* 23 (1): 817.

Evered, K. T. 2011. “The Opium Poppy in Türkiye: Alternative perspectives on a controversial crop.” *Focus on Geography* 54 (1): 1–10.

Facchini, P. J., Hagel, J. M., Liscombe, D. K., Loukanina, N., MacLeod, B. P., Samanani, N., and Zulak, K. G. 2007. “Opium poppy: Blueprint for an alkaloid factory.” *Phytochemistry Reviews* 6 (1): 97–124.

Fukushima, A., and Kusano, M. 2013. “Recent progress in the development of metabolome databases for Plant Systems Biology.” *Frontiers in Plant Science* 4: 73.

Gilbert, H. J. 2010. “The biochemistry and structural biology of plant cell wall deconstruction.” *Plant Physiology* 153 (2): 444-455.

Gracz-Bernaciak, J., Mazur, O., and Nawrot, R. 2021. “Functional studies of plant latex as a rich source of bioactive compounds: focus on proteins and alkaloids.” *International Journal of Molecular Sciences* 22 (22): 12427.

Gu, L., Zhang, Z. Y., Quan, H., Li, M. J., Zhao, F. Y., Xu, Y. J., ... and Lan, X. Z. 2018. “Integrated analysis of transcriptomic and metabolomic data reveals critical metabolic pathways involved in rotenoid biosynthesis in the medicinal plant Mirabilis himalaica.” *Molecular Genetics and Genomics* 293*:* 635-647.

Güçlü, G. B., Gürkök, T., Koyuncu, M., Arslan, N., and Parmaksız, İ. 2014. “Genetic characterization of Turkish commercial opium poppy (*Papaver somniferum* L.) cultivars using ISSR and SSR markers.” *Journal of New Results in Science* 3 (7): 48-57.

Guo, J., Huang, Z., Sun, J., Cui, X., and Liu, Y. 2021. “Research progress and future development trends in medicinal plant transcriptomics.” *Frontiers in Plant Science* 12: 691838.

Gurkok, T., Ozhuner, E., Parmaksiz, I., Özcan, S., Turktas, M., Ipek, A., ... and Unver, T. 2016. “Functional characterization of 4′ OMT and 7OMT genes in BIA biosynthesis.” *Frontiers in Plant Science* 7: 98.

Gurkok T, Turktas M, Parmaksiz I, and Unver T 2015. “Transcriptome profiling of alkaloid biosynthesis in elicitor induced opium poppy.” *Plant Molecular Biology Reporter* 33: 673-688.

Hagel, J. M., and Facchini, P. J. 2013. “Benzylisoquinoline alkaloid metabolism: A century of discovery and a brave new world.” *Plant and Cell Physiology* 54 (5): 647–672.

Heinrich, M., Mah, J., and Amirkia, V. 2021. “Alkaloids used as medicines: Structural phytochemistry meets Biodiversity—an update and forward look.” *Molecules* 26 (7): 1836.

Heyman, H. M., and Dubery, I. A. 2016. “The potential of mass spectrometry imaging in plant metabolomics: a review.” *Phytochemistry Reviews* 15: 297-316.

Hong, J., Yang, L., Zhang, D., and Shi, J. 2016. “Plant metabolomics: an indispensable system biology tool for plant science.” *Intrnational Journal of Molecular Sciences* 17 (6): 767.

Huang, F.C., and Kutchan, T.M. 2000. “Distribution of morphinan and benzo[c]phenanthridine alkaloid gene transcript accumulation in *Papaver somniferum.” Phytochemistry* 53 (5): 555-564.

Huang, P., Xia, L., Zhou, L., Liu, W., Wang, P., Qing, Z., and Zeng, J. 2021. “Influence of different elicitors on BIA production in *Macleaya cordata*.” *Scientific Reports* 11 (1): 619.

Hughes, C. S., Moggridge, S., Müller, T., Sorensen, P. H., Morin, G. B., and Krijgsveld, J. 2019. “Single-pot, solid-phase-enhanced sample preparation for proteomics experiments.” *Nature Protocols* 14 (1): 68–85.

Idle, J. R., and Gonzalez, F. J. 2007. “Metabolomics.” *Cell Metabolism* 6 (5): 348-351.

Kara, N., and Baydar, H. 2021. “The alkaloid content of poppy (*Papaver somniferum* L.) varieties in Turkey by their correlation and path coefficient relationships.” *International Journal of Agriculture Environment and Food Sciences* 5 (4): 450-455.

Kocabaş, D. S., Köle, M., and Yağcı, S. 2020. “Development and optimization of hemicellulose extraction bioprocess from poppy (*Papaver somniferum* L.) stalks assisted by instant controlled pressure drop (DIC) pretreatment.” *Biocatalysis and Agricultural Biotechnology* 29: 101793.

Kolberg, L., Raudvere, U., Kuzmin, I., Adler, P., Vilo, J., and Peterson, H. 2023. “g: Profiler—interoperable web service for functional enrichment analysis and gene identifier mapping (2023 update).” *Nucleic Acids Research* 51 (W1): W207-W212.

Kundrátová, K., Bartas, M., Pečinka, P., Hejna, O., Rychlá, A., Čurn, V., and Červeň, J. 2021. “Transcriptomic and proteomic analysis of drought stress response in opium poppy plants during the first week of germination.” *Plants* 10 (9): 1878.

Lee, E.-J., Hagel, J. M., and Facchini, P. J. 2013. “Role of the phloem in the biochemistry and ecophysiology of benzylisoquinoline alkaloid metabolism.” *Frontiers in Plant Science* 4: 182.

Li, J., Li, Y., Dang, M., Li, S., Chen, S., Liu, R., ... and Deng, X. 2022. “Jasmonate-responsive transcription factors NnWRKY70a and NnWRKY70b positively regulate benzylisoquinoline alkaloid biosynthesis in lotus (*Nelumbo nucifera*).” *Frontiers in Plant Science* 13: 862915.

Li, J., Van Vranken, J. G., Pontano Vaites, L., Schweppe, D. K., Huttlin, E. L., Etienne, C., ... and Paulo, J. A. 2020a. “TMTpro reagents: a set of isobaric labeling mass tags enables simultaneous proteome-wide measurements across 16 samples.” *Nature Methods* 17 (4): 399-404.

Li, Q., Ramasamy, S., Singh, P., Hagel, J., Dunemann, S., Chen, X., Chen, R., Yu, L., Tucker, J., Facchini, P., and Yeaman, S. 2020b. “Gene clustering and copy number variation in alkaloid metabolic pathways of opium poppy.” *Nature Communications* 11 (1): 1190.

Li, Y., Li, S., Thodey, K., Trenchard, I., Cravens, A., and Smolke, C. D. 2018. "Complete biosynthesis of noscapine and halogenated alkaloids in yeast." *Proceedings of the National Academy of Sciences* 115 (17): E3922-E3931.

Lin, Z., Ren, Y., Shi, Z., Zhang, K., Yang, H., Liu, S., and Hao, P. 2020. "Evaluation and minimization of nonspecific tryptic cleavages in proteomic sample preparation." *Rapid Communications in Mass Spectrometry* 34 (10): e8733.

Liu, J., Cai, J., Wang, R., and Yang, S. 2016. "Transcriptional regulation and transport of terpenoid indole alkaloid in *Catharanthus roseus*: exploration of new research directions." *International Journal of Molecular Sciences* 18 (1): 53.

Mann, M., Hendrickson, R. C., and Pandey, A. 2001. "Analysis of proteins and proteomes by mass spectrometry." *Annual Review of Biochemistry* 70 (1): 437-473.

Mansfield, D. 2001. "An analysis of licit opium poppy cultivation: India and Turkey." *Unpublished document available on www. geopium. org*.

Marriott, P. E., Gómez, L. D., and McQueen-Mason, S. J. 2016. "Unlocking the potential of lignocellulosic biomass through plant science." *New Phytologist* 209 (4): 1366-1381.

Martínez-Esteso, M. J., Martínez-Márquez, A., Sellés-Marchart, S., Morante-Carriel, J. A., and Bru-Martínez, R. 2015. "The role of proteomics in progressing insights into plant secondary metabolism." *Frontiers in Plant Science* 6: 504.

Maurino, V. G., and Engqvist, M. K. 2015. "2-Hydroxy acids in plant metabolism." *The Arabidopsis book/American Society of Plant Biologists,* 13.

Mergner, J., Frejno, M., List, M., Papacek, M., Chen, X., Chaudhary, A., Samaras, P., Richter, S., Shikata, H., Messerer, M., Lang, D., Altmann, S., Cyprys, P., Zolg, D. P., Mathieson, T., Bantscheff, M., Hazarika, R. R., Schmidt, T., Dawid, C., … and Kuster, B. 2020a. "Mass-spectrometry-based draft of the Arabidopsis proteome." *Nature* 579 (7799): 409–414.

Mergner, J., Frejno, M., Messerer, M., Lang, D., Samaras, P., Wilhelm, M., ... and Kuster, B. 2020b. “Proteomic and transcriptomic profiling of aerial organ development in Arabidopsis.” *Scientific Data* 7 (1): 334.

Mikulášek, K., Konečná, H., Potěšil, D., Holánková, R., Havliš, J., and Zdráhal, Z. 2021. “SP3 protocol for Proteomic plant sample preparation prior LC-MS/MS.” *Frontiers in Plant Science* 12: 635550.

Morishige, T., Tsujita, T., Yamada, Y., and Sato, F. 2000. “Molecular characterization of the S-adenosyl-L-methionine: 3′-hydroxy-N-methylcoclaurine 4′-O-methyltransferase involved in isoquinoline alkaloid biosynthesis in Coptis japonica.” *Journal of Biological Chemistry* 275 (30): 23398-23405.

Morris, J. S., Caldo, K. M. P., Liang, S., and Facchini, P. J. 2021. “PR10/Bet v1-like proteins as novel contributors to plant biochemical diversity.” *ChemBioChem* 22 (2): 264-287.

Nessler, C. L., Allen, R. D., and Galewsky, S. 1985. “Identification and characterization of latex-specific proteins in opium poppy.” *Plant Physiology* 79 (2): 499-504.

Neubert, H., Bonnert, T. P., Rumpel, K., Hunt, B. T., Henle, E. S., and James, I. T. 2008. “Label-free detection of differential protein expression by LC/MALDI mass spectrometry.” *Journal of Proteome Research* 7 (6): 2270-2279.

Norn, S., Kruse, P. R., and Kruse, E. 2005. “History of opium poppy and morphine.” *Dansk Medicinhistorisk Arbog* 33: 171-184.

Nguyen, T. D., and Dang, T. T. T. 2021. “Cytochrome P450 enzymes as key drivers of alkaloid chemical diversification in plants.” *Frontiers in Plant Science* 12: 682181.

Okada, T., Mochamad Afendi, F., Altaf-Ul-Amin, M., Takahashi, H., Nakamura, K., and Kanaya, S. 2010. “Metabolomics of medicinal plants: the importance of multivariate analysis of analytical chemistry data.” *Current Computer-aided Drug Design* 6 (3): 179-196.

Onoyovwe, A., Hagel, J. M., Chen, X., Khan, M. F., Schriemer, D. C., and Facchini, P. J. 2013. “Morphine biosynthesis in opium poppy involves two cell types: Sieve elements and laticifers.” *The Plant Cell* 25 (10): 4110–4122.

Ounaroon, A., Decker, G., Schmidt, J., Lottspeich, F., and Kutchan, T. M. 2003. “(R, S)-Reticuline 7-O-methyltransferase and (R, S)-norcoclaurine 6-O-methyltransferase of *Papaver somniferum*–cDNA cloning and characterization of methyl transfer enzymes of alkaloid biosynthesis in opium poppy.” *The Plant Journal* 36 (6): 808-819.

Ozber, N., Carr, S. C., Morris, J. S., Liang, S., Watkins, J. L., Caldo, K. M., ... and Facchini, P. J. 2022. “Alkaloid binding to opium poppy major latex proteins triggers structural modification and functional aggregation.” *Nature Communications* 13 (1): 6768.

Ozber, N., and Facchini, P. J. 2022. “Phloem-specific localization of benzylisoquinoline alkaloid metabolism in opium poppy.” *Journal of Plant Physiology* 271: 153641.

Özgen, Y., Arslan, N., and Bayraktar, N. 2017.” Türkiye açısından önemli bitki haşhaşın önemi ve tarımı.” *Ziraat Mühendisliği* (364): 4-8.

Park, M. R., Chen, X., Lang, D. E., Ng, K. K., and Facchini, P. J. 2018. “Heterodimeric O-methyltransferases involved in the biosynthesis of noscapine in opium poppy.” *The Plant Journal* 95 (2): 252-267.

Pathak, S., Lakhwani, D., Gupta, P., Mishra, B. K., Shukla, S., Asif, M. H., and Trivedi, P. K. 2013. “Comparative transcriptome analysis using high papaverine mutant of *Papaver somniferum* reveals pathway and uncharacterized steps of papaverine biosynthesis.” *PLoS ONE* 8 (5): e65622.

Pauwels, L., Inzé, D., and Goossens, A. 2009. “Jasmonate-inducible gene: what does it mean?” *Trends in Plant Science* 14 (2): 87-91.

Pienkny, S., Brandt, W., Schmidt, J., Kramell, R., and Ziegler, J. 2009. "Functional characterization of a novel benzylisoquinoline O-methyltransferase suggests its involvement in papaverine biosynthesis in opium poppy (*Papaver somniferum* L)." *The Plant Journal* 60 (1): 56-67.

Pilatzke-Wunderlich, I., and Nessler, C. L. 2001. "Expression and activity of cell-wall-degrading enzymes in the latex of opium poppy, *Papaver somniferum* L." *Plant Molecular Biology* 45: 567-576.

Quanbeck, S. M., Brachova, L., Campbell, A. A., Guan, X., Perera, A., He, K., Rhee, S. Y., Bais, P., Dickerson, J. A., Dixon, P., Wohlgemuth, G., Fiehn, O., Barkan, L., Lange, I., Lange, B. M., Lee, I., Cortes, D., Salazar, C., Shuman, J., … Nikolau, B. J. 2012. "Metabolomics as a hypothesis-generating functional genomics tool for the annotation of Arabidopsis thaliana genes of "unknown function."" *Frontiers in Plant Science* 3: 15.

Rai, A., and Saito, K. 2016. "OMICS data input for Metabolic Modeling." *Current Opinion in Biotechnology* 37: 127–134.

Ray, T., Pandey, S. S., Pandey, A., Srivastava, M., Shanker, K., and Kalra, A. 2019. "Endophytic consortium with diverse gene-regulating capabilities of benzylisoquinoline alkaloids biosynthetic pathway can enhance endogenous morphine biosynthesis in *Papaver somniferum*." *Frontiers in Microbiology* 10: 925.

Rodrigues, E. P., Torres, A. R., Batista, J. S., Huergo, L., and Hungria, M. 2012a. "A simple, economical and reproducible protein extraction protocol for proteomics studies of Soybean Roots." *Genetics and Molecular Biology* 35 (1): 348–352.

Samanani, N., Alcantara, J., Bourgault, R., Zulak, K. G., and Facchini, P. J. 2006. "The role of phloem sieve elements and laticifers in the biosynthesis and accumulation of alkaloids in opium poppy." *The Plant Journal* 47 (4): 547-563.

Seger, C., and Salzmann, L. 2020. "After another decade: LC–MS/MS became routine in clinical diagnostics." *Clinical Biochemistry* 82: 2-11.

Sharma, P., Jha, A. B., Dubey, R. S., and Pessarakli, M. 2012. “Reactive oxygen species, oxidative damage, and antioxidative defense mechanism in plants under stressful conditions.” *Journal of Botany* 2012 (1): 217037.

Sherman, B. T., Hao, M., Qiu, J., Jiao, X., Baseler, M. W., Lane, H. C., ... and Chang, W. 2022. “DAVID: a web server for functional enrichment analysis and functional annotation of gene lists (2021 update).” *Nucleic Acids Research* 50 (W1): W216-W221.

Singh, A., Menéndez-Perdomo, I. M., and Facchini, P. J. 2019. “Benzylisoquinoline alkaloid biosynthesis in opium poppy: An update.” *Phytochemistry Reviews* 18 (6): 1457–1482.

Singh, N., Jain, N., Kumar, R., Jain, A., Singh, N. K., and Rai, V. 2015. “A comparative method for protein extraction and 2-D gel electrophoresis from different tissues of *Cajanus cajan*.” *Frontiers in Plant Science* 6: 1-7.

Singh, S. P., Khanna, K. R., Dixit, B. S., and Srivastava, S. N. 1990. “Fatty acid composition of opium poppy (*Papaver somniferum*) seed oil.” *Indian Journal of Agricultural Science* 60 (5): 358-359.

Skalicky, M., Hejnak, V., Novak, J., Hejtmankova, A., and Stranska, I. 2014. “Evaluation of selected poppy (*Papaver somniferum* L.) cultivars: Industrial Aspect.” *Turkish Journal Of Field Crops* 19 (2): 189–196.

Snyder, L. R., Kirkland, J. J., and Dolan, J. W. 2011. *Introduction to Modern Liquid Chromatography*. John Wiley and Sons.

Srivastava, N. K., and Sharma, S. 1990. “Effect of triacontanol on photosynthesis, alkaloid content and growth in opium poppy (*Papaver somniferum* L.).” *Plant Growth Regulation* 9: 65-71.

Thoma, F., Somborn-Schulz, A., Schlehuber, D., Keuter, V., and Deerberg, G. 2020. “Effects of light on secondary metabolites in selected leafy greens: A review.” *Frontiers in Plant Science* 11: 497.

Tuli, L., and Ressom, H. W. 2009. “LC–MS based detection of differential protein expression.” *Journal of Proteomics and Bioinformatics* 2 (10): 416-438.

Tyanova, S., Temu, T., Sinitcyn, P., Carlson, A., Hein, M. Y., Geiger, T., ... and Cox, J. 2016. “The Perseus computational platform for comprehensive analysis of (prote) omics data.” *Nature Methods* 13 (9): 731-740.

Uemura, M., and Hausman, J.-F. 2012. “Plant Strategies for survival in changing environment.” *Physiologia Plantarum* 147 (1): 1–3.

Viana, L. da, Silva, P. P., Nascimento, V. X., Riffel, A., and Sant’Ana, A. E. 2020. Comparison of methods for the extraction of proteins from root and leaf tissue of sugarcane (saccharum spp.) for proteomic analysis. *Australian Journal of Crop Science,* 14(8), 1221–1229.

Walker, J. M. 2009. “The bicinchoninic acid (BCA) assay for protein quantitation *The Protein Protocols Handbook:* 11–14.

Waris, M., Kocak, E., Gonulalan, E. M., Demirezer, L. O., Kır, S., and Nemutlu, E. 2022. “Metabolomics analysis insight into medicinal plant science*.” TrAC Trends in Analytical Chemistry* 157: 116795.

Waszczak, C., Carmody, M., and Kangasjärvi, J. 2018. “Reactive oxygen species in plant signaling.” *Annual Review of Plant Biology* 69 (1): 209-236.

Wei, S. 2010. “Methyl jasmonic acid induced expression pattern of terpenoid indole alkaloid pathway genes in Catharanthus roseus seedlings.” *Plant Growth Regulation* 61 (3): 243-251.

Weid, M., Ziegler, J., and Kutchan, T. M. 2004. “The roles of latex and the vascular bundle in morphine biosynthesis in the opium poppy, *Papaver somniferum*.” *Proceedings of the National Academy of Sciences* 101 (38): 13957–13962.

Wijekoon, C. P., and Facchini, P. J. 2012. “Systematic knockdown of morphine pathway enzymes in opium poppy using virus-induced gene silencing.” *The Plant Journal* 69 (6): 1052-1063.

Williams, D., and De Luca, V. 2023. “Plant cytochrome P450s directing monoterpene indole alkaloid (MIA) and benzylisoquinoline alkaloid (BIA) biosynthesis.” *Phytochemistry Reviews* 22 (2): 309-338.

Williams, S. 2010. “On islands, insularity, and opium poppies: Australia's secret pharmacy.” *Environment and Planning D: Society and Space* 28 (2): 290-310.

Williams, S. 2013. “Licit Narcotics Production in Australia: Legal Geographies Nomospheric and Topological.” *Geographical Research* 51 (4): 364-374.

Windle, J. 2014.” A very gradual suppression: A history of Turkish opium controls, 1933–1974.” *European Journal of Criminology* 11 (2): 195-212.

Winzer, T., Gazda, V., He, Z., Kaminki, F., Kern, M., Larson, T. R., Li, Y., Meade, F., Teodor, R., Vaistij, F. E., Walker, C., Bowser, T. A., and Graham, I. A. 2012. “A *Papaver somniferum* 10-gene cluster for synthesis of the anticancer alkaloid noscapine.” *Science* 336 (6089): 1704–1708.

Winzer, T., Kern, M., King, A. J., Larson, T. R., Teodor, R. I., Donninger, S. L., ... and Graham, I. A. 2015. “Morphinan biosynthesis in opium poppy requires a P450-oxidoreductase fusion protein.” *Science* 349 (6245): 309-312.

Yang, L., Miao, L., Gong, Q., and Guo, J. 2022. “Advances in studies on transcription factors in regulation of secondary metabolites in Chinese medicinal plants.” *Plant Cell, Tissue and Organ Culture* 151 (1): 1-9.

Yang, X., Gao, S., Guo, L., Wang, B., Jia, Y., Zhou, J., ... and Ye, K. 2021. “Three chromosome-scale *Papaver* genomes reveal punctuated patchwork evolution of the morphinan and noscapine biosynthesis pathway.” *Nature Communications* 12 (1): 6030.

Yazici, L., and Yılmaz, G. 2021. “Investigation of alkaloids in opium poppy (*Papaver somniferum* L.) varieties and hybrids.” *Journal of Agricultural Sciences* 27 (1): 62-68.

Zecha, J., Satpathy, S., Kanashova, T., Avanessian, S. C., Kane, M. H., Clauser, K. R., Mertins, P., Carr, S. A., and Kuster, B. 2019. “TMT labeling for the masses: A robust and cost-efficient, in-solution labeling approach.” *Molecular and Cellular Proteomics* 18 (7): 1468–1478.

Zhao, Y., Zhang, Z., Li, M., Luo, J., Chen, F., Gong, Y., Li, Y., Wei, Y., Su, Y., and Kong, L. 2019. “Transcriptomic profiles of 33 opium poppy samples in different tissues, growth phases, and cultivars.” *Scientific Data* 6 *(*1): 66.

Zhu, W., Yang, B., Komatsu, S., Lu, X., Li, X., and Tian, J. 2015. “Binary stress induces an increase in indole alkaloid biosynthesis in *Catharanthus roseus*.” *Frontiers in Plant Science* 6*:*582.

Ziegler, J., Diaz-Chávez, M. L., Kramell, R., Ammer, C., and Kutchan, T. M. 2005. “Comparative macroarray analysis of morphine containing *Papaver somniferum* and eight morphine free *Papaver* species identifies an O-methyltransferase involved in benzylisoquinoline biosynthesis.” *Planta* 222: 458-471.